

APPLICATION OF TIRE DERIVED AGGREGATE AS HIGHWAY EMBANKMENT FILL MATERIAL

by

Daniel Teklu Meles

A thesis submitted in partial fulfillment of the requirements for the degree of

Doctor of Philosophy

in

Geotechnical Engineering

Department of Civil and Environmental Engineering
University of Alberta

© Daniel Teklu Meles, 2014

ABSTRACT

Discarded tires have been an environmental concern in different parts of the world. One mass application to avoid such environmental concern is to use them as embankment fill material in civil engineering projects. In such applications, discarded tires are usually used in a shred form referred as Tire Derived Aggregate (TDA). Tire derived aggregate has desirable properties for most civil engineering applications; it is lightweight, free-draining, and has good thermal resistivity. In the past, it has been successfully used as fill material in various engineering projects. Tire derived aggregate has also been used as fill material by mixing with soil. Despite the superior geotechnical characteristics and successful application, predicting settlement in the field based on laboratory tests has been a problem. Moreover, only TDA produced from Passenger and Light Truck Tire referred as PLTT has been used in the past. However, in regions with heavy industrial and mining activities, such as the Province of Alberta, Canada, Off-The-Road (OTR) tires have become a significant source for TDA production. The major challenge for the use of TDA from OTR is the lack of laboratory data or field experience.

In this study, the application and engineering properties of TDA produced from PLTT and OTR, and PLTT-mixed with soil as fill material for highway embankment application has been investigated using large-scale laboratory or full-scale field experiments. The compression behavior of TDA, taking particle size and source of tire as experimental variable, has been investigated using large-scale laboratory testing apparatus. Based on results from the large-scale

laboratory compression test, nonlinear elastic material model has been developed for TDA. The developed material model has been used in numerical analysis to predict settlement measured in the field for the construction of a test embankment. The result from numerical analysis agrees reasonable well with the measured settlement in the field.

Various data were also collected from the field experiment where TDA or TDA-mixed with soil was used as fill material. The ease of construction for using TDA or TDA-mixed with soil as fill material, field mixing of TDA and soil, immediate and time-dependent settlement, potential for internal heating and overall performance have been evaluated from the data collected. Analyses of the field data support the use of PLTT, OTR, and TDA-mixed with soil as a fill material for highway embankment. The construction can be completed with conventional construction equipment and the performance is quite satisfactory. Moreover, such construction is beneficial to the environment by recycling a waste material.

PREFACE

This dissertation is presented in the “paper-format” style. Chapters 2, 3, and 4 have been published in different journals as explained below. Chapter 2 of this thesis has been published as Meles, D., Bayat, A., and Soleymani, H. 2013, “Compression Behavior of Large-Sized Tire Derived Aggregate for Embankment Application,” *Journal of Material in Civil Engineering, ASCE*, 25(9), 1285-1290. I was responsible for the laboratory experiment and data analysis as well as manuscript composition. A. Bayat was the supervisory and corresponding author and designed the research program. He was also involved in manuscript composition and contributed to manuscript edits. H. Soleymani assisted in the manuscript edits and manuscript composition. Chapter 3 has been published as Meles, D., Bayat, A., and Chan, D. 2014, “One-Dimensional Compression Model for Tire Derived Aggregate using Large-Scale Testing Apparatus,” *International Journal of Geotechnical Engineering*, 8(2), 197-204. I was responsible for the laboratory experiment and data analysis as well as manuscript composition. A. Bayat was the supervisory and corresponding author and designed the research programme. He also assisted in manuscript edits and composition. D. Chan assisted in manuscript compositions and edits. Chapter 4 of this thesis has been published as Meles, D., Bayat, A., Shaffi, M., H., Nassiri, S., and Gul, M. 2014, “Investigation of Tire Derived Aggregate as a Fill Material for Highway Embankment,” *International Journal of Geotechnical Engineering*, 8(2), 182-190. I was responsible for the data collection and analysis as well as manuscript composition. A. Bayat was the supervisory and corresponding author, designed

the research programme and was involved in manuscript composition and assisted manuscript edits. H. M. Shaffi assisted data collection and data analysis. S. Nassiri assisted with data collection, data analysis and contributed to manuscript edits. Gul, M. assisted in manuscript edits.

Dedicated to my mother,

Yeshi Damessa

Dearest Mom,

*This is for you; thank you for being my motivation throughout my
life!*

ACKNOWLEDGEMENT

I would like to sincerely thank Dr. Alireza Bayat and Dr. Dave Chan for their commitment to the research undertaken and for providing valuable technical guidance. Dr. Bayat's patience, encouragement and friendly approach are greatly appreciated. I have also greatly benefited from Dr. Chan being part of the research. Thank you for all support.

Financial and material support provided by University of Alberta, Alberta Transportation, Alberta Recycling, the City of Edmonton and Canada Foundation for Innovation is greatly appreciated. I would like also to thank the technical support staffs in the Geotechnical and Structural Engineering sections, Mrs. Christine Hereygers, Mr. Greg Miller, Mr. Cameron West and Mr. Rizaldy Mariano for the technical support they provide me in the laboratory. You guys are great and your contribution to this research is very valuable.

I am deeply grateful to Mohammad Hussien Shafiee and Dr. Somayeh Nassiri for your help during instrumentation and data collection for the field experiment. Mohammad's support during sampling will not be forgotten. I would like also thank Dr. Yaolin Yi, Dr. Somayeh Nassiri, Mrs. Tejay Gardiner, and Ms. Lauren Wozny for their help on editorial review of this thesis.

I also thank my friends (too many to list here but you know who you are!) for providing support, encouragement, and friendship those I needed. I will always remember the generous support I got from Abrimo, Lease, Tsagech and Mesga during that extreme cold winter to transport samples from field for laboratory

testing. You guys are wonderful. I would like also to thank Samson Takela who has been my roommate during my study. Sami, your encouragement and the discussion we had together in all those years will have a special place in my life.

I am also very thankful for my friends I encountered during my study. Mohan, Renato, Hossien, and Ken, you guys are very great. I will never forget the many wonderful coffee time discussions and fun activities we have done together. Ken, I am also deeply grateful for your help and encouragement during my laboratory testing at Edmonton Waste Management Centre of Excellence. You are very special and a best model for a good friend.

Finally, and most importantly, are my special thanks to my family; my mother Yeshi Damessa, my brothers Hailsh and Tesfech, and my sisters Mulu and Asni. Your support, encouragement and love helped me overcome the most difficult obstacles.

Let all the glory be to God the Almighty.

TABLE OF CONTENTS

LIST OF TABLES.....	xiii
LIST OF FIGURES.....	xv
CHAPTER 1 INTRODUCTION.....	1
BACKGROUND.....	1
OVERVIEW OF TIRE RECYCLING IN ALBERTA.....	4
COMPOSITION OF SCRAP TIRE.....	5
SCRAP TIRE PRODUCTION.....	6
SIZE AND PARTICLE GRADATION.....	8
COMPACTED UNIT WEIGHT.....	8
COMPRESSIBILITY.....	9
ELASTIC MODULUS.....	12
POISSON’S RATIO.....	14
TIRE SHRED/SOIL MIX.....	15
CONSTRUCTION PRACTICE.....	15
WATER-QUALITY EFFECTS.....	18
FIRE HAZARDS.....	19
DURABILITY.....	21
RESEARCH OBJECTIVES.....	22
ORGANIZATION OF THESIS.....	23
PUBLICATIONS RELATED TO THIS RESEARCH.....	25
Journal papers.....	25
Conference and presentation.....	25
Report.....	26
REFERENCES.....	27
CHAPTER 2 COMPRESSION BEHAVIOUR OF LARGE-SIZED TIRE DERIVED AGGREGATE FOR EMBANKMENT APPLICATION.....	36
ABSTRACT.....	36
INTRODUCTION.....	36
CHARACTERIZATION OF TEST MATERIAL.....	39
Gradation, specific gravity and water absorption.....	41
APPARATUS AND TEST PROCEDURE.....	42
RESULTS AND DISCUSSION.....	45

One-dimensional compression	45
Loading-unloading tests	50
ONE-DIMENSIONAL STRESS-STRAIN MODEL	50
CONCLUSIONS	52
REFERENCES.....	53
CHAPTER 3 ONE-DIMENSIONAL COMPRESSION MODEL FOR TIRE DERIVED AGGREGATE USING LARGE-SCALE TESTING APPARATUS.....	58
ABSTRACT.....	58
INTRODUCTION.....	58
PREVIOUS STUDIES.....	60
Compacted unit weight.....	60
Compression behavior	62
EXPERIMENTAL PROGRAM.....	63
MATERIALS	64
APPARATUS AND TEST PROCEDURE	66
RESULT AND DISCUSSIONS	70
Compaction test.....	70
Compacted unit weight for the compression tests.....	72
Vertical compressibility	73
One-dimensional compression model.....	75
At-rest lateral earth pressure coefficient (K_0) and Poisson's ratio.....	78
CONCLUSIONS	79
REFERENCES.....	81
CHAPTER 4 INVESTIGATION OF TIRE DERIVED AGGREGATE AS A FILL MATERIAL FOR HIGHWAY EMBANKMENT.....	86
ABSTRACT.....	86
INTRODUCTION.....	86
RESEARCH OBJECTIVES AND APPROACH.....	88
PROJECT OVERVIEW	89
MATERIALS	89
Tire derived aggregate.....	89
Soil.....	91
EMBANKMENT DESIGN	92
TDA sections.....	92

TDA and soil mixture section.....	93
INSTRUMENTATION	93
CONSTRUCTION.....	95
Mixing TDA and soil in the field	95
Construction process	96
Observations during construction	98
ANALYSIS OF FIELD DATA	98
Settlement of the test embankment	99
Temperature change in the test embankment.....	104
FWD test results.....	105
CONCLUSIONS	108
REFERENCES.....	110
CHAPTER 5. PERFORMANCE OF HIGHWAY EMBANKMENT CONSTRUCTED FROM TIRE DERIVED AGGREGATE.....	114
ABSTRACT.....	114
INTRODUCTION.....	115
PURPOSE AND SCOPE.....	117
OVERVIEW OF THE TEST EMBANKMENT.....	118
IMMEDIATE SETTLEMENT DURING CONSTRUCTION.....	120
TIME-DEPENDENT SETTLEMENT	122
FALLING WEIGHT DEFLECTOMETER (FWD) TESTING.....	125
PRE-SCREENING OF DEFLECTION DATA	126
DEFLECTION DATA.....	127
BACKCALCULATION ANALYSIS OF MODULI	134
PRACTICAL APPLICATIONS.....	136
CONCLUSION	137
REFERENCES.....	139
CHAPTER 6 FINITE ELEMENT ANALYSIS OF HIGHWAY EMBANKMENT MADE FROM TIRE DERIVED AGGREGATE	144
ABSTRACT.....	144
INTRODUCTION.....	145
COMPRESSION MODEL FOR TDA.....	148
Materials	148
Testing apparatus.....	148

Constrained compression model.....	149
Derivation of nonlinear elastic stress-strain behavior for TDA.....	149
FIELD EXPERIMENT	151
Project layout and construction of the test embankment.....	151
NUMERICAL MODELING OF TEST EMBANKMENT	153
Finite Element Analysis using SIGMA/W	153
Material model for TDA.....	154
Material model other than TDA	156
FINITE ELEMENT ANALYSIS PROCEDURE	157
Comparisons of FE results with field observations.....	159
DESIGN CHARTS TO COMPUTE OVERBUILD IN TDA LAYER(S).....	162
CONCLUSION	166
REFERENCES.....	168
CHAPTER 7. SUMMARY, CONCLUSIONS AND RECOMMENDATIONS	172
GENERAL SUMMARY	172
COMPRESSION BEHAVIOR OF TDA	173
MATERIAL MODEL FOR TDA.....	175
DATA COLLECTED FROM INSTRUMENTED FULL SCALE FIELD	
EXPERIMENT	176
CONCLUSIONS	176
RECOMMENDATIONS FOR FUTURE WORK.....	180
REFERENCES.....	181

LIST OF TABLES

Chapter 1

Table 1.1: Typical composition of passenger and truck tire in North America (Pehlken and Essadiqi 2005).....	5
Table 1.2: Classification based on the size of shredded tire pieces (ASTM D 6270 2008).....	7
Table 1.3: Summery of various reported compression behavior of TDA in the literature.....	11
Table 1.4: Reported values for constrained modulus and calculated values of Young's modulus E using equation 2 (Edeskar 2004).....	13
Table 1.5: Summery of various reported case histories in literature for the use of TDA as fill material.....	17

Chapter 2

Table 2.1: Material description, specific gravity and water absorption.....	42
Table 2.2: Summary of stress-strain for PLTT and OTR of TDA with six cycles of loading-unloading.....	51

Chapter 3

Table 3.1: Previously reported compaction mold size and compacted density in the laboratory.....	61
Table 3.2: Physical properties of the TDA used in this study.....	66

Table 3.3: Unit weight of the sample used for the compression test.....73

Table 3.4: Elastic parameters for the TDA used in this study.....79

Chapter 5

Table 5.1: Average deflection in microns and deflection basin parameters at each deflection sensor.....133

Table 5.2: Backcalculated moduli from August 28, 2013 FWD data using the first six sensors nearest to the center of the loading plate.....136

LIST OF FIGURES

Page

Chapter 1

Figure 1.1. Major components of tire shredder: (a) shredding blade, (b) tire shredder sieve, (c) the whole tire shredder.....7

Chapter 2

Figure 2.1. Photograph of Shredded tires used in the study: (a) PLTT, (b) OTR..40

Figure 2.2. Particle- size distribution of TDA used in the study.....42

Figure 2.3. Photograph of compression apparatus at EWMCE for Testing TDA.43

Figure 2.4. Compression behaviour of TDA for different initial unit weight of samples: (a) OTR, (b) PLTT.....47

Figure 2.5. Stress versus void ratio of TDA for different initial unit weight of samples; (a) OTR (b) PLTT.....48

Figure 2.6. Stress-strain plot of TDA samples in this study and from Warith and Rao (2006).49

Figure 2.7. Comparison of compression of PLTT and OTR at initial void ratio = 1.15.....49

Figure 2.8. Vertical stress on natural logarithm scale vs. axial strain for TDA from OTR.....52

Chapter 3

Figure 3.1. Particle size distribution of TDA used for the compression test.....	65
Figure 3.2. Photograph of the small compaction test equipment.....	66
Figure 3.3. Photograph of the large compression test equipment.....	68
Figure 3.4. Comparison of test results in this study with Humphrey and Sandford (1993)	71
Figure 3.5. Vertical strain versus average vertical stress for: (a) Type A PLTT, (b) Type B PLTT and (c) Type B OTR tested in the 1230 mm diameter PVC pipe...	74
Figure 3.6. Typical plot of σ/ε versus σ from one dimensional compression test data for Type B PLTT.....	77
Figure 3.7. Comparison of laboratory compression curve and compression curve re-plotted from one-dimensional compression model for: (a) Type A PLTT, (b) Type B PLTT, and (c) Type B OTR.....	78
Figure 3.8. Typical plot of horizontal stress versus average vertical stress for Type B PLTT.....	79

Chapter 4

Figure 4.1. Pictures of PLTT (left) and OTR (right) used in the project.....	91
Figure 4.2. Grain size distribution of sand, PLTT and OTR used for the construction of the test embankment.....	92

Figure 4.3. Typical cross section and instrumentation for the test embankment (all units in meters)	95
Figure 4.4. Excavation for test embankment covered with geotextile at the bottom and on the side slopes.....	97
Figure 4.5. Settlement plate measurements for the: bottom layers of (a) PLTT and (b) OTR sections, and top layers of (c) PLTT and (d) OTR sections.....	102
Figure 4.6. Temperature measurement for PLTT, OTR and TDA mixed with soil sections in: (a) bottom layer, and (b) upper layer.....	105
Figure 4.7. Peak deflections beneath the center of the FWD loading plate for different load drops.....	108
Figure 4.8. Normalized deflection basin under the maximum applied load (12.4 kN) for the four sections.....	108
 Chapter 5	
Figure 5.1. Typical cross section and instrumentation for the test embankment (all units in meters).....	120
Figure 5.2. Time-dependent settlement for PLTT and OTR sections.....	124
Figure 5.3. Photo of transvers crack observed at the start of the PLTT section..	125
Figure 5.4. Deflection below: (a) center of loading plate, (b) the furthest deflection sensor	131

Figure 5.5. Deflection basin for FWD tests performed on August 28, 2013....132

Figure 5.6. Deflection basin parameters (DBPs) for FWD test performed on August 28, 2013.....132

Chapter 6

Figure 6.1. Variation of modulus as a function of vertical stress for PLTT and OTR151

Figure 6.2. Typical section, construction stage and location of Settlement Plates (SP) for the test embankment (all units in meters).....153

Figure 6.3. Settlement measured in the field and FE analysis results: (a) on top of bottom TDA layer in PLTT and OTR sections; (b) on top of upper TDA layer in PLTT and OTR sections; (c) on top of bottom TDA-soil layer in TDA- soil section.....161

Figure 6.4. Sample model used to develop the design chart for TDA thickness of 3 m.....163

Figure 6.5: Overbuild design chart: (a) Type B:\ PLTT; (b) Type B OTR; and (c) Type A PLTT.....166

CHAPTER 1 INTRODUCTION

BACKGROUND

Discarded tires have been a problem in different parts of the world. There are environmental concerns associated if not properly stored. Growth in population and the expansion of the transportation industries make safe disposal even challenging (Edeskar 2004). In the province Alberta, Canada, over five million tires are discarded each year (ARMA 2013). In the past, these tires have been used by the tire recycling industry to make various manufactured products, such as rubber crumb and tire derived aggregate (TDA) primarily used for landfill drainage application.

The primary use of TDA in Alberta, Canada, has been as leachate collection systems in rural landfills (ARMA 2013). As this market is becoming mature, it is necessary to look elsewhere for large volume consumption of recycled scrap tires. One application is to use them as fill material in geotechnical application. In civil engineering applications, usually recycled tires are used in a shred form referred to as “tire shred/Tire Derived Aggregate”. Tire shred and TDA are synonyms for most engineering application. Tire shreds are pieces of scrap tires that are generally between 50 and 300 mm in size, whereas TDA between 12 and 300 mm (ASTM D 6270-08). Tire derived aggregate has desirable properties for most civil engineering applications; it is lightweight, free-draining, and has good thermal resistivity. It has been used as fill material for embankments, retaining walls and

bridge abutments, as well as insulation to limit frost penetration. Additionally, it has also been used as a drainage layer for roads (Humphrey 2008).

Various successful TDA projects have been reported in the literature, including several studies conducted in the United States and Canada (Bosscher et al. 1992, Humphrey et al. 2000; Dickson et al. 2001, Tandon et al. 2007; Mills and McGinn 2010). Tire derived aggregate has also been mixed with soil to use as fill material for embankment (Zornberg et al. 2004; Yoon et al. 2006; Tandon et al. 2007). Despite the superior geotechnical characteristics and successful application in the past, use of TDA in Alberta was only limited for landfill drainage application.

Tire derived aggregate can be produced from different tire sources. In this thesis: PLTT refers to TDA made from passenger and light truck tire with a rim diameter up to 495 mm, and OTR refers to TDA made from off-the-road tire with a rim diameter up to 990 mm (ARMA 2013). PLTT was mostly used in the past for civil engineering applications (Strenk et al. 2007). This is primarily because of the availability of scrap PLTT and ease of production. However, in regions with heavy industrial and mining activities, such as Alberta, OTR tires have become a significant source for TDA production. The increase in the amount of discarded OTR tires and the tire recycling industry's growing capability to process all types of discarded tire have encouraged Alberta Recycling and Alberta Transportation to look for other potential engineering application of TDA from OTR. The major challenge for the use of TDA from other tires such as OTR is the lack of laboratory or field experience. Most of the laboratory and field studies in the past focused on PLTT (Humphrey and Manion 1992; Bosscher et al. 1997; Shalaby

and Khan 2005; Strenk et al. 2007; Warith and Rao 2006). The OTR differ from PLTT in particle size, shape, thickness, and amount of protruding wire from the cutting surface.

Tire derived aggregate is a highly compressible material whose deformation characteristics, rather than strength characteristics, govern its design and performance in most applications (Bosscher et al. 1997). The compression behaviour of TDA has been the subject of previous laboratory investigations; however, these investigations have been conducted primarily on TDA with one-third the size of TDA used for engineering applications. Very little information is available on the compression behavior of large-sized TDA on compacted sample, particularly regarding TDA with a maximum size of 300 mm. Moreover, the compression behaviour of TDA in the field is different from that in the laboratory. A case history to study the use of TDA as lightweight fill material for highway embankment on the north abutment of the Merrymeeting Bridge in Topsham, Main and an approach embankment fill for a bridge over the Main Turnpike in Portland, Main, U.S. also showed a discrepancy between the strains predicted based on the laboratory compression curve and the strains measured in the field following construction (Humphrey et al. 2000).

Various studies were reported in the past to develop material model for TDA (Gharegrat 1993; Bosscher et al. 1997; Lee et al. 1999; Heimdahl et al. 1999; Shalaby and Khan 2002; 2005; Youwai and Bergado 2003). In all these works except Shalaby and Khan (2002; 2005), TDA material behavior was modeled based on the laboratory test using tire chips or tire shreds with maximum particle

size smaller than the TDA size used in field applications. TDA used for the field application has maximum size in the range of 300 to 400 mm (ASTM 2008), and usually the larger sizes are elongated in shape and more flexible for bending. Strenk et al. (2007) has shown the sensitivity of TDA compression behavior (constrained modulus) with maximum TDA particle size. Considering the limitation of previous material model with respect to the size of TDA particle, it is proposed in this research to develop material model for TDA based on large-scale laboratory compression experiment on compacted samples. Variation in the size of TDA particles and the tire source for TDA production are taken as experiment variables. The research also provides various field data important to compare the characteristics and performance of PLTT, OTR and PLTT-mixed with soil as a fill material.

OVERVIEW OF TIRE RECYCLING IN ALBERTA

In Alberta, discarded tires are usually collected through site pick-ups, municipal tire collection sites or at landfills and shipped to registered scrap tire processors to produce shred or crumb forms. Almost all the scrap tires generated are collected through the province's tire recycling program managed by Alberta Recycling Management Authority. The program recycles more than 15 kilograms of tire per person annually, more than any other provincial tire program. Since the start of tire recycling in 1992, seventy-four million tires have been diverted from landfills (ARMA 2013).

The previous recycling programmes used discarded tires to make granulated rubber incorporated to asphalt binder for asphalt pavement, raw material for

playground cover, and make rubber roofing. Recently, shredded options and using for civil engineering applications are gaining popularity due to low processing fees, large volume consumption of discarded tires and the interesting engineering properties such as being lightweight, free-draining, and thermal resistive (several times higher than soil).

COMPOSITION OF SCRAP TIRE

Exact tire compositions are not known as the composition varies from one manufacturer to another. Knowing the compositions will be even more difficult in case of scrap tire as scrap tire contain waste tires produced by different manufacturer. Typical composition of passenger and truck tire in North America as reported by Pehlken and Essadiqi (2005) is presented in Table 1.1.

Table 1.1: Typical composition of passenger and truck tire in North America (Pehlken and Essadiqi 2005).

Composition	Passenger tire (% by weight)	Truck tire (% by weight)
Natural rubber	14	27
Synthetic rubber	27	14
Carbon black	28	28
Steel	14 - 15	14 - 15
Fibres, fillers, accelerators, etc.	16 - 17	16 - 17
Average total weight	New = 11 kg Scrap = 9 kg	New = 54 kg Scrap = 45 kg

SCRAP TIRE PRODUCTION

Scrap tires can be shredded into a variety of sizes ranging from large chunks to smaller chips. In Alberta, discarded tires are shredded into pieces using mechanical grinding. Using this method, whole tires can be reduced to finely ground rubber particles using a tire shredder. Scrap tires are shredded to a specific size to meet the requirements of their intended use. ASTM D 6270 (2008) has classified tire pieces into various categories that can be used for various applications as shown in table 1.2. For example, TDA with size 12–305 mm is generally used for various geotechnical applications. The sizes of the end products are controlled by the number of passes through the shredder (multiple passes for smaller shreds), and a classifier. The classifiers consist of sieves of specific size and the shredded material is passed through them; the material retained on the sieves is conveyed back to the shredder for further processing. Some shreds or chips may have pieces of steel belt exposed along the edges, which should be controlled during production. The amount of exposed steel may vary depending on how sharp the knives are. Figure 1.1 presents picture of major components parts of tire shredder during shredding operation using the mechanical method.



(a)



(b)



(c)

Figure 1.1: Major components of tire shredder: (a) shredding blade, (b) tire shredder sieve, (c) the whole tire shredder.

Table 1.2: Classification based on the size of shredded tire pieces (ASTM D 6270 2008).

Size (mm)	Classification
<0.425	Powdered rubber
0.425-2	Ground rubber
0.425-12	Granulated rubber
12-50	Tire chips
50-305	Tire shreds
12-305	Tire derived aggregate
>50 by 50 by 50 but less than 762 by 50 by 100	Rough shred

SIZE AND PARTICLE GRADATION

The parameters related to particle size and gradation that is of engineering interest include, maximum overall particle dimension, aspect ratio (i.e., ratio of particle length to width), distribution of particle sizes, and amount of exposed wire. The size of TDA particles have been expressed based on the gradation curve obtained using a sieve. It was also common practice to include the percentage of TDA particles comprising exposed metal. Tire shreds were reported to have uniformly gradation, and their maximum size, aspect ratio and amount of exposed wire varied according to the manufacturing process and intended applications (Humphrey 2008).

COMPACTED UNIT WEIGHT

TDA or tire chips have a maximum density that is approximately one-third to one-half typical soil (Humphrey 2008). The compacted unit weight of TDA has been investigated by Humphrey and Manion (1992), Ahmed (1993), Humphrey and Sandford (1993), and Moo-Young et al. (2003). The experimental observation in these studies showed that unlike soil, compacted unit weight of TDA was mainly affected by compaction method and compaction conditions, whereas compaction effort (beyond a certain level) and moisture content has little effect on compacted density. Vibratory method was also found to be ineffective in compacting tire shreds (Ahmed 1993). Geosyntec consultants (2008) has given a range of unit weight values based on the compaction method as: no compaction or, light compaction, laboratory compaction and field compaction. In cases of no or light compaction, unit weight ranges from 3.4 to 4.9 kN/m³. Whereas,

laboratory and field compaction methods result in unit weights of 5 to 6.9 kN/m³ and 6.1 to 9.1 kN/m³, respectively.

In previous research works the compacted unit weight in the laboratory have been investigated for TDA with maximum size up to 75 mm (Humphrey 2008), and dynamic method of compaction, similar to that defined in ASTM D 698 (2007) or D 1557 (2009) for soil was used to compact the sample in the laboratory (Humphrey and Sandford 1993; Moo-Young et al. 2003). However, unlike soil particles, individual TDA particles are compressible and will reduce the impact of the rammer load. Moreover, the laboratory method of compaction specified for soil in ASTM D 698 (2007) or D 1557 (2009) is not satisfied, as TDA for civil engineering applications retains more than 30% of TDA on a 19 mm sieve. Moreover, to study compacted unit weight of TDA in the laboratory for size of TDA particle greater than 75 mm is tedious and impractical using method of compaction reported in the literature.

COMPRESSIBILITY

Bosscher et al. (1997) described TDA as a highly compressible material whose deformation characteristics, rather than strength characteristics, govern its design and performance in most applications. The compression behaviour of TDA also highly affects the design and performance of the structure constructed from TDA. Knowing compressibility will help to determine: settlement that will occur during construction and after fill is placed, in-place unit weight of compressed tire shred and settlement or deflection caused by temporary load after construction is complete. The compression behavior of TDA has been the subject of previous

laboratory studies. Early contributions on compression behavior of TDA from previous studies have been summarized in Table 1.3. As presented in Table 1.3, all the reported data indicated the high compressible nature of TDA, and showed similar trend in the test data. However, the derived compression behavior often showed significant variation. Strenk et al. (2007) studied variability on several engineering properties of TDA based on comprehensive literature survey of experimental program. He indicated that the cause for variation in derived engineering properties of TDA including compression behavior among reported test results could be from difference in tire sources/suppliers, tire types, particle size, manufacturing (shredding) process and the non-standardized and/or modified laboratory testing methods and equipment used in the experimental program. Moreover, because conventional soil testing equipment is defined for specimens having a limited particle size, most studies were performed on granulated rubber or tire chips, whereas much larger tire shreds are used in most field applications. Wartman et al. (2007) also found that the compressibility of TDA depends on size of TDA particle and applied stress (Wartman et al. 2007).

Besides the immediate compression, TDA also shows time-dependent compression. Time-dependent compression is largely a function of TDA content and time (Wartman et al. 2007). Various studies suggest that the majority of the creep settlements occur within two months (Tweedie et al. 1998; Drescher et al. 1999). In practice, time-dependent compression is sometimes addressed by allowing some time to elapse after TDA placement and before placement of settlement-sensitive components.

Table 1.3: Summary of various reported compression behavior of TDA in the literature

Maximum TDA size (mm)	Compressibility (%)	Specific test Conditions (Stress in kPa)	Size of compression Mold	Reference
50	33-37	200 (compacted)	Diameter=254mm and Height=247mm	Humphrey et al., 1992; ASTM, 2008
50	52	200 (loose)		
25	45	200 (loose)		
75	38-41	200 (compacted)	Diameter=305 mm and Height=318 mm	Manion and Humphrey, 1992; ASTM, 2008
50	40-43	460 (compacted)		
75	36	690 (compacted)	152 mm diameter compaction mold	Edil and Bosscher, 1992
38	47	200 (Lose)	Diameter=305mm and Height=317.5mm	Ahmed and Lovell, 1993
	27	200 (compacted)		
30	25	5	Diameter=209mm and Height=330mm	Newcomb and Drescher, 1994
	40	409		
4.75 - 38	27-32	55	Triaxial Machine	Benda, 1995
76	18.-28	25		Nickels and Humphrey, 1997; ASTM, 2008
38	27	55 (compacted)	Triaxial Machine having Diameter= 100 mm and Height= 200 mm	Wu et al., 1997
19	26.5			
9.5	31.6 - 25.4			
2	27			
12 - 139	31			
12 - 139	31	32	Diameter=360mm and Height=300mm	Reddy and Saichek, 1998
12 - 139	50	163		
12 - 139	65	1005		
50 max	36.5	600 (after 20 cyclic loading, and initially from loss state)	Diameter=900mm and Height=1000mm	Shalaby and Khan, 2002
150 max	38.5			
300 max	41			
< 50	25	110 (compacted)	610 by 610mm	Moo-Young, 2003
50-100	35			
100-200	48			
200-300	50			

ELASTIC MODULUS

The elastic modulus is an important parameter to characterize stress-strain relation. The elastic modulus of tire rubber ranges from 1.2 MPa to 5.1 MPa (Beatty 1981). Tire derived aggregate and tire chips have smaller elastic modulus because they are made from pieces of rubber. Early studies characterize the elastic modulus for tire chips determined through a triaxial test and or by measuring vertical compressibility.

Benda (1995) and Wu et al. (1997) determined elastic modulus using triaxial apparatus. Elastic modulus varying from 344 kPa to 820 kPa in the study by Benda (1995), and 450 kPa to 820 kPa in the study by Wu et al. (1997) were reported. Benda (1995) used a confining stress varying from 34 kPa to 55 kPa, and Wu et al. (1997) used an extension test with constant $\sigma_1 = 55$ kPa.

Yang et al. (2002) performed a triaxial test on tire chips with size varying from 2 to 10 mm and determined the initial modulus. Using the result from their study and data reported by Ahmed (1993), Benda (1995), Masad et al. (1996) and Lee et al. (1999), Yang et al. (2002) observed the variation of elastic modulus with confining pressure. They found that the initial tangent modulus increases with confining pressure σ_3 as shown by equation 1.

$$E = 13.2\sigma_3 - 0.0191\sigma_3^2 \quad 1$$

Where E (kPa)= elastic modulus; and σ_3 = confining pressure (kPa)

Humphrey and Sandford (1993) determined the elastic modulus from constrained modulus (M_c) using equation 2 (Lambe and Whitman 1979). Results of Young's

modulus evaluated from the constrained modulus and Poisson's ratio for different tire shreds, at 110 kPa, are presented in Table 1.4 (Edeskar 2004).

$$E = \frac{(1+\nu)(1-2\nu)M_c}{(1-\nu)} \quad 2$$

Where M_c = constrained modulus; ν = Poisson's ratio; and E = elastic modulus.

Table 1.4: Reported values for constrained modulus and calculated values of Young's modulus E using equation 2 (Edeskar 2004).

Maximum size (mm)	Constrained modulus (M_c) [kPa]	Elastic modulus(E) [kPa]	Remark
38	1270	770	At surcharge load of 110 kPa
51	1680	1120	
51	1470	1250	
76	1730	1130	

Heimdahl and Drescher (1999) observed anisotropy of elastic modulus for large-sized tire shreds. They found that large-sized tire shreds, placed randomly in a fill, tend to arrange themselves because of compaction or high gravity loads and align predominantly in the horizontal plane resulting in a layered structure, whose in-plane properties are expected to differ from the out-of-plane properties. They concluded that the in-plane Young's modulus was about three times greater than the out-of-plane Young's modulus, and the settlement obtained from the anisotropy assumption was smaller than the isotropic assumption.

Shalaby and Khan (2002) developed nonlinear resilient response of three-sized tire shreds obtained from large-scale constrained compression test. They found that the stress-strain response of the tire shreds obtained from laboratory testing was dependent on stress levels showing resilient modulus of the tire shreds increase with increase in bulk density. However, the method has limitations: the

laboratory compression test was conducted on a rigid steel cylinder; vertical stress was only measured at the top of the sample, for such large-scale testing apparatus friction on the side is very significant and highly affect the accuracy of the result; and tire shreds were placed in loose state in the cylinder of height 900 mm and the sample was compacted once the tire shreds placed in the cylinder.

POISSON'S RATIO

Tire rubber has a large Poisson's ratio (μ), a value of 0.5 was reported by Beatty (1981); however, as tire rubber is broken down to produce TDA, the value of Poisson's ratio for TDA is smaller. Most of the reported values of Poisson's ratio in the literature were determined either by measuring the vertical and horizontal stresses under the vertical load and computing Poisson's ratio from theoretical equations (equation 5 and 6) or by strain measurements in triaxial cells under axial compression conditions. ASTM D 6270 (2008) recommends using the results from confined compression tests and calculating Poisson's ratio using equation 3 and 4. Humphrey and Sandford (1993) conducted laboratory experiment as recommended by ASTM D 6270 (2008) to determine K_o and μ using equations (3-4). They reported values of μ that varies from 0.2 to 0.32 as a function of TDA tire sources and maximum size.

$$K_o = \frac{\sigma_h}{\sigma_v} \quad 3$$

$$\mu = \frac{K_o}{(1+K_o)} \quad 4$$

Where K_o = at-rest lateral earth pressure coefficient, μ =Poisson's ratio, σ_h = horizontal stress and σ_v = vertical stress

TIRE SHRED/SOIL MIX

The engineering properties of tire shred/soil mix have been studied by different researcher both in the laboratory, and in the field using test embankment, and from performance of full scale civil engineering projects (Ahmed 1993; Masda et al. 1994; Edil and Bosscher 1994 and Yoon et al. 2005). Most of the previous studies showed that, compared to use of TDA alone, a soil/TDA mixture has higher unit weight, lower compressibility, lower hydraulic conductivity and lower combustion potential. However as the percentages of the soil in the mix increased, the unit weight and lateral earth pressures acting against retaining structures will be higher and the drainage capacity of the fill mixture will likely be reduced. Besides TDA-soil mixture may lead to additional construction costs, difficulty in mixing and formation of sink holes after construction especially when the amount of soil used in the mix is small.

CONSTRUCTION PRACTICE

Various studies were reported in the past to observe construction and performance of TDA in the field for embankment application (Bosscher et al. 1992; Humphrey et al. 200; Dickson et al., 2001; Zornberg et al., 2004; Yoon et al., 2005; Tandon et al., 2007; Mills and McGinn, 2010). Method of field compaction and reported values on unit weight and strain at the end of construction are summarized in Table 1.5.

Important findings from these studies:

- Placement and compaction of tire shreds could be performed with conventional construction equipment.

- Sufficient soil cover is required to decrease the compressibility. The higher the depth of the soil cover the better the performance.
- Void ratio of the tire chips affects the stiffness.
- TDA is an economical alternative for light weight fill applications.
- The design specification given in ASTM D 6270-08 for limiting internal heating was successful.
- Mixing tire shreds with soil gave better results with respect to compression and for controlling internal heating.
- The compression behaviour of TDA in the field is different from that in the laboratory compression

Table 1.5: Summary of various reported case histories in literature for the use of TDA as fill material

Name of the project and TDA fill height	Unit weight (kN/m ³)	Comments on unit weight and TDA type	Field compaction method	Strain for fill placement	Reference	
Highway embankment in Southwest Oregon (TDA layer up to 3.6 m thick)	7.2	Compacted unit weight for 610 mm maximum size	0.9 m lift and three pass of D8 bulldozer (one pass was back and forth in longitudinal and transverse direction)	15% compression under soil and pavement surcharge	Upton and Machan, 1993	
	8.3	In place unit weight for 610 mm maximum size				
Portland Jetport (two layers of TDA each layer 3 m thick)	7.7	In place unit weight for Type B	0.3m lift and six pass of a vibratory roller with minimum 9.1 metric tons	Measured strain was 9.9% for the upper layer and 15.6% for the lower layer	Humphery et al., 2000	
North Abutment TDA fill (TDA layer up to 4.3 m thick)	8.8	In place unit weight for a combination of Type B and Type A	0.3m lift thickness and six passes of a smooth drum vibratory roller with a static weight of 9.4 metric tons	Measured strain was 9%		
Test pad (TDA layer 0.3 m thick)	6.6	Field compaction for 152 mm maximum size	six pass of sheepsfoot roller weighing 6.7 tons	NA	Zornberg et al., 2000	
Binghamton project (TDA layer up to 3 m thick)	6	Final in place unit weight after fill placement	Spreading and compaction of tire shred was made using front-end loader and steel drum roller respectively	Compressed about 9%	Dickson et al., 2001	
North Yarmouth, Maine (TDA layer up to 0.6 m thick)	6.1	Field compaction for 300-mm maximum size	NA	NA	Humphrey, 2008	
Guidance Manual for engineering use of Scrap Tires	5 to 6.9	Lab compacted densities		NA	NA	Geosyntec consult, 2008
	6.4 to 7.5	Field compacted densities				
St. Stephen reconstruction project (two layers of TDA with bottom and top layer 2.3 and 3 m thick respectively)	8.1	compressed in place unit weight for type B	0.4 m (loose) lift and a minimum of six passes with vibratory smooth-drum roller with a minimum static weight of 9 tons	Bott. TDA layer=12% and Top TDA layer=5.3%	Mills and McGinn 2010	

WATER-QUALITY EFFECTS

Various studies were reported in the past to address environmental concerns on water-quality effect of using TDA for civil engineering applications (e.g. Bosscher et al. 1992; Humphrey 1999; Humphrey and Katz 2000; Humphrey and Swett 2006). Humphrey and Swett (2006) provided detailed evaluation on the water-quality effect of TDA based on reported field studies. The potential of TDA to generate leachate has been examined for cases with TDA placed both above and below ground water table. For both cases where TDA used above and below water table applications, the statistical field data reported in the study by Humphrey and Swett (2006) indicated that TDA would not cause primary drinking water standards to be exceeded. Moreover, TDA was unlikely to increase the levels of metals with primary drinking water standards above naturally occurring background levels. Dissolved iron and manganese with a secondary drinking standard, it was likely that water in direct contact with TDA, either in above or below the ground water table applications, would have elevated concentration likely to be exceeded the secondary drinking water standards. Moreover, the concentration of iron and manganese was higher for below groundwater applications. For water in direct contact with TDA placed below the groundwater table, it was likely that the concentration of zinc would be increased, but with levels below the applicable secondary drinking water standards. There was no evidence for other chemicals with secondary drinking water standards that TDA affects naturally occurring background levels. Other important observation in the study by Humphrey and Swett (2006) was for five out six field sites with monitoring well adjacent to TDA fills; it was found that flow through soil for a

distance of 0.6 to 3 m was generally adequate to attenuate the concentration of iron, manganese, and zinc to near naturally occurring background levels. As there was sufficient studies in the literature that support the water quality effects of TDA have no health related concern, no further study was conducted in this research.

FIRE HAZARDS

Different case histories had shown that thick tire shreds or pile of tire experience a serious self-heating reaction and fire hazard (Eyles et al 1990; Winnipeg Sun 2001; Humphrey 2004). Tire fires pollute the air with large quantities of smoke, hydrocarbons and residue, and are difficult to extinguish. Also, the oils created by the breakdown of heated tires spread into the soil and pollute ground water. In addition to environmental damage, clean-up after a tire fire is very expensive. Humphrey (2004) discussed three case histories located in Ilwaco, Washington, Garfield County, Washington, and Glenwood Canyon, Colorado that experienced serious heat within six months after construction in 1995. Humphrey (2004) also stated that a survey of tire processors conducted in 1996 showed that 15% of the tire processors, who stockpiled products ranging from crumb-rubber to 75 mm in size, had experienced internal heating. There was also some waste tire fire hazards reported in Canada: the Hagersville tire fire in Ontario occurred in a storage yard (Eyles et al. 1990), and the Rosser tire fire in Manitoba on a private access road (Winnipeg Sun, 2001).

The cause of fires in shredded tire stockpiles is not well understood. However, several researchers have studied the issue and have identified the following

potential heat sources that may lead to combustion (Humphrey, 2004; ASTM D 6270, 2008): chemical or microbial oxidation of exposed metal wires, chemical or microbial oxidation of the tires, and microbes consuming liquid petroleum products. Further, factors thought to create conditions favorable for oxidation of exposed steel or rubber include: free access to air, free access to water, retention of heat caused by the high insulation value of TDA in combination with a large fill size and excessive amounts of granulated rubber particles and the presence of inorganic and organic nutrients that would enhance microbial action (ASTM D 6270, 2008).

To limit the possibility of internal heating, a design guideline (ASTM D 6270, 2008) was prepared for the use of TDA material for engineering applications. The design guideline sets out procedures to reduce the potential for internal heating, the spread, burn time and environmental impact of a shredded tire fire. The guidelines focuses primarily on limiting maximum thickness of TDA layer, enclosure of TDA fill, and TDA particle size gradation and material requirement. The design guidelines in ASTM D 6270 (2008) however is less stringent for projects with thinner TDA layers. For example TDA used as Class I (fill with TDA layer less than 1-m thick) require no special enclosure design compared to Class II (fill with TDA layers in the range of 1 to 3 m). Detail on enclosure requirement for Class II fill TDA, material requirement for Class I and Class II TDA fill, and TDA particle size distribution: Type A for Class I and Type B for Class II are given on ASTM D 6270 (2008). So far, no internal heating in TDA fill is reported from engineering projects designed in accordance with ASTM D

6270 (2008), and observations of existing projects do not show internal heating. But it has been a common practice to monitor the potential for internal heating when TDA is used in bulk amount.

DURABILITY

Chu (1998) tested the degradation of tire shred by exposing the tire shred to varying climatic conditions for 18 months, and measured the degradation by comparing particle size distribution before and after. He found that the particle size was the same before and after it was exposed to climatic change, concluding that the tire shred was not degradable for the exposed time frame and climatic variation. Other long-term durability tests reported include AB-Malek and Svensson (1986), who studied the physical condition of vulcanised natural rubber submerged in 24 m of sea water for a period of 42 years. The pH-value and amount of dissolved oxygen at the location of the storage place was 7.8 and 8.77 mg/l respectively. The conditions could be described as slightly alkaline and oxidising. They found that no serious deterioration occurred, and the maximum amount of water absorbed after 42 years of submersion was 4.7%. Leclerq et al. (1990) also concluded that the surrounding environment below the ground surface was favourable for geosynthetics, in terms of degradation, because the temperature below ground is low, the materials are protected from UV- radiation and the pH in groundwater is not extreme. The previous studies showed that except for the corrosion of the protruding steel, tire shreds have high durability.

RESEARCH OBJECTIVES

The primary objective of this research was to study the engineering properties of TDA using large-scale laboratory experiment, and evaluate the performance of TDA or TDA-mixed with soil as highway embankment fill material using an instrumented full-scale field experiment. In addition to PLTT, the research present the engineering properties and field performance of TDA solely made from OTR for the first time.

The specific objective of the research includes:

- Characterizing the compression behavior of TDA considering size of TDA and source of tire for TDA production as experimental variable through various large-scale testing apparatus.
- Suggest method to prepare compacted samples for large-scale compression test.
- Present a functional relation between stress and strain for Type A PLTT, Type B PLTT, and Type B OTR.
- Present a functional relation for constrained modulus as a function of vertical stress for Type A PLTT, Type B PLTT, and Type B OTR for the first time.
- Investigate and compare data collected during and after construction of an instrumented test embankment that contained four sections made from PLTT, OTR, TDA-mixed with soil and soil without TDA with respect to ease of construction, field mixing of TDA and soil, immediate compression, and susceptibility to internal heating and stiffness.

- Validate the developed material model based on large-scale laboratory compression test for Type B PLTT and Type B OTR numerically using the settlement data measured in the field.
- Compare performance of PLTT, OTR, TDA-mixed with soil and control section made from soil without TDA from visual assessment and field data collected for one year after placement of asphalt layer.

ORGANIZATION OF THESIS

This thesis is presented in the “paper-format” style. Each chapter of the thesis presents separate but related studies. Chapters 2, 3, and 4 have been published and Chapters 5 and 6 have been submitted in peer-reviewed journals. Details of experimental testing programs, analysis, discussion and conclusions for each of the major components of this research are provided in the following chapters. Though not included in the thesis, additional four articles have been published in reviewed conferences from the research.

Chapter 2 presents compression behavior of TDA produced from PLTT and OTR with size up to 125 mm from laboratory tests. Compression tests were conducted under constrained condition for samples prepared at different unit weight for both PLTT and OTR with major focus to determine compression behavior of OTR for the first time. In this chapter, the compression test results for both PLTT and OTR are analyzed, effect of initial unit weight on compression behaviour is investigated and compression tests result for PLTT are compared with previously reported laboratory compression tests with similar experimental set up. Moreover,

results obtained in this chapter lay the base for the experimental set up and material model developed for TDA in later chapters.

Chapter 3 presents large-scale laboratory compression tests conducted on TDA with size up to 300 mm. TDA properties, including compression behavior, the coefficient of lateral earth pressure at rest, and Poisson's ratio, are provided, while variation in the gradation of TDA particles and the tire type for TDA production were experiment variables. This chapter also proposes a method to prepare compacted TDA samples for large-scale laboratory testing.

Chapter 4 presents the various data collected during and after construction of a test embankment that contained four sections (PLTT, OTR, TDA-mixed with soil and control sections). The data collected from the field experiment among the four sections are also compared, including the ease of construction, field mixing of TDA and soil, vertical settlement, potential for internal heating and deflection under Falling Weight Deflectometer (FWD) testing.

Chapter 5 evaluate performance of TDA and TDA-mixed with soil using the data collected from field monitoring, and in-situ field test conducted during and for one year after completion of test embankment described in chapter 4.

Chapter 6 proposes material model for TDA produced from PLTT and OTR. This chapter also include detail numerical analyses to predict the settlement measured during construction of the test embankment provided in chapter 5 and verify the developed material model. Moreover, design charts to compute overbuild on the top elevation of TDA layer(s) to compensate for immediate compression under an applied load during construction are provided.

The last chapter, Chapter 7, summarizes the results from this study. It also provides recommendations for future research.

PUBLICATIONS RELATED TO THIS RESEARCH

Journal papers and conference papers were published from the results of this research work. The following are summary of publications from this research work:

Journal papers

1. Meles, D., Bayat, A., and Soleymani, H. 2013. Compression behavior of large-sized Tire Derived Aggregate for embankment application. *Journal of Material in Civil Engineering*, ASCE, 25(9), 1285-1290.
2. Meles, D., Bayat, A, Shaffi, M., H., Nassiri, S., and Gul, M. 2014a. Investigation of Tire Derived Aggregate as a Fill Material for Highway Embankment. *International journal of geotechnical engineering*, 8(2), 182-190.
3. Meles, D., Bayat, A, and Chan, D. 2014b. One-dimensional compression model for tire derived aggregate using large-scale testing apparatus. *International journal of geotechnical engineering*, 8(2), 197-204.

Conference and presentation

1. Meles, D., Bayat, A and Skirrow, R. 2013. Field & Laboratory Characterization of Tire Derived Aggregate in Alberta: 2013 Transportation Association of Canada (TAC) Conference and Exhibition, Winnipeg, Manitoba

2. Meles, D., Bayat, A., Nassiri, S., and Skirrow, R. 2013. Performance and Time-Dependent Compression Behavior of Highway Fill Material Constructed Using Tire-Derived Aggregate: GeoMontreal 2013, Canadian Geotechnical Society
3. Meles, D., Bayat, A., and Chan, D. 2013. Compression Behavior of Compacted Tire-Derived Aggregate Using a Static Compaction Method: Transportation Research Board, 92 Annual meeting January 13-17, Washington, D.C., Session 622, Performance measure for Constructed Embankment
4. Meles, D., Bayat, A., Shafiee, M.H., Nassiri, S., and Gul, M. 2013. Field Study on Construction of Highway Embankment Made from Two Tire-Derived Aggregate Types and Tire-Derived Aggregate Mixed with Soil as Fill Materials: Transportation Research Board, 92 Annual meeting January 13-17, Washington, D.C., Session 622, Performance measure for Constructed Embankment

Report

1. Melese, D., Yi, Y., Nassiri, S., and Bayat, A. 2013. Evaluation of application of tire-derived aggregate for highway embankment. Final Research Report, Alberta Recycling, Edmonton.

REFERENCES

- AB-Malek, K., and Stevansson, A. 1986. The effects of 42 years immersion in sea water on natural rubber. *Journal of Materials Science*, 21, 147-154.
- Ahmed, I. 1993. Laboratory study on properties of rubber soils. Rep.No. FHWA/IN/JHRP-93/4, Dept. of Civil Engineering, Purdue Univ., West Lafayette, Ind.
- Ahmed, I., and Lovell, C. W. 1993. Rubber soils as lightweight geomaterial. *Transportation Research Record*, 1422, National Research Council, Transportation Research Board, Washington, D.C., 61–70.
- Alberta Recycling Management Authority. 2013. Tire recycling program. Edmonton, AB. [online] Available: <<http://www.albertarecycling.ca/>>. [Accessed on June 1, 2013].
- ASTM. 2008. Standard practice for use of scrap tires in civil engineering applications. ASTM D 6270-08, ASTM International, West Conshohocken, PA.
- ASTM. 2009. Standard test methods for laboratory compaction characteristics of soil using modified effort. ASTM D 1557-09, ASTM international, West Conshohocken, PA.
- ASTM. 2007. Standard test methods for laboratory compaction characteristics of soil using standard effort. ASTM D 698-07, ASTM International, West Conshohocken, PA.
- Benda, C.C. 1995. Engineering properties of scrap tires used in geotechnical applications. Report 95-1, Materials and Research Division, Vermont agency of transportation, Montpelier, VT.

- Beaty, J.R. 1981. Physical properties of rubber compounds. Chapter 10 of mechanics of pneumatic tires, Clark, S.K. ed., United States Department of Transportation, Highway Traffic Safety Administration, Washington, D.C.
- Bosscher, P. J., Edil, T. B. and Eldin, N. N. 1992. Construction and performance of a shredded waste tire test embankment. Transportation Research Record 1345, National Research Council, Transportation Research Board, Washington, D.C., 44–52.
- Bosscher, P. J., Edil, T. B., and Kuraoka, S. 1997. Design of highway embankments using tire chips. Journal of Geotechnical and Geoenvironmental Engineering, 123(4), 295–304.
- Chu, C-J. 1998. A geotechnical investigation of the potential use of shredded scrap tires in soil stabilization. Ph.D. Dissertation, Kent State University, Kent, Ohio.
- Dickson, T.H., Dwyer D.F., and Humphrey D.N. 2001. Prototype tire-shred embankment construction. Transportation Research Record 1755, National Research Council, Transportation Research Board, Washington, D.C., 160-167.
- Drescher, A., and Newcomb, D.E. 1994. Development of design guidelines for use of shredded tires as a lightweight fill in road subgrade and retaining walls. Report No. MN/RC-94/04, Department of Civil and Mineral Engineering, University of Minnesota, Minneapolis, MN, 1994.

- Drescher, A., Newcomb, D, and Heimdahl, T. 1999. Deformability of shredded tires. Minnesota Department of Transportation, MN/RC -1999-13.
- Edeskar, T. 2004. Technical and environmental properties of tire shreds focusing on ground engineering applications. SE-971 87 Lulea, Department of Civil and Mining Engineering, Lulea University, Lulea, Sweden.
- Edil, T. B., and Bosscher, P. J. 1992. Development of engineering criteria for shredded or whole tires in highway applications. Report No. WI 14-92, Department of Civil and Environmental Engineering, University of Wisconsin, Madison, Wisconsin.
- Edil, T. B., and Bosscher, P. J. 1994. Engineering properties of tire chips and soil mixtures. *Geotechnical Testing Journal*, Vol. 17, No. 4, pp. 453-464.
- Eyles, J., Sider, D., Baxter, J., Taylor, S. M., and Willms, D. 1990. The impacts and effects of the Hagersville tire fire: Preliminary analysis and findings. In *Environment Ontario (Ed.), The challenge of a new decade (Vol. 2, pp. 818-829)*. Toronto: Environment Ontario.
- Geosyntec consultants 2008. Guidance manual-for engineering use of Scrap Tires. Prepared for Maryland Department of the Environmental Scrap Tire Program, Geosyntec project No: ME0012, Maryland, USA.
- Gharegrat, H. 1993. Finite element analyses of pavements underlain by a tire chip layer and of retaining walls with tire chip backfill. MSCE thesis, University of Maine, Orono, ME.
- Heimdahl, T. C., and Drescher, A. 1999. Elastic anisotropy of tire shreds. *Journal of Geotechnical and Geoenvironmental Engineering*, 125(5), 383-389.

- Humphrey, D.N. 1999. Water quality results for Whitter farm road tire shred field trial. Department of Civil and Environmental Engineering, University of Maine, Orono, ME.
- Humphrey, D. N. 2008. Tire derived aggregates as lightweight fill for embankments and retaining wall. International Workshop on Scrap Tire Derived Geomaterials– Opportunities and Challenges, Yokosuka, Japan, 59-81.
- Humphrey, D.N., and Katz, L.E. 2000. Five-year field study of the effect of tire shreds placed above the water table on groundwater quality. Transportation Research Record 1714, National Research Council, Transportation Research Board, Washington, DC, 18-24.
- Humphrey, D. N., and Manion, W. P. 1992. Properties of tire chips for lightweight fill. Proceeding: Grouting, Soil Improvement, and Geosynthetics, ASCE, New York, 1344–1355.
- Humphrey, D. N. and Sandford, T.C. 1993. Tire chips as lightweight subgrade fill and retaining wall backfill. Symposium on Recovery and Effective Reuse of Discarded Material and By-Products for Construction of Highway Facilities, Federal Highway Administration, Washington, DC.
- Humphrey, D. N., Sandford, T. C., Cribbs, M. M., and Manion, W. P. 1993. Shear strength and compressibility of tire chips for use as retaining wall backfill. Transportation Research Record 1422, National Research Council, Transportation Research Board, Washington, D.C., 29–35.

- Humphrey, D.N., and Swett, M. 2006. Literature review of the water quality effects of tire derived aggregate and rubber modified asphalt pavement. Department of Civil and Environmental Engineering, University of Maine, Orono, ME, for U.S. Environmental Protection Agency Resource Conservation Challenge, November 29, 2006.
- Humphrey, D. N., Whetten, N., Weaver, J., and Recker, K. 2000. Tire shreds as lightweight fill for construction on weak marine clay. Proceeding International Symposium on Coastal Geotechnical Engineering in Practice, Balkema, Rotterdam, The Netherlands, 611–616.
- Manion, W. P., and Humphrey, D. N. 1992. Use of tire chips as light weight and conventional embankment fill, Phase I-laboratory. Technical paper 91-1, Technical Services Division, Maine department of transportation, Maine.
- Lamb, T.W. and Whitman, R.V. 1969. Soil Mechanics. John Wiley & Sons, New York.
- Lee, J. H., Salgado, R., Bernal, A. and Lovell, C. W. 1999. Shredded tires and rubber-sand as lightweight backfill. Journal of Geotechnical and Geoenvironmental Engineering, 125(2), 132-141.
- Leclerq, B., Schaeffner, M., Delmas, P., Blivet, J. C., and Matichard, Y. 1990. Durability of geotextiles: Pragmatic approach used in France. Geotextiles, Geomembranes and Related Products, Ed. Hoedt, D., Balkema, Rotterdam, 679-684.

- Masad, E., Taha, R., Ho, C., and Papagiannakis, T. 1996. Engineering properties of tire/soil mixtures as lightweight fill material. *Geotechnical Testing Journal*, 193, 297–304.
- Mills, B and McGinn, J. 2010. Design, construction, and performance of highway embankment failure repair with Tire-derived Aggregate. *Transportation Research Record 2170*, National Research Council, Transportation Research Board, Washington, D.C., 90-99.
- Moo-Young, Sellasie, K., Zeroka, D., and Sabnis, G. 2003. Physical and chemical properties of recycled tire shreds for use in construction, *Journal of Environmental Engineering*, 129(10), 921-929.
- Newcomb, D. E. and Drescher, A. 1994. Engineering properties of shredded tires in lightweight fill applications. *Transportation Research Record 1437*, National Research Council, Transportation Research Board, Washington, D.C., 1-7.
- Nickels, W.L. 1995. The effect of tire shreds as subgrade fill on paved roads. M.S. Thesis, Department of Civil Engineering, University of Maine, Orono, Maine, 215.
- Pehlken, A., and Essadiqi, E. 2005. Scrap tire recycling in Canada. CANMET material technology laboratory, MTL 2005-08 (CF).
- Reddy, K, R. and Saichek, R. E. 1998. Assessment of damage to geomembrane liners by shredded scrap tires. *Geotechnical Testing Journal*, 21 (4), 307-316.

- Shalaby, A. and Khan, R.A. 2002. Temperature monitoring and compressibility measurement of a tire shred embankment: Winnipeg, Manitoba, Canada. Transportation Research Record 1808, National Research Council, Transportation Research Board, Washington, D.C., 67-75.
- Shalaby, A., and Khan, R.A. 2005. Design of unsurfaced roads constructed with large-size shredded rubber tires: a case study. Resource Conservation and Recycling Journal, Elsevier B.V., Vol. 44, 318-332.
- Strenk, P.M., Wartman, J., Grubb, D.G., Humphrey, D. N. and Natale, M. F., 2007. Variability and scale-dependency of tire derived aggregate. Journal of Material in Civil Engineering, ASCE, 19(3), 233-241.
- Tandon, V., Velazco, D.A., Nazarian, S. and Picornell, M. 2007. Performance monitoring of embankment containing tire chips: case study. Journal of Performance of Construction Facilities, ASCE, 21(3), 207-214.
- Tweedie, J.J., Humphrey, D.N., and Sandford, T.C. 1998. Full scale field trials of tire shreds as lightweight retaining wall backfill, at-rest condition. Transportation Research Record 1619, National Research Council, Transportation Research Board, Washington, D.C., 64-71.
- Upton, R.J., and Machan, G. 1993. Use of shredded tires for lightweight fill. Transportation Research Record 1422, National Research Council, Transportation Research Board, Washington, D.C., 36-45.
- Warith, M.A., Sundhakar, M.R. 2006. Predicting the compressibility behavior of tire shred samples for landfill applications. Journal of Waste Management, 26 (3), 268-277.

- Wu, W., Benda, C., and Cauley, R. 1997. Triaxial determination of shear strength of tire chips. *Journal of Geotechnical and Geoenvironmental Engineering*, ASCE, 123 (5), 479-482.
- Wartman, J., Natale, M.F., and Strenk, P.M. 2007. Immediate and time-dependent compression of tire derived aggregate. *Journal of Geotechnical and Geoenvironmental Engineering*, ASCE, 133 (3), 245-256.
- Winnipeg Sun 2001. The fire started accidentally continues to smolder just west of Winnipeg. Winnipeg free press.
- Yang, S., Lohnes, R. A., and Kjartanson, B. H. 2002. Mechanical properties of shredded tires. *Geotechnical Testing Journal*, 25(1), 44-52.
- Youwai, S., and Bergado, D. T., 2003. Strength and deformation characteristics of shredded rubber tire-sand mixtures. *Canadian Geotechnical Journal*, 40(1), 254-264.
- Yoon, S., Prezzi, M., Sidiki, N.Z., and Kim, B. 2006. Construction of test embankment using a sand-tire shred mixtures as fill material. *Journal of Waste Management*, 26(9), 1033-1044.
- Zornberg, J. G., Costa, Y. D., and Vollenweider, B. 2004. Performance of prototype embankment built with tire shreds and nongranular soil. *Transportation Research Board 1874*, National Research Council, Transportation Research Board, Washington, D.C., 70-77.

CHAPTER 2 COMPRESSION BEHAVIOUR OF LARGE-SIZED TIRE DERIVED AGGREGATE FOR EMBANKMENT APPLICATION

This paper was previously reviewed and published in the Journal of Materials in Civil Engineering (ASCE). It is modified (formatting only) and presented as published part of this Ph.D. thesis as Chapter 2.

Reference: Meles, D., Bayat, A., and Soleymani, H. 2013. Compression behavior of large-sized Tire Derived Aggregate for embankment application. Journal of Material in Civil Engineering, ASCE, 25(9), 1285-1290.

CHAPTER 2 COMPRESSION BEHAVIOUR OF LARGE-SIZED TIRE DERIVED AGGREGATE FOR EMBANKMENT APPLICATION

ABSTRACT

Tire Derived Aggregate (TDA) has been successfully used for highway embankment applications in the past. Previous applications mainly used small and medium tire sizes as TDA sources. There are no published test results in the literature regarding the compression behaviour of TDA made solely from Off-the-Road tires (OTR). In this study, large-scale, one-dimensional compression tests are carried out to study the compression behaviour of TDA from OTR as well as from Passenger and Light Truck Tires (PLTT). Samples for the tests are prepared by varying the initial unit weights. The results show that there is a general trend of decreasing compressibility with increasing initial unit weight for both TDA sources. The compression test results are also used to compare compression behaviour between the two TDA sources. It is found that the compression behaviour of TDA from OTR and PLTT is more or less similar. Moreover, one-dimensional stress-strain regression equations were developed for TDA from OTR.

INTRODUCTION

Due to population growth and the expansion of the transportation industry, the amount of waste tires generated each year is increasing exponentially, making safe disposal of these waste products a challenge (Edeskar, 2004). One mass application of waste tires in civil engineering projects is to use tire derived

aggregate (TDA) as embankment material. Civil engineering applications have several advantages over other applications in that, for instance, they require less processing time and consume large volumes of waste tires (Edeskar, 2004). In addition to the environmental benefits of creating a clean environment and preserving natural resources such as aggregates, recycling waste tires provides the economic benefit of avoiding or reducing the usual practice of landfilling. For example, approximately 50,000 t of scrap tires are generated in Alberta each year. Almost all are diverted to productive end uses which save the equivalent 394,000 m³ of landfill space annually. In dollar terms, this translates to an estimated total savings of \$230 million since the recycling program began in 1992 (ARMA, 2011).

Several studies have been conducted to identify the feasibility of using shredded tires as a lightweight fill material in highway projects, such as embankment or backfill behind retaining walls (Drescher and Newcomb, 1994; Hoppe, 1994; Tweedie et al., 1998; Tandon et al. 2007; Humphrey, 2008; Mills and McGinn 2010). These studies suggest that TDA performed similarly or even better than the conventional fill. TDA has an additional advantage over conventional fill material in that it is lightweight. Tire derived aggregate embankments, however, should be designed to minimize the potential for internal heating. Design guidelines are provided in ASTM D 6270-08 to minimize the possibility for heating by removing or at least mitigating factors that create favourable conditions for this reaction. The design guideline provides detailed specifications on the amount of

steel wire permitted to protrude from the surface and particle size distribution, which are two significant factors in the use of TDA.

Tire derived aggregate can be produced from various tire sources. In this paper, passenger and light truck tires (PLTT) refers to TDA made from PLTT designed for use on passenger, light and multipurpose passenger vehicles with rim diameters of up to 0.5 m (19.5 in.). Off-the-road tires (OTR) refers to TDA made from OTR designed for use on vehicles or equipment (e.g. construction, mining, earthmovers) with rim diameters of up to 1 m (39 in.) (ARMA 2011). Previous civil engineering applications primarily used PLTT (Strenk et al., 2007). The main reasons for such a broad application of PLTT are waste tire availability and ease of production process. In some regions with heavy industrial and mining activities, (e.g., Alberta, Canada) discarded tires from OTR become a significant source of TDA. Typically, these tires are left in open spaces or deposited in landfills. The capability of tire recycling industries to process all types of waste tire into TDA and the growing stockpiles of discarded OTR from industrial activities encouraged the authors to investigate the possibility of recycling discarded OTR. Future applications for OTR include embankment fill material for highway projects.

The major challenge for the use of TDA from other tires such as OTR is the lack of laboratory or field experience. Most of the laboratory and field studies in the past focused on PLTT (Humphrey & Manion, 1992; Bosscher et al., 1997; Shalaby & Khan, 2005; Strenk et al., 2007; Warith & Rao, 2006). The geometric shapes of OTR differ from PLTT in size, shape, thickness, and amount of wire

protruding from the cutting surface. Therefore, an attempt has been made in this study to characterize the physical and mechanical properties of TDA from OTR and PLTT in the laboratory. Also, the PLTT that has been used successfully in the past is compared with OTR test results.

The prediction of field compression based on one-dimensional compression test laboratory results overestimated measured compression values in the field. A case history on Portland Jetport Interchange (Humphrey et al., 2000) showed that compressed unit weight and compression behaviour that was predicted based on laboratory results varied with the actual values measured at the end of the construction period. Geosyntec consultants (2008) summarize compaction methods studied by various authors. They found that field compaction usually results in higher unit weights when compared to laboratory compaction methods for large-sized TDA. One possible reason for the overestimation of field performance may be variations in compacted unit weights between the field and the laboratory. Therefore, the study also sees the effect of initial unit weights on one-dimensional stress-strain behaviour for both TDA sources. Moreover, one-dimensional stress-strain regression equations as a function initial unit weight are developed for OTR.

CHARACTERIZATION OF TEST MATERIAL

TDA materials used in the experiments were supplied by CuttingEDGE Tire Recycling LP and Liberty Tire Recycling located in Alberta, Canada. The TDA production process starts by removing the inner portion of the sidewalls. The remaining parts are then placed in a shredder, where they are cut into different

sizes and shapes. Figure 2.1(a and b) shows photographs of the TDA material used in the study.

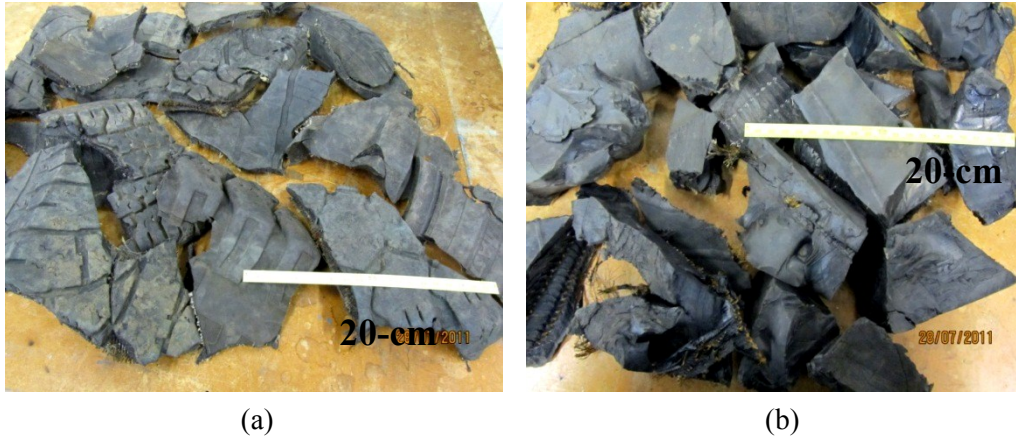


Figure 2.1: Photograph of Shredded tires used in the study: (a) PLTT, (b) OTR.

Visual observations were carried to investigate the difference in the geometric shape, thickness and steel wire protruding from the cutting edge. Typical shapes and thicknesses of both TDA types are shown in Table 2.1. The thicknesses for PLTT and OTR were measured manually by taking an average of 50 random shredded tire samples. Compared to PLTT, OTR contain TDA particles irregular in shape and relatively more steel wire protruding from the cutting surface. Nonetheless, in both PLTT and OTR, the steel protruding from the surface is very short and in compliance with the ASTM D6270-2008 requirement. PLTT contained TDA particles that were mostly thin and plate-like in shape. However, the larger pieces were dome shaped, resulting from the curvature of the whole (original) tire. OTR contained TDA particles mostly irregular in shape.

Gradation, specific gravity and water absorption

Gradation tests were determined in accordance with ASTM C 136 (ASTM 2006b). Sieves opening with size ranging from 6 to 308 mm were used. The particle size distribution of TDA material used in the study is shown in Figure 2.2. As we can see, the particle size distribution is typically uniform, with sizes ranging from 125 to 38 mm and a uniformity coefficient of less than 4.

Specific gravity and water absorption tests were conducted in accordance with ASTM C 127 (ASTM 2006a). At the start of the water absorption tests, air-dried samples were used instead of oven-dried samples. Table 2.1 summarizes specific gravity and water absorption for TDA used in the study. Specific gravity and water absorption are 1.27 and 1.1 percent for OTR, and 1.31 and 1.9 percent for PLTT, respectively. The range of specific gravity obtained in this study agrees with the result reported by Edil and Bosscher (1994) for large-sized TDA, ranging from 1.13 to 1.36. The magnitude of water absorption observed in the present study is slightly lower than the previously observed results of 2 to 4.3 percent by Humphrey (2008). The smaller values in this study may be the result of using large-sized TDA, which has a relatively smaller surface area compared to the size of TDA summarized by Humphrey (2008).

Table 2.1: Material description, specific gravity and water absorption.

Type of TDA	Average Thickness* (mm)	Standard Deviation *	Specific Gravity	Water Absorption (%)	Uniformity Coefficient (C_u)	Particle Shape
PLTT	10	0.11	1.31	1.8	1.8	Thin and Plate-like
OTR	30	0.91	1.27	1.1	3	Irregular

* sample size = 50

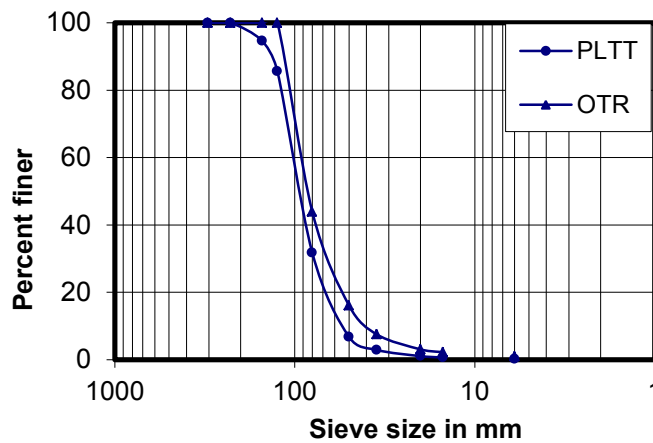


Figure 2.2: Particle size distribution of TDA used in the study.

APPARATUS AND TEST PROCEDURE

The experimental program was designed to study the one-dimensional compression behaviour of both TDA types. Compression tests were conducted, using a large-scale compression cell at the Edmonton Waste Management Center of Excellence (EWMCE). Figure 2.3 shows the compressibility testing apparatus. The equipment contained four compression cells of equal sizes, all connected to one hydraulic system. Each compression cell has an inside diameter of 57 cm, a height of 112 cm, and a thickness of 20 mm thick. The 20-mm polyethylene wall is thick enough to restrain the lateral deformations under axial loading. The inner

diameter of the compression cell was approximately four times larger than the largest TDA piece. The equipment was able to apply pressure up to 200 kPa. Loads were applied incrementally on top of the samples using a steel plate with a thickness of 2 cm and a diameter of 56 cm.



Figure 2.3: Photograph of compression apparatus at EWMCE for Testing TDA.

Friction between the TDA particles and the inner surface of the cells was a major concern in the use of such large-scale compression equipment. To minimize the side friction, three trial tests were performed on PLTT samples. In the first trial, compression tests were conducted such that the TDA particles were in direct contact with the sides of the cells. For the second trial, the interior surfaces of the cells were lubricated with grease. For the third trial, the interior surfaces were first lubricated using grease and later covered by a plastic sheet. In each case, a load cell was used to measure the pressure at the bottom of the cell to find the load reduction due to the friction. The first trial gave maximum frictional loss, with

stress at the bottom measuring up to 60 percent less than stress at the top. The third trial measured a minimal amount of stress at the bottom that was 25 to 30 percent lower than the stress at the top. The third trial thus was adopted for the experiment. To further account for side friction, the average stress at the top and bottom of the sample were used at each stage of load increment to compute the strain. The stresses at the top of the sample were measured using a load gauge attached to the compression apparatus, and the stresses at the bottom were measured using a load cell.

Two sets of experiments were conducted on the large-scale compression apparatus. The first sets of experiments were performed to study the compression properties of OTR and PLTT at different initial unit weights. Due to the large size of the equipment and difficulties to compact the samples in the compression cell, only a limited number of compression tests were conducted. For PLTT, unit weights of 4.9, 5.6 and 6.0 kN/m³, and for OTR, unit weights of 4.8, 5.8, 6.0 and 6.5 kN/m³ were used. The lowest unit weights were obtained by loosely dumping TDA in the compression cell and were only subjected to a vertical load of 50 to 60 kPa. The remaining tests were made by applying vertical load up to 200 kPa, which was the capacity of the compression equipment. The range of unit weights was selected randomly to be in between the loose unit weight and field-compacted unit weight, as reported by Geosyntec consultants (2008).

The second experiment was intended to find the compression of TDA under loading and unloading conditions. Samples at the initial unit weight of 5.7 kN/m³ were prepared for each TDA type and subjected to repeated loading and

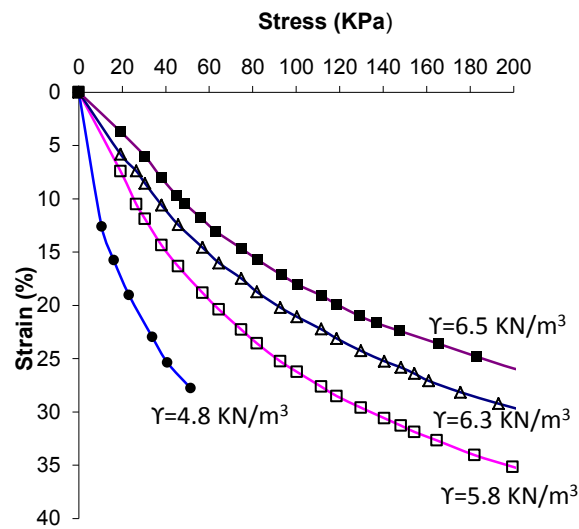
unloading cycles for two stress levels. First, the samples were subjected to loading up to a stress of 60 kPa and then unloaded to a zero vertical stress. Loads were applied manually using a hand pump attached to a compression cell. Based on an average of various tests, a stress of 150 kPa was applied in 1 minute. When the load reached maximum stress, deformation measurements were taken and the load was immediately reduced to zero stress. The plastic strain for each cycle was then computed by subtracting the strain upon unloading from the total strain at maximum stress. The loading cycle was repeated until the plastic strain upon unloading became insignificant, after which point the same sample was subjected to another load cycle with a stress level increased to 200 kPa.

RESULTS AND DISCUSSION

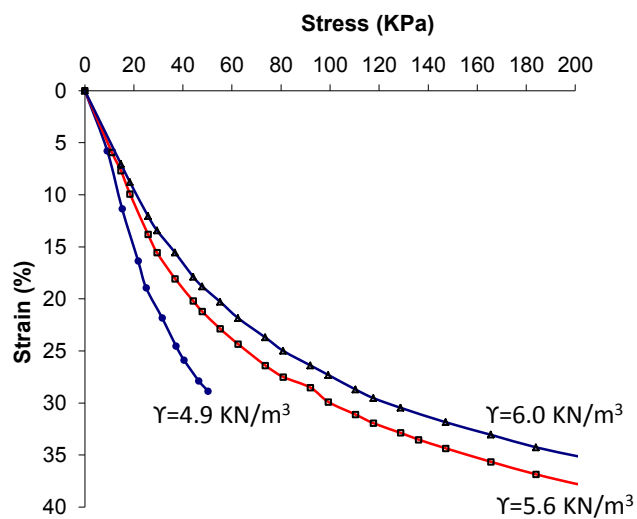
One-dimensional compression

Uniaxial compression tests were conducted on both TDA materials to characterize their compression behaviour. The stress-strain curves for each TDA material were then plotted. Figures 2.4(a and b) show the stress-strain relationship for OTR and PLTT materials, respectively. In all of the TDA types, the initial unit weight of the samples affects the shape of the compression curves. The effect is significant at lower stress, as the slopes of the initial parts of the compression curves decrease as the initial unit weights of the samples increase. Quantitative comparison is also shown to indicate how unit weight affects the prediction of compression at a vertical stress of 50 kPa. A vertical stress of 50 kPa was taken to be the representative of typical overburden stresses in TDA for a variety of common geotechnical applications (Wartman et al., 2007). For OTR, an increase

in the initial unit weight from 5.8 to 6.5 kN/m³ at a vertical stress of 50 kPa results in a decrease in the vertical strain from 17 to 11 percent. Similarly, at the same vertical stress, an increase in the initial unit weight from 4.9 to 5.6 kN/m³ for PLTT results in a decrease in vertical strain at the same vertical stress by 22 percent.



(a) OTR

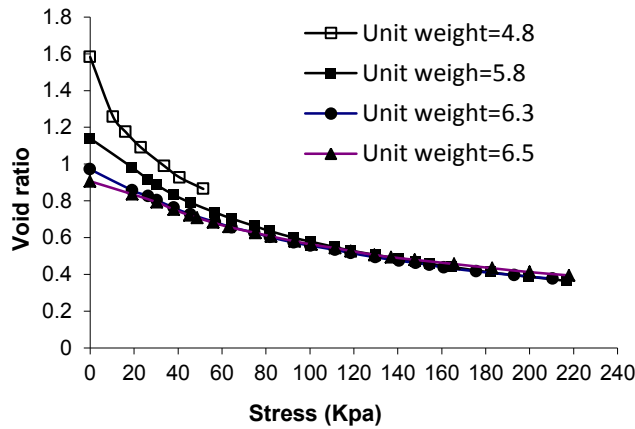


(b) PLTT

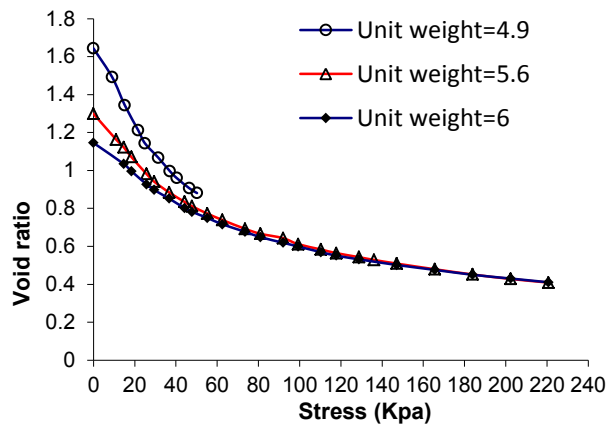
Figure 2.4: Compression behaviour of TDA for different initial unit weight of samples: (a) OTR, (b) PLTT.

Figure 2.5(a and b) show the relation between void ratio and stress. Void ratio is computed from specific gravity, which is assumed not to change during compression. Like the previous stress strain plot, the initial unit weight also affects the void ratio stress curves. However, these effects are not carried through at higher stress levels. At stress of approximately 100 kPa for OTR and 80 kPa for PLTT, the void ratio versus stress curves at different initial unit weights start to overlap. Beaven et al. (2006) also observed that the effects of initial density were largely destroyed by compression to 80 kPa.

To check repeatability, two tests—one from OTR and one from PLTT at density 4.8 and 4.9 kN/m³, respectively—were repeated thrice, from which adequate degrees of repeatability were obtained. Moreover, Figure 2.6 shows the one-dimensional compression curves obtained in this experiment are compared with the compression curves obtained by Warith and Rao (2006). The compression curve in Figure 2.6 was plotted from the Warith and Rao (2006) regression equation, with the initial unit weight of the samples tested varying from 5–5.3 kN/m³. Due to the wide use of TDA from light-truck tires in the past, only the compression test results from PLTT in the present study are compared. Figure 2.6 shows, at the same vertical stresses, the strain for three samples tested by Warith and Rao (2006) lies between the strains for samples tested at the initial unit weight of 4.9 and 5.6 kN/m³ in this study.



(a)



(b)

Figure 2.5: Stress versus void ratio of TDA for different initial unit weight (in kN/m^3) of samples: (a) OTR, (b) PLTT.

As part of the current study, the compression behaviour of OTR is compared with that of PLTT, which has been successfully used in previous projects. For comparison purposes, the initial void ratio is used rather than the initial unit weight. This is because PLTT and OTR have different specific gravities, which results in a different initial pore volume at the same initial unit weight. The comparison has been shown using stress-strain curve plotted for the same void ratio ($e_0 = 1.15$), as shown in Figure 2.7. Although, based on visual observations,

OTR and PLTT show some differences in the geometric shape of their individual particles, there is no significant change in compression behaviour at the same initial void ratio.

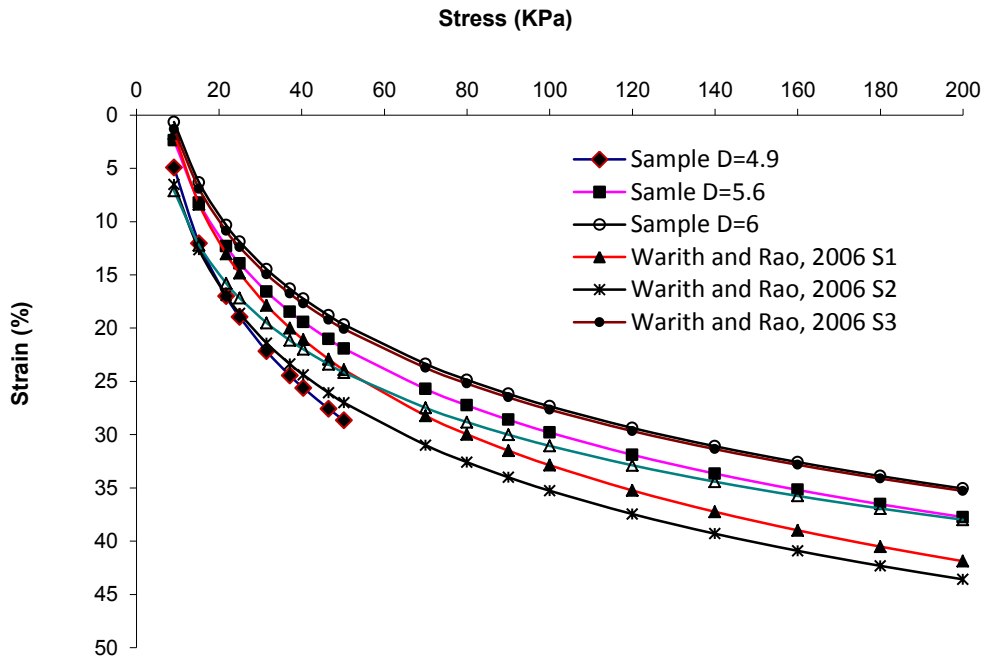


Figure 2.6: Stress-strain plot of TDA samples in this study and from Warith and Rao (2006).

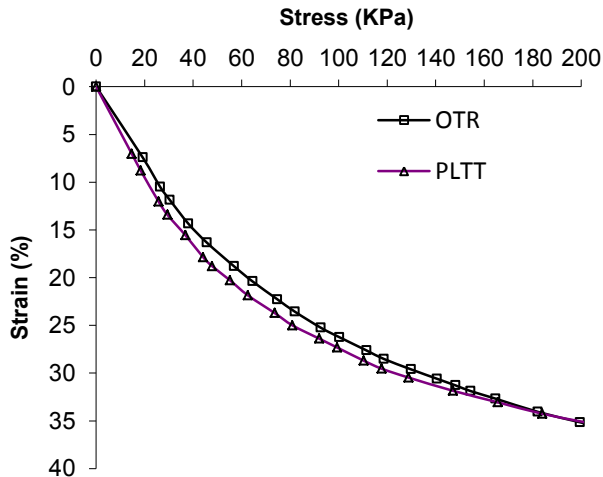


Figure 2.7 Comparison of compression of PLTT and OTR at initial void ratio=1.15

Loading-unloading tests

Table 2.2 summarizes the results of loading-unloading compression tests. In both TDA types, the plastic deformation upon unloading decreases significantly after the first cycle of the test. Similar observations were also made by Bosscher et al. (1992) and Zornberg et al. (2004). Field observations Bosscher et al.'s (1992) showed that only the first pass during the field compaction appears to induce a small amount of permanent compaction, with the other pass being totally ineffective. Zornberg et al. (2004) also made similar observations in their preliminary field testing program while studying performance of prototype embankment. They concluded that the change in dry density was insignificant after the second pass.

ONE-DIMENSIONAL STRESS-STRAIN MODEL

Previous laboratory studies have provided compression curves for TDA made from PLTT (Humphrey & Manion, 1992; Bosscher et al., 1997; Shalaby & Khan, 2005; Strenk et al., 2005; Warith and Rao, 2006). There was no previous compression curve in the literature that was developed for TDA made solely from OTR. Therefore, in this study, one-dimensional compression curves that may be used for design are given for OTR by varying initial unit weights of the sample tested. Fig. 8 shows that the one-dimensional stress-strain for OTR gave a straight line when plotted with a vertical strain on a normal scale against the natural logarithm of average vertical stress. The regression equations developed based on a straight line fit are shown in Eqs. (1)-(4) as a function of the initial unit weight.

All of the samples gave a straight line fit with R^2 values greater than 99 percent. Hence, the regression equations can be used to predict immediate compression during design, if field compaction results in unit weight are equivalent to laboratory densities:

$$\varepsilon = 10.726 \ln(\sigma) - 31.221, \text{ for initial unit weight } 6.5 \text{ kN/m}^3 \quad (1)$$

$$\varepsilon = 11.229 \ln(\sigma) - 30.326, \text{ for initial unit weight } 6.3 \text{ kN/m}^3 \quad (2)$$

$$\varepsilon = 12.459 \ln(\sigma) - 31.037, \text{ for initial unit weight } 5.8 \text{ kN/m}^3 \quad (3)$$

$$\varepsilon = 10.436 \ln(\sigma) - 13.476, \text{ for initial unit weight } 4.8 \text{ kN/m}^3 \quad (4)$$

where ε = strain expressed as a ratio of change in height (Δh) by original height (H_o) in percentage, and $\ln(\sigma)$ = the natural logarithm of average vertical stresses in kPa.

Table 2.2: Summary of stress-strain for PLTT and OTR of TDA with six cycles of loading-unloading.

Type of TDA	Load Cycle	Bulk Unit Weight at Start of Loading (KN/m ³)	Total Strain at Max. Stress (%)	Max. Applied Stress (KPa)	Plastic Strain Upon Unloading (%)
PLTT	1	5.72	23.01	53.92	8.21
	2	6.23	17.78		1.23
	3	6.31	17.07		0.10
	4	6.31	27.48	133.79	1.46
	5	6.43	26.83		0.85
	6	6.48	26.52		0.32
OTR	1	5.71	19.72	57.73	5.0
	2	6.01	16.38		1.69
	3	6.11	15.45		0.61
	4	6.15	26.27	146.09	0.70
	5	6.21	26.05		0.51
	6	6.24	25.77		0.41

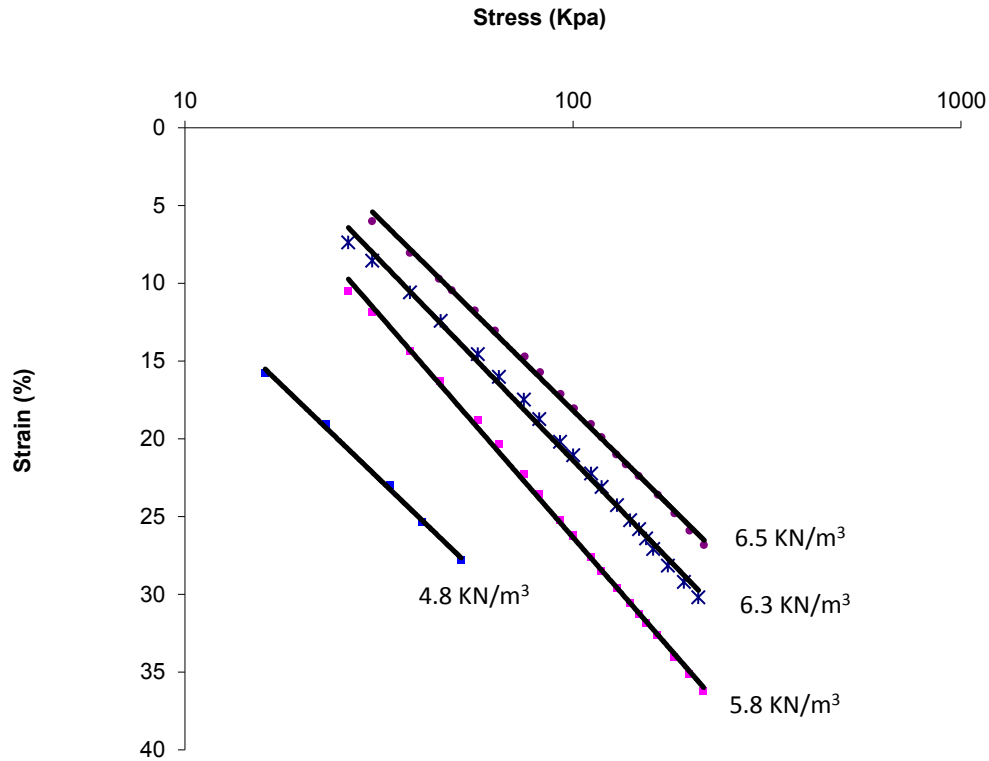


Figure 2.8: Vertical stress on natural logarithm scale vs. axial strain for TDA from OTR.

CONCLUSIONS

Based on the test results in this study for physical and mechanical properties of TDA from PLTT and OTR, the following conclusions can be made:

- The compression curve obtained for OTR has the same shape as PLTT, and in both TDA types, the compression curve depends on the initial unit weight of the sample and stress level.
- The laboratory loading-unloading compression test indicated that only the first load cycle results in a significant plastic deformation for both TDA sources.

- A comparison of compression behaviour indicates that both PLTT and OTR show more or less similar stress strain behaviour when compared at the same initial void ratio.
- The one-dimensional compression equations developed for OTR with different unit weights can be used to predict immediate settlement during design if the unit weight after field compaction is known. Care should be used to select the appropriate laboratory compression curve that has an equivalent compacted unit weight with the field.
- OTR can be used for similar application as PLTT as long as the appropriate design guideline in ASTM D 6270-08 is used. It is worth noting that the applications of OTR require field observations and monitoring.

REFERENCES

- Alberta Recycling Management Authority, 2011. Tire recycling. <http://www.albertarecycling.ca/> (Jul. 20, 2011).
- ASTM. 2006a. Test method for density, relative density (specific gravity), and absorption of coarse aggregate. ASTM D C127-06, ASTM International, West Conshohocken, PA.
- ASTM. 2006b. Test method for sieve analysis of fine and coarse aggregates. ASTM D C136-06, ASTM International, West Conshohocken, PA.
- ASTM. 2008. Standard practice for use of scrap tires in civil engineering applications. ASTM D 6270-08, ASTM International, West Conshohocken, PA.

- Beaven, R. P., Powrie, W., Hudson, A. P., and Parkes, D. J. 2006. Compressibility of tyres for use in landfill drainage systems. *Waste Resource Management*, 159(4), 173–180.
- Bosscher, P. J., Edil, T. B., and Eldin, N. N. 1992. Construction and performance of a shredded waste tire test embankment. *Transportation Research Record* 1345, Transportation Research Board, Washington, DC, 44–52.
- Bosscher, P. J., Edil, T. B., and Kuraoka, S. 1997. Design of highway embankments using tire chips. *Journal Geotechnical and Geoenvironmental Engineering*, 123(4), 295–304.
- Drescher, A., and Newcomb, D. E. 1994. Development of design guidelines for use of shredded tires as a lightweight fill in road subgrade and retaining walls. Report No. MN/RC-94/04, Dept. of Civil and Mineral Engineering, University of Minnesota, Minneapolis.
- Edeskar, T. 2004. Technical and environmental properties of tire shreds focusing on ground engineering applications. SE-971 87 Lulea, Department of Civil and Mining Engineering, Lulea Univ., Lulea, Sweden.
- Edil, T. B., and Bosscher, P. J. 1994. Engineering properties of tire chips and soil mixtures. *Geotechnical Testing Journal*, 17(4), 453–464.
- Geosyntec Consultants. 2008. Guidance manual-for engineering use of scrap tires. Project no. ME0012, prepared for Maryland department of the environmental scrap tire program, Columbia, MD.

- Hoppe, E. J. 1994. Field study of shredded-tire embankment. Report No. FHWA/VA-94-IR1, Virginia Department of Transportation, Richmond, VA.
- Humphrey, D. N. 2008. Civil engineering application of tire derived aggregate. Alberta Recycling Management Authority, Edmonton, AB, Canada.
- Humphrey, D. N., and Manion, W. P. 1992. Properties of tire chips for lightweight fill, Proceeding Grouting, Soil Improvement, and Geosynthetics, ASCE, New York, 1344–1355.
- Humphrey, D. N., Whetten, N., Weaver, J., and Recker, K. 2000. Tire shreds as lightweight fill for construction on weak marine clay, Proceeding International Symposium on Coastal Geotechnical Engineering in Practice, Balkema, Rotterdam, Netherlands, 611–616.
- Mills, B., and McGinn, J. 2010. Design, construction, and performance of highway embankment failure repair with tire-derived aggregate. Transportation Research Record 1345, Transportation Research Board, Washington, DC, 90–99.
- Shalaby, A., and Khan, R. A. 2005. Design of unsurfaced roads constructed with large-size shredded rubber tires: A case study. Resources Conservation Recycling, Elsevier B.V., 44(4), 318–332.

- Strenk, P. M., Wartman, J., Grubb, D. G., Humphrey, D. N., and Natale, M. F. 2007. Variability and scale-dependency of tire derived aggregate. *Journal of Materials in Civil Engineering*, ASCE, 19(3), 233–241.
- Tandon, V., Velazco, D. A., Nazarian, S., and Picornell, M. 2007. Performance monitoring of embankment containing tire chips: Case study. *Journal of Performance and Construction Facility*, ASCE, 21(3), 207–214.
- Tweedie, J. J., Humphrey, D. N., and Sandford, T. C. 1998. Full scale field trials of tire shreds as lightweight retaining wall backfill, at-rest condition. Transportation Research Board, Washington, DC.
- Warith, M. A., and Rao, S. M. 2006. Predicting the compressibility behavior of tire shred samples for landfill applications. *Journal of Waste Management*, 26(3), 268–277.
- Wartman, J., Natale, M. F., and Strenk, P. M. 2007. Immediate and time-dependent compression of tire derived aggregate. *Journal of Geotechnical and Geo environmental Engineering*, ASCE, 133(3), 245–256.
- Zornberg, J. G., Costa, Y. D., and Vollenweider, B. 2004. Performance of prototype embankment built with tire shreds and nongranular soil. *Transportation Research Record 1874*, Transportation Research Board, Washington, DC, 70–77.

CHAPTER 3 ONE-DIMENSIONAL COMPRESSION MODEL FOR TIRE DERIVED AGGREGATE USING LARGE-SCALE TESTING APPARATUS

This paper was previously reviewed and published in the International Journal of Geotechnical Engineering. It is modified (formatting only) and presented as published part of this Ph.D. thesis as Chapter 3.

Reference: Meles, D., Bayat, A, and Chan, D. 2014. One-dimensional compression model for tire derived aggregate using large-scale testing apparatus. International journal of geotechnical engineering, 8(2), 197-204.

CHAPTER 3 ONE-DIMENSIONAL COMPRESSION MODEL FOR TIRE DERIVED AGGREGATE USING LARGE-SCALE TESTING APPARATUS

ABSTRACT

The engineering properties of Tire Derived Aggregate (TDA) have been the subject of previous laboratory investigations; however, these investigations have been conducted primarily on TDA one-third the size of TDA used for engineering applications. In this study, the compression behavior of compacted TDA samples with a maximum particle size of 300 mm, typically used for engineering applications, has been investigated using custom made testing apparatus designed to accommodate the large-sized TDA. TDA Properties important to engineering applications, including compression behavior, the coefficient of lateral earth pressure at rest, and Poisson's ratio, are provided, while variation in the gradation of TDA particles and the tire type for TDA production are experiment variables. This study also proposes a method to prepare compacted TDA samples for large-scale testing.

INTRODUCTION

More than 5 million tires are discarded each year in the province Alberta, Canada (ARMA 2013). In the past, these tires have been used by the tire recycling industry to make various manufactured products, rubber crumb, and Tire derived aggregate (TDA) primarily used for landfill drainage application. Recently, the growing construction and mining industries have contributed to the existing stockpile of discarded tire. The increase in the amount of discarded tire and the

tire recycling industry's growing capability to process all types of discarded tire have encouraged Alberta Recycling and Alberta Transportation to look for other potential uses of TDA.

Tire derived aggregate has the desirable properties for most civil engineering applications; it is lightweight, free-draining, and has good thermal resistivity. It has been used as fill material for embankments, retaining walls and bridge abutments, as well as insulation to limit frost penetration. Additionally, it has also been used for french drains and as a drainage layer for roads (Humphrey 2008). Various successful TDA projects have been reported in the literature, including several studies conducted in the USA and Canada (Bosscher et al. 1992, Dickson et al. 2001, Tandon et al. 2007; Mills and McGinn 2010). A major problem with the use of TDA for such applications is the lack of large-scale laboratory experiments that characterize the deformation behavior of TDA in the field.

Tire derived aggregate is a highly compressible material whose deformation characteristics, rather than strength characteristics, govern its design and performance in most applications (Bosscher et al. 1997). The compression behavior of TDA has been studied previously in laboratories (Humphrey and Sandford 1993; Bosscher et al. 1997; Warith et al. 2006; Wartman et al. 2007; Humphrey 2008, Meles et al. 2013). In these works, the compression behavior was mostly determined on compacted samples using tire chips or tire shreds with a maximum particle size one-third the size of TDA used in field applications. Very little information is available on the compression behavior of large-size TDA, particularly regarding TDA with a maximum size of 300 mm.

The use of TDA as a fill material for highway embankment or fill behind retaining walls requires the consideration of design parameters such as Young's modulus, constrained modulus, the coefficient of lateral earth pressure, and Poisson's ratio. In Previous studies, these parameters were determined on compacted TDA samples in the laboratory using a one-dimensional compression test (Humphrey and Sandford 1993). Humphrey and Sandford (1993) determined the elastic parameters for TDA with maximum particle sizes ranging from 38 to 76 mm. However, TDA used for field applications has maximum particle sizes that range from 300 to 400 mm (ASTM D 6270 2008).

PREVIOUS STUDIES

Compacted unit weight

Previous studies conducted on TDA have used a dynamic method of compaction, similar to that defined in ASTM D 698 or D 1557 for soil, which modifies only the compaction mold size (Humphrey and Sandford 1993; Moo-Young et al. 2003). The large mold requires that the number of layers of compaction, the number of blows of the rammer per layer, or both, be increased to produce the desired compaction energy per unit volume. Typical sizes of the compaction mold and maximum dry densities obtained from the previous laboratory studies are summarized in Table 3.1. However, unlike soil particles, individual TDA particles are compressible and will reduce the impact of the rammer load. Moreover, the laboratory method of compaction specified for soil in ASTM D 698 or D 1557 is not satisfied, as TDA for civil engineering applications retains more than 30% of TDA on a 19 mm sieve.

Table 3.1: Previously reported compaction mold size and compacted density in the laboratory.

Size of TDA	Size of compaction mold	Compacted unit weight (Mg/m³)	Compaction type	Reference
Maximum 38 mm	254 mm diameter	0.618	compacted in three layer with 60% standard Proctor energy	Humphrey and Sandford (1993)
Maximum 76 mm		0.619		
Maximum 51 mm		0.642		
Maximum 51 mm		0.625		
< 50 mm	304.8 mm diameter	0.64	compacted using 60% standard Proctor energy	Moo-Young et al. (2003)
50 to 100 mm		0.72		
100 to 200 mm		0.66		
200 to 300 mm		0.62		

The dynamic method of TDA compaction in the laboratory has other disadvantages; specifically, the impracticality of studying the compacted unit weight for TDA larger than 75 mm. To test large-sized TDA requires a compaction mold larger than that reported in Table 1. Such molds make it difficult to achieve a compaction energy required to execute standard or modified Proctor compaction tests manually. Moreover, as the size of the TDA increases, the bouncing effect of individual TDA pieces on compaction also increases, making the dynamic method less effective. The lack of a viable compaction method has proven problematic, particularly when attempting other tests under a compacted state. For example, a compression test for TDA with a maximum particle size of 300 mm requires sample sizes several times larger than the size of the TDA particles, which requires significantly larger test equipment. Such a large-sized sample is impractical to prepare using the dynamic method of compaction. It is believed that this may be one reason for the lack of reported

compression tests for TDA with a maximum particle size of 300 mm in a compacted state.

Compression behavior

The compressibility of compacted TDA samples with a maximum particle size of up to 75 mm has been previously investigated (Humphrey and Sandford 1993). In the study by Humphrey and Sandford (1993), vertical strains up to 29% were measured for samples compacted in five layers, with 60% Standard Proctor energy in the compression mold under a vertical stress of 69 kPa. These laboratory-measured strains are greater than the field-measured strains reported in previous case studies (Humphrey et al. 2000; Dickson et al. 2001 and Mills and McGinn 2010). A case history to study the use of TDA as lightweight fill material for highway embankment on the north abutment of the Merrymeeting Bridge in Topsham, Main and an approach embankment fill for a bridge over the Main Turnpike in Portland, Main, U.S. also showed a discrepancy between the strains predicted based on the laboratory compression curve and the strains measured in the field following construction (Humphrey et al. 2000).

The exact reasons for the deviation between predictions based on laboratory tests and actual measurements in the field are not clear, but they may include the following: a majority of previous laboratory tests were performed on TDA with a maximum particle size of 75 mm, which is smaller TDA used in the field; there may be a variation between laboratory and field compacted densities; the dynamic compaction similar to that used for soil in the laboratory sample may not

adequately simulate field compaction with respect to particle arrangement; and, the anisotropic behavior of TDA.

This paper presents key engineering properties of TDA needed for design as lightweight fill material and fill behind retaining walls. These properties were determined in the laboratory for TDA samples collected from the field where the samples had been used as embankment fill and insulation to limit frost penetration. The large TDA size and high compressibility of the TDA necessitated that conventional test procedure be modified, especially the method of compaction used to prepare samples for the compression test. This also required that a custom testing apparatus be designed. Stress-strain model and at-rest lateral earth pressure coefficients are given from the results of the large-scale, one-dimensional compression test.

EXPERIMENTAL PROGRAM

The experimental program was designed to study the compression behavior and to determine lateral earth pressure coefficient at rest (K_o) for compacted TDA samples with a maximum particle size of 300 mm. Variation in the gradation of TDA particles and the source of tire for TDA production were the major variables in the experiment. TDA used as a fill material is categorized into two classes; Class I: fill with TDA layers less than 1-m thick, and Class II: fill with TDA layers in the range of 1 to 3 m thick (ASTM D 6270 2008). ASTM D 6270 (2008) specifies different particle gradation requirements for the use of TDA for the two classes, where Type A shall meet material requirement for Class I fill and Type B for Class II fill. The testing program considered TDA that met gradation

requirements as Type A and Type B according to ASTM D 6270 (2008). The testing program also considered TDA produced from two tire sources: passenger and light truck tires (PLTT), with a rim diameter of up to 49.5 cm; and off-the-road (OTR) tires, with a rim diameter of up to 99 cm (ARMA 2013).

Owing to the TDA particle size and the resultant testing apparatus used in the experiment, it was impossible to apply the previous compaction method used by Humphrey and Sandford (1993) and Moo-Young et al. (2003) in preparation for the compression test. Therefore, a different compaction method was used in this study. In addition to studying the compression behavior of TDA, this study was also designed to test the effectiveness of this new compaction method. To compare the results of compaction with Humphrey and Sandford (1993), the compaction test was conducted on TDA with a maximum particle size of 75-mm.

MATERIALS

TDA used for the compaction test was provided by Liberty Tire Recycling Alberta, Canada, and was produced from PLTT. The material contained TDA pieces with a maximum size of 75 mm. The TDA used to study the compression behavior and the coefficient of lateral earth pressure at rest (K_o) was taken from the field. This TDA was used as a fill material and an insulation layer for an access road connecting the Anthony Henday Ring Road to the Edmonton Waste Management Centre (EWMC) in Edmonton, Alberta, Canada. The road is part of a research initiative, the Integrated Road Research Facility (IRRF), established to evaluate the long-term performance of TDA as embankment fill material and an insulation layer.

Three types of TDA were used in the road project: Type A PLTT was used as insulation layer, and Type B PLTT and Type B OTR were used as embankment fill material. The fundamental properties, including gradation, specific gravity, and water absorption, of all three types of TDA were studied in the laboratory. Gradation testing was conducted in accordance with ASTM C 136 (2006) by using large-scale sieves with openings ranging from 6 to 308 mm. The typical particle size distribution curves are shown in Figure 3.1. All three types of TDA had uniform gradation, with a coefficient of uniformity (C_u) less than 4. Specific gravity and water absorption tests were also conducted in accordance with ASTM C 127 (2005). For water absorption tests, air-dried samples were used instead of oven-dried samples. Table 3.2 summarizes the specific gravity and water absorption values for the three types of TDA used in this study.

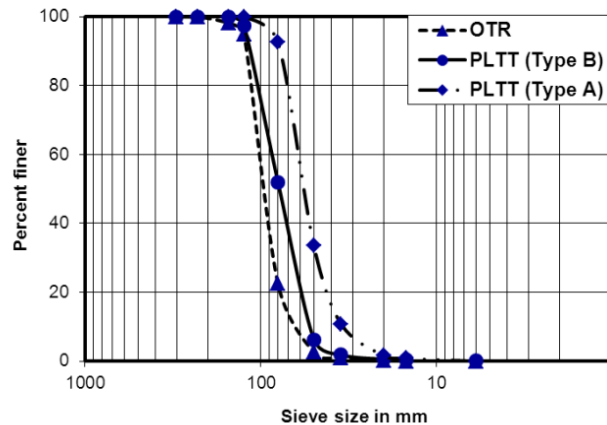


Figure 3.1: Particle size distribution of TDA used for the compression test.

Table 3.2: Physical properties of the TDA used in this study.

TDA type	Specific gravity	Water absorption	Uniformity coefficient (c_u)	Maximum particle size (mm)
TDA Max 75 mm	1.17	3.5	NA	75
PLTT (Type A)	1.31	3.0	1.7	110
PLTT (Type B)	1.32	2.7	1.4	300
OTR (Type B)	1.19	1.3	1.8	300

APPARATUS AND TEST PROCEDURE

Two types of Polyvinyl chloride (PVC) pipes with different diameters of 310 and 1230 mm were used in this study. A 310-mm-diameter pipe was used as compaction mold to study the applicability of the compaction method used to prepare compacted samples of TDA for compression testing. The container used for the compaction test contained schedule 40 PVC pipe with a 310-mm internal diameter, 470-mm height, and 8-mm thickness. An MTS 400 compression machine with a capacity of 400 kN was used to apply stress for compaction, and load was applied by a rigid loading plate with a 300-mm diameter. A photograph of the compaction test apparatus is shown in Figure 3.2.



Figure 3.2: Photograph of the small compaction test equipment.

The compaction test was conducted by first applying a vertical stress to TDA that increased from 0 to 300 kPa using the MTS machine, and then immediately unloading the stress to 0 kPa. The 300-kPa vertical stress is usually the minimum ground contact pressure exerted by compaction equipment during compaction in the field (DAS 2013). Three samples (sample 1, 2 and 3) of TDA with different compaction thicknesses and energies were prepared for the compaction test. Sample 1 was loosely placed in the compaction mold without any compaction pressure. Sample 2 was loosely placed in the mold and vertical pressure was increased to 300 kPa and then removed; the cycle of loading and unloading vertical stress was repeated three times. Sample 3 filled the mould with three layers of TDA, approximately 200 mm thick each. For each layer, TDA was placed loosely and then subjected to three cycles of loading and unloading at a vertical stress of 300 kPa. The layer thickness of 200 mm was selected to ensure that the total compaction energy would be approximately 60% standard Proctor energy to compare with Humphrey and Sandford (1993).

The 1230 mm pipe used to study the TDA's compression behavior and lateral earth pressure at rest (K_o) was designed based on the recommendations of ASTM D 6270 (2008). It was made from PVC pipe with a 1230-mm internal diameter, 1500-mm length, and 27-mm wall thickness. The PVC pipe has open ends with a Young's Modulus and Poisson's ratio of 266 MPa and 0.38, respectively. Two steel plates, with thicknesses of 35 mm and diameters of 1200 mm, were used at the top and bottom of the pipe. One steel plate was attached to the loading machine and vertical load was applied on the top of the TDA sample. The second

plate was placed on the bottom of the pipe, 300 mm above the ground, resting on top of four load cells, which were calibrated to measure the vertical force at the bottom the sample. A total of 12 strain gages were attached to the external wall of the pipe with a horizontal orientation: four were placed 300 mm above the bottom plate and the remaining two placed 600 mm above the bottom plate. These gages were calibrated to measure the longitudinal strain on the pipe, which was later used to back-calculate the horizontal stress exerted by the TDA on the inside of the container. The additional six strain gages were placed vertically along the external wall of the pipe, near the other horizontally-placed strain gages. The vertical gages were calibrated to measure the vertical compression of the pipe during the test. A photograph of the testing apparatus is shown in Figure 3.3.

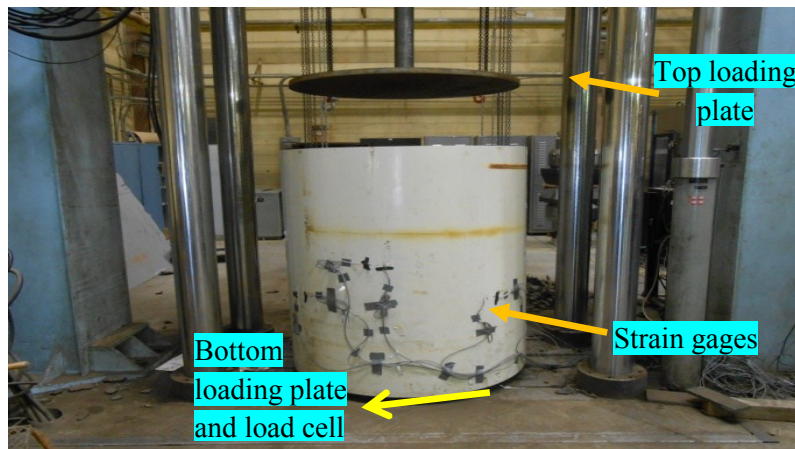


Figure 3.3: Photograph of the large compression test equipment.

Loose samples for the compression test were prepared by placing TDA into the 1230 mm diameter PVC pipe without any compaction. For the compacted sample, TDA was filled in the PVC pipe in four 300-mm thick layers, which is equivalent to the field compaction thickness. For each layer, TDA was placed loosely and then subjected to three cycles of loading and unloading to a maximum vertical

stress of 300 kPa. Only three cycles were used in each layer as further loading and unloading cycles were not effective in compacting the sample. Once the container was filled with the four layers, a vertical load was applied at a constant strain rate of 13 mm/min. All tests were performed on air-dried TDA specimens as previous research showed that water had an insignificant effect on TDA's compression characteristics (Tatlisoz et al. 1997).

Each compression test was repeated at least twice to see if adequate repeatability was achieved for the test procedure. Side friction between the inside wall of the pipe and TDA sample was a major concern during the compression test due to the large-scale compression apparatus. The PVC pipe was open at both ends, and the bottom steel plate was raised 300 mm from the ground to accommodate the load cell. By leaving 100 mm space between the ground and PVC pipe after the compacted sample was prepared, the pipe was allowed to move vertically during the application of the compression load. This vertical movement greatly reduced the wall friction between the inside wall of the pipe and TDA during the application of the compression load. By allowing vertical movement of the pipe, the bottom cell recorded about 90-80% of the vertical load applied by the loading equipment at the top.

Readings from the strain gages and load cell as well as the vertical load and deformation from the loading machine were collected in 1-second intervals using an automatic data acquisition system. The readings from the load cell and vertical load from the loading machine were then divided by the area of the loading plate to calculate the stress at the bottom and top of the TDA samples, respectively. The

deformation measured during the test was divided by the initial height of the sample prior to the test to calculate the strain. The average stress between the top and the bottom sample was then used to plot the stress-strain curves of the TDA samples. The longitudinal and transverse readings from the four strain gages located at the bottom of the pipe were used to compute the internal pressure and then later used to compute the horizontal stress.

RESULT AND DISCUSSIONS

Compaction test

Results from the compaction tests on the 300 mm-diameter compaction mold are presented in Figure 3.4. The compacted densities based on an average of the three samples for each test varied from 4.6 to 6.3 kN/m³. The lowest density, 4.6 kN/m³, was obtained for Sample 1, which was prepared by filling the mold with TDA without applying any compaction energy. Sample 3, which was prepared to simulate the way TDA is compacted in the field, gave the highest compacted density of 6.3 kN/m³. Sample 2, which was given an intermediate compaction effort, yielded a compacted density of 5.7 kN/m³. Figure 3.4 also shows an increase in compaction energy, which was achieved by varying lift thickness results to increase compacted unit weight. It was also observed that only the first three loading and unloading cycles were effective in compacting the TDA samples for each given lift thickness.

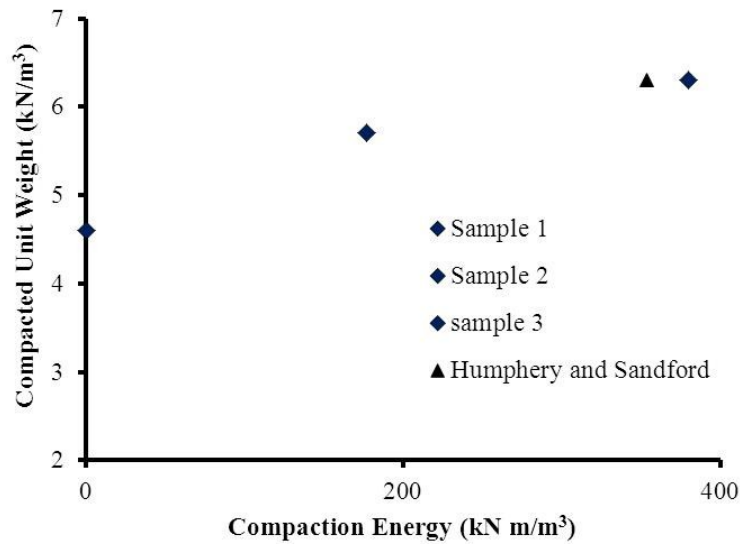


Figure 3.4: Comparison of test results in this study with Humphrey and Sandford (1993).

The compacted densities obtained in this study were compared with the maximum dynamic compacted density obtained by Humphrey and Sandford (1993) as shown in Figure 3.4. The compacted density that this study obtained for Sample 3, where TDA was compacted by 64% Standard Proctor energy, is equivalent to the compacted density obtained by Humphrey and Sandford (1993). Humphrey and Sandford (1993) used a 254-mm-diameter compaction mold to compact their TDA in five layers, with 60% standard Proctor energy. They obtained compacted densities ranging from 6.0 kN/m³ to 6.3 kN/m³. Moreover, visual observation of Sample 3 during this study revealed that even though most TDA pieces were initially placed into the mold at random, they were aligned horizontally after compaction. Similar observations were made in the field after using compaction equipment (Drescher et al. 1999), with most TDA pieces horizontally aligned following compaction. Therefore, the method of laboratory compaction used in

this study simulates field conditions closely with respect to the arrangement of TDA particles after compaction. This is important in studying TDA compressional behavior as laboratory experiment conducted by Heimdahl et al. (1999) on biaxial apparatus revealed a difference in Young's moduli for TDA pieces aligned perpendicular and parallel to the direction of loading.

Compacted unit weight for the compression tests

The unit weights of the samples before and after compression tests in the 1230 mm-diameter PVC pipe are presented in Table 3.3. The unit weights vary from 4.4 to 6.1 kN/m³. Type B PLTT gives the lowest unit weight under both loose and compacted states compared to Type A PLTT and Type B OTR. This discrepancy might be related to the differences in the maximum particle size and geometry. Type B PLTT contained TDA particles with a maximum size of up to 300 mm, and the larger pieces were primarily elongated in shape with high aspect ratios. On the contrary, Type A PLTT contained TDA pieces of up to 110 mm in size, with the larger pieces primarily equidimensional in shape. Therefore, the presence of elongated, large TDA pieces in Type B PLTT can produce larger, more frequent void space during placement and compaction when compared to Type A PLTT. The higher unit weight for Type B OTR compared to Type B PLTT may be related to the differences in geometry of TDA pieces due to the source of tire they were produced from; type B OTR contained TDA pieces made from larger and thicker tires. As a result, the TDA pieces in the OTR were inflexible, and most pieces were granular and cubical in shape. With no flexibility in the pieces and the presence of a granular particle, Type B OTR geometry may favor more

efficient packing, producing a higher unit weight during placement and compaction.

Table 3.3: Unit weight of the sample used for the compression test.

TDA type	Unit weight of sample before the test (kN/m³)	Testing condition
Type A: PLTT	5.4	No compaction
	6.1	Compacted
Type B: PLTT	4.4	No compaction
	5.9	Compacted
Type B: OTR	4.9	No compaction
	6.1	Compacted

Vertical compressibility

The plots of the average vertical stress versus vertical strain for Type A PLTT, Type B PLTT, and Type B OTR are shown in Figures 3.5 (a), (b), and (c), respectively. In all cases, it is found that loosely placed TDA compressed more than the compacted samples, and the stress-strain curve have a similar shape. The initial portions of the stress-strain curves are relatively steep at lower stress, with a slight slope at higher stress. As shown in Figures 3.5 (a) and (b), it appears that TDA containing large pieces compresses more than TDA containing small pieces; this is consistent with findings reported by Strenk et al. (2007). Figures 3.5 (a), (b,) and (c) also show that Type B OTR is the least compressible of all three samples. Quantitative comparison between the samples can be made by examining the vertical strain at an average vertical stress of 50 kPa. A vertical stress of 50 kPa is considered to be representative of typical overburden stress in TDA applications for variety of common geotechnical projects (Wartman et al. 2007). At an average vertical stress of 50 kPa, Type A PLTT, Type B PLTT, and

Type B OTR show vertical strains of 16%, 18%, and 14%, respectively. These strains are two to three orders of magnitude higher than typical strains found in soils used as fill material for common geotechnical applications. This data also suggests that for the similar-sized TDA, PLTT compresses by more than 28% from OTR, and Type B PLTT compresses by more than 12.5 % from Type A PLTT.

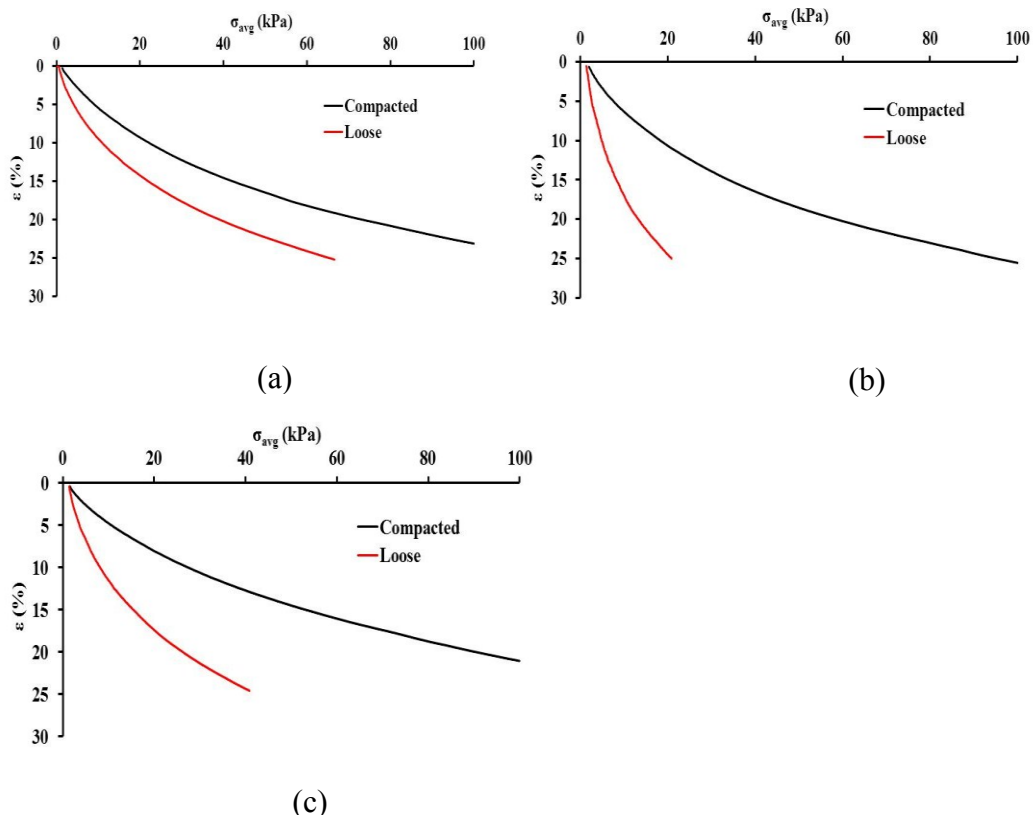


Figure 3.5: Vertical strain versus average vertical stress for: (a) Type A PLTT, (b) Type B PLTT, and (c) Type B OTR tested in the 1230 mm diameter PVC pipe.

TDA compresses when load is applied due to three mechanisms: (a) the rearrangement/sliding of TDA pieces, which is generally irrecoverable; (b) the bending/flattening of TDA, which is responsible for a majority of compression

and is usually recoverable upon unloading; and (c) the elastic compression of TDA pieces which is also recoverable and negligible at lower stress (Ahmed and Lovell 1993). For the compacted samples in this study, the first mechanism mainly occurred during compaction while preparing the sample for the compression test. It was observed that the compression of the samples was recovered upon unloading after the compression test. The contribution of the third mechanism is small for the stress range used in this study (Ahmed and Lovell 1993; Wartman 2007). As indicated by Ahmed and Lovell (1993), the second mechanism seems to play a major role for TDA compression samples in this study. As explained in the section “*compacted unit weigh for the compression tests*”, OTR contains TDA pieces which are thick and inflexible compared to PLTT, which includes thin, flexible particles. Thus, OTR particles should have more resistance to bending/flattening compared to PLTT pieces, and this may result in less compression in OTR compared to both Type A and Type B PLTT. Because of their shape, OTR particles also favor more efficient packing compared to PLTT when prepared for compression tests.

One-dimensional compression model

A typical plot of the average vertical stress versus vertical strain for TDA is nonlinear. The curve can be described by the following hyperbolic equation (Drnevich 1975):

$$\sigma = \frac{D_t \varepsilon}{1 - \frac{\varepsilon}{\varepsilon_m}} \dots\dots\dots (1)$$

where σ =axial stress; D_i =initial tangent modulus; ε =axial strain; and ε_m =strain to which the stress-strain curve is asymptotic.

Several methods are available to determine the values of ε_m and D_i in Equation 1. One method involves the use of one-dimensional compression test data (Drnevich 1975). Equation (1) may be rearranged to give:

$$\frac{\sigma}{\varepsilon} = D_i + \frac{\sigma}{\varepsilon_m} \dots\dots\dots (2)$$

which is a straight line with intercept D_i and slope $1/\varepsilon_m$. To determine the value of D_i and ε_m , σ/ε versus σ for one dimensional compression test data are plotted, and the resulting data points are fitted with a straight line. A typical plot of σ/ε versus σ for Type B PLTT is presented in Figure 3.6. The intercept gives D_i and the inverse of slope gives ε_m . Using the values of D_i and ε_m , the following one-dimensional compression models are developed for Type A PLTT, Type B PLTT, and Type B OTR using the results of the compacted samples respectively:

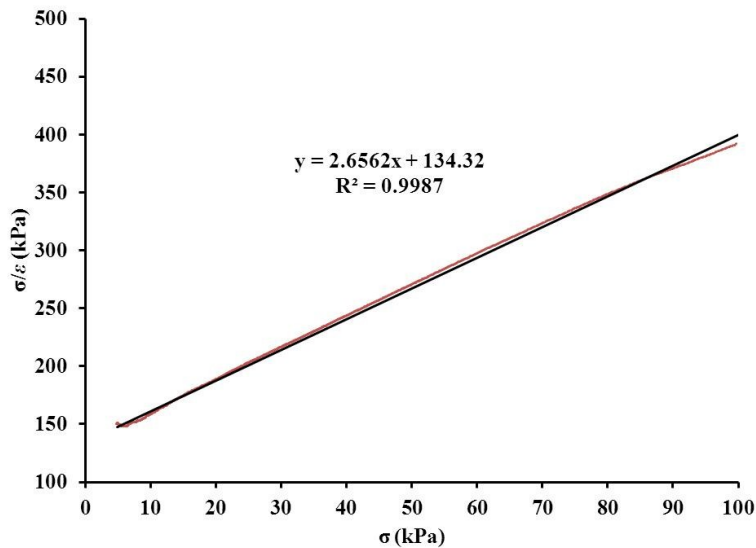


Figure 3.6 Typical plot of σ/ε versus σ from one dimensional compression test data for Type B PLTT

$$\sigma = \frac{163\varepsilon}{(1-2.72\varepsilon)} \dots\dots\dots (3)$$

$$\sigma = \frac{134\varepsilon}{(1-2.65\varepsilon)} \dots\dots\dots (4)$$

$$\sigma = \frac{196\varepsilon}{(1-2.77\varepsilon)} \dots\dots\dots (5)$$

where σ =axial stress in kPa and ε =axial strain in decimal.

Equations (3), (4), and (5) are used to re-plot the laboratory compression curve for the compacted samples discussed in the section “vertical compressibility”. The comparison of the compression curve obtained from the model and laboratory experiment is presented in Figure 3.7. There is significant similarity between the experimental curve and curves re-plotted from the model equations.

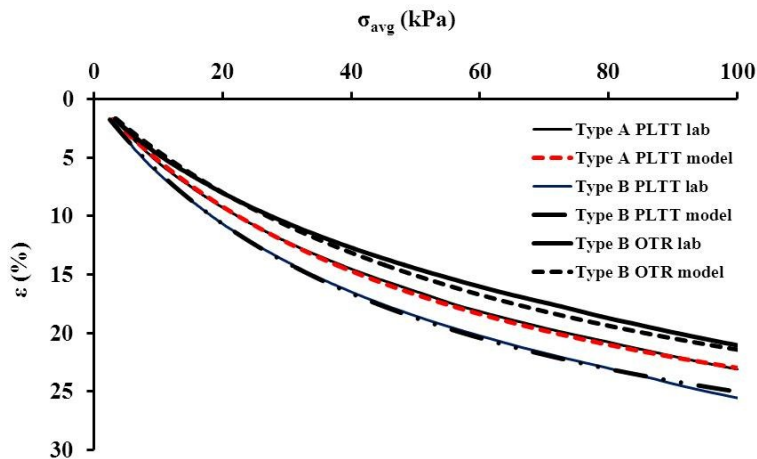


Figure 3.7: Comparison of laboratory compression curve and compression curve re-plotted from one dimensional compression model for: (a) Type A PLTT, (b) Type B PLTT, and (c) Type B OTR.

At-rest lateral earth pressure coefficient (K_o) and Poisson's ratio

Horizontal strain gages were used to measure the increase in horizontal stresses as the sample was loaded. The coefficients of lateral earth pressure at rest (K_o) were then calculated from the slope of horizontal stress at the gage height versus the average vertical stress plot. A typical horizontal stress versus average vertical stress plot for compacted Type B PLTT is presented in Figure 3.8. The initial portion of the curve has a slighter slope up to the average vertical stress of approximately 80 kPa, following which the slope is relatively steeper. The increase in slope at a higher stress has been hypothesized to be related to the compression mechanism of TDA: the flatter slope at lower stress is due to the compression of void space between particles, and the steeper slope at higher stress is due to the deformation of the rubber pieces (Humphrey and Sandford 1993). The same behavior has also been observed for Type A PLTT and Type B OTR. The K_o value based on a straight line fit for the stress range in this study varies from 0.43 to 0.33, as shown in Table 3.4. This data suggests that Type A PLTT with smaller TDA size has a higher K_o value compared to PLTT Type B with larger TDA size. Humphrey and Sandford (1993) also conducted a similar experiment and determined the K_o value for tire chips with different maximum sizes. The results of their experiment showed a decrease in the K_o value with an increase in the maximum tire chip size, which agrees with the findings of this

study. Poisson's ratio can also be computed from K_o values shown in Table 4. The Poisson's ratio for the TDA in this study varies from 0.3 to 0.25, which is 50% to 60% less than the Poisson's ratio of solid tire rubber of approximately 0.5.

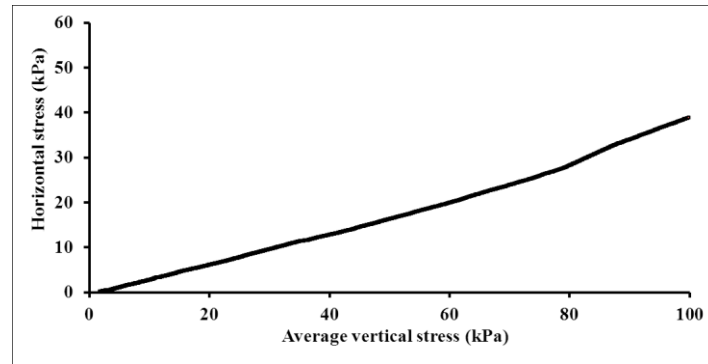


Figure 3.8: Typical plot of horizontal stress versus average vertical stress for Type B PLTT.

Table 3.4: Elastic parameters for the TDA used in this study.

TDA type	K_o	μ	$D_{initial}$ (kPa)
Type A: PLTT	0.43	0.30	163
Type B: PLTT	0.38	0.28	134
Type B : OTR	0.33	0.25	196

CONCLUSIONS

Based on the results of compaction and large-scale compression tests of PLTT and OTR, the following conclusions can be made:

Compaction test on TDA with maximum size of 75 mm:

- Using the method of compaction proposed in this study, it is possible to achieve a compacted unit weight similar to the dynamic compacted unit weight.

- Tire derived aggregate strips initially placed at random are aligned perpendicularly to the direction of the application of loads after compaction, similar to observations made after field compaction.
- The method of compaction developed in this study can be used to prepare large-size compacted TDA samples.

Large-scale compression test results:

- Type B PLTT gives the smallest unit weight under both loose and compacted states compared to Type A PLTT and Type B OTR.
- It is found that loosely placed TDA compresses more than the compacted samples, and the stress-strain curve for all TDA samples tested have similar shape.
- For TDA produced from PLTT, the study indicates that TDA containing large pieces compresses more than TDA containing smaller pieces.
- For the method of compaction used to prepare compacted samples, the compression test results indicate that TDA made from OTR is less compressible than TDA made from PLTT.
- The one-dimensional compression model developed for Type A PLTT, Type B PLTT, and Type B OTR can be used to predict immediate settlement during design.
- The laboratory results also suggest that there may be some advantages to use Type B PLTT compared to Type A PLTT as retaining wall backfill since it has a lower K_o value.

REFERENCES

- Ahmed, I. and Lovell, C.W. 1993. Rubber soils as lightweight geomaterials. Transportation Research Record, 1422, National Research Council, Transportation Research Board, Washington, D.C., 61-70.
- Alberta Recycling Management Authority. 2013. Tire Recycling Program. Edmonton, AB. [online] Available: <<http://www.albertarecycling.ca/>>. [Accessed on June 1, 2013].
- ASTM. 2005. Test method for density, relative density (specific gravity), and absorption of coarse aggregate. ASTM C127-04, ASTM International, West Conshohocken, PA.
- ASTM. 2006. Test method for sieve analysis of fine and coarse aggregates. ASTM C136-06, ASTM International, West Conshohocken, PA.
- ASTM. 2007. Standard test methods for laboratory compaction characteristics of soil using standard effort. ASTM D 698-07, ASTM International, West Conshohocken, PA.
- ASTM. 2008. Standard practice for use of scrap tires in civil engineering applications. ASTM D 6270-08, ASTM International, West Conshohocken, PA.
- ASTM 2009. Standard test methods for laboratory compaction characteristics of soil using modified effort. ASTM D 1557-09, ASTM International, West Conshohocken, PA.

- Bosscher, P. J., Edil, T. B. and Eldin, N. N. 1992. Construction and performance of a shredded waste tire test embankment. Transportation Research Record 1345, National Research Council, Transportation Research Board, Washington, D.C., 44–52.
- Bosscher, P. J., Edil, T. B., and Kuraoka, S. 1997. Design of highway embankments using tire chips. Journal of Geotechnical and Geoenvironmental Engineering, 123(4), 295–304.
- Das, B. M. 2013. Fundamentals of Geotechnical Engineering. Global Engineering: Christopher M. Short, USA.
- Dickson, T.H., Dwyer D.F., and Humphrey D.N. 2001. Prototype tire-shred embankment construction. Transportation Research Record, 1755, National Research Council, Transportation Research Board, Washington, D.C., 160-167.
- Drescher, A., Newcomb, D. and Heimdahl, T. 1999. Deformability of shredded tires. Minnesota Department of Transportation, St. Paul, MN, USA.
- Drnevich, V. 1975. Constrained and shear moduli for finite elements. Journal of the Geotechnical Engineering Division, 101(5), 459-473
- Heimdahl, T. C. and Drescher, A. 1999. Elastic anisotropy of tire shreds. Journal of Geotechniques and Geoenvironmental Engineering, ASCE, 125, (5), 383-389.

- Humphrey, D. N. 2008. Tire Derived Aggregates as Lightweight Fill for Embankments and Retaining Wall. International Workshop on Scrap Tire Derived Geomaterials– Opportunities and challenges, Yokosuka, Japan, 59-81.
- Humphrey, D. N. and Sandford, T.C. 1993. Tire chips as lightweight subgrade fill and retaining wall backfill. Symposium on Recovery and Effective Reuse of Discarded Material and By-Products for Construction of Highway Facilities, Federal Highway Administration, Washington, DC.
- Humphrey, D.N., Whetten, N., Weaver, J., and Recker, K. 2000. Tire shreds as lightweight fill for construction on weak marine clay. Proceeding International Symposium on Coastal Geotechnical Engineering in Practice, Balkema, Rotterdam, The Netherlands, 611–616.
- Meles, D., Bayat, A., and Soleymani, H. 2013. Compression behavior of large-sized Tire Derived Aggregate for embankment application. Journal of Material in Civil Engineering, ASCE, 25(9), 1285-1290.
- Mills, B., and McGinn, J. 2010. Design, construction, and performance of highway embankment failure repair with tire derived aggregate. Transportation Research Record, 1345, National Research Council, Transportation Research Board, Washington, D.C., 90-99.
- Moo-Young, Sellasie, K., Zeroka, D., and Sabnis, G. 2003. Physical and chemical properties of recycled tire shreds for use in construction. Journal of Environmental Engineering, 129(10): pp. 921-929.

- Strenk, P.M., Wartman, J., Grubb, D.G., Humphrey, D. N., and Natale, M. F. 2007. Variability and Scale-Dependency of Tire Derived Aggregate. *Journal of Material in Civil Engineering*, ASCE, 19(3), 233-241.
- Tandon, V., Velazco, D.A., Nazarian, S. and Picornell, M. 2007. Performance monitoring of embankment containing tire chips: case study. *Journal of Performance of Construction Facilities*. ASCE, 21(3), 207-214.
- Tatlisoz, N., Benson, C. H., and Edil, T. B. 1997. Effect of fines on mechanical properties of soil-tire chip mixtures. Testing soil mixed with waste or recycled materials, *STP 1275*, M. Wasemiller, and K.Hoddinott, eds., ASTM, West Conshohocken, PA., 93–108.
- Warith, M.A., Sundhakar, M.R. 2006. Predicting the compressibility behavior of tire shred samples for landfill applications. *Journal of Waste Management*, (26), 268-277.
- Wartman, J., Natale, M.F., and Strenk, P.M. 2007. Immediate and time-dependent compression of tire derived aggregate. *Journal of Geotechnical and Geoenvironmental Engineering*, ASCE, 133 (3), 245-256

CHAPTER 4 INVESTIGATION OF TIRE DERIVED AGGREGATE AS A FILL MATERIAL FOR HIGHWAY EMBANKMENT

This paper was previously reviewed and published in the International Journal of Geotechnical Engineering. It is modified (formatting only) and presented as published part of this Ph.D. thesis as Chapter 4.

Reference: Meles, D., Bayat, A, Shaffi, M., H., Nassiri, S., and Gul, M. 2014. Investigation of Tire Derived Aggregate as a Fill Material for Highway Embankment. International Journal of Geotechnical Engineering, 8(2), 182-190.

CHAPTER 4 INVESTIGATION OF TIRE DERIVED AGGREGATE AS A FILL MATERIAL FOR HIGHWAY EMBANKMENT

ABSTRACT

This study investigates the compression behavior and performance of Tire derived aggregate (TDA) used to construct an 80 m long embankment for a highway test road in Edmonton, Alberta, Canada. The road contained four test sections made from passenger and light truck tires (PLTT), off-the-road (OTR) truck tires, TDA-soil mixture, and native soil. Thirty temperature probes and 25 settlement plates were embedded into the road to monitor the embankment. Falling Weight Deflectometer (FWD) test were also conducted under different load levels to determine the embankment material's deflection behaviour after the placement of the soil cover. Through observation, field data and FWD testing, it was determined that PLTT is more compressible than OTR and the TDA-soil mixture, and TDA-soil mix section showed equivalent performance with the control section. Additionally, all the temperature probes revealed no internal heating during the eight-month monitoring period.

INTRODUCTION

Tire derived aggregate (TDA) has proved useful for various civil engineering applications (Humphrey 2008). Tire derived aggregate is defined as “pieces of scrap tires that have a basic geometrical shape and are generally between 12 and 305 mm in size and are intended for use in civil engineering applications” (ASTM D6270 2008). Passenger and light truck tires (PLTT) refers to TDA made from

passenger, light, and multipurpose passenger vehicles with a rim diameter of up to 495 mm. Off-the-road (OTR) refers to TDA made from off-the-road tires with a rim diameter of up to 990 mm, typical of large industrial vehicles (ARMA 2012). Tire derived aggregate is lightweight, free-draining, and thermal resistive (several times higher than soil), and produce low earth pressure (Humphrey 2008). As the unit weight of TDA is approximately 1/3 to 1/2 of the unit weight of soil, it is a suitable alternative as lightweight embankment fill material, especially when the subgrade is weak and requires costly stabilization and modifications. Moreover, the use of TDA in civil engineering has economic and environmental significance, such as eliminating the need to store discarded tires in landfills.

Several field studies were conducted in the United States to identify the feasibility of using shredded tires as lightweight embankment fill in highway projects (Humphrey et al. 2000; Dickson et al. 2001; Edil 2004; Yoon et al. 2006; Tandon et al. 2007). These studies suggested that TDA can be used as lightweight fill material, and its placement and compaction can be easily performed with conventional construction equipment. However, embankments constructed with TDA should be designed to minimize the potential of internal heating. Design guidelines to control internal heating can be found in ASTM D 6270 (2008).

Passenger and light truck tires are commonly used in civil engineering applications (Strenk et al. 2007). This is primarily because of the availability of scrap PLTT and ease of production. However, in regions with heavy industrial and mining activities, such as the Province of Alberta, Canada, OTR tires have

become a significant source for TDA production. The capability of Albertan tire recycling industries to process all types of discarded tires into TDA as well as the growing stockpiles of discarded OTR tires have encouraged Alberta Recycling and Alberta Transportation to investigate TDA as embankment fill material for highway projects. The geometric properties of the OTR particles differ from PLTT in size, shape and thickness. To the best of the authors' knowledge, TDA made from OTR tires has not been used for highway embankment fill. Therefore, this study also intends to verify the feasibility of OTR tires as embankment fill for highway construction.

RESEARCH OBJECTIVES AND APPROACH

The primary objective of this study is to compare the characteristics of PLTT, OTR tires, TDA-soil mixture and native soil, including the ease of construction, field mixing of TDA and soil, vertical settlement, potential for internal heating and deflection under Falling weight deflectometer (FWD) testing.

The construction processes among the four sections with similar geometry were compared through observation and discussions with the operator and construction crew. During the duration of the embankment construction, activities were closely observed and all challenges reported by the operators were recorded.

Instrumentation was used to monitor and compare the change in temperature inside the fill and the vertical settlement among the different sections. The immediate and time-dependent settlement was measured using settlement plates. Temperature inside the fill sections was monitored using thermistors for signs of

internal heating. Lastly, once the subgrade was placed on top of the test embankment, FWD tests were performed along the embankment to compare the deflections between the four test sections.

PROJECT OVERVIEW

The test embankment was constructed for an access road project that connects the Anthony Henday ring road to the Edmonton Waste Management Center (EWMC) in Edmonton, Alberta, Canada. As stated previously, the test embankment has four sections and runs from east to west. The furthest east section is made of PLTT, which is the primary source of TDA. A smooth transition is provided from the existing ground to the PLTT test section by gradually increasing the TDA thickness from zero at station 130 + 067 to full at station 130 + 080. The second section is constructed with OTR tires, and the third is made of TDA-soil mixture (using native soil). Mixing TDA with soil can reduce the potential for internal heating and decrease the compressibility of TDA (Yoon et al. 2006); hence, the third section provides a transition zone to the adjacent normal ground. The last (furthest west) section of the test road is made from conventional fill (native soil) and serves as the control section.

MATERIALS

Tire derived aggregate

Prior to construction, the quantities of both types of TDA required for the embankment were estimated based on the geometry of the embankment and by assuming both TDAs had a compressed unit weight of 8.1 kN/m^3 (Mills and

McGinn 2010). The production of TDA took approximately two months, with PLTT provided by Liberty Tire Recycling Canada and OTR provided by CuttingEDGE Tire Recycling. The TDA was inspected visually during production to ensure the product contained minimal dust, and did not contain oversized or undersized pieces or foreign materials such as gasoline, grease, diesel fuel and oil. In addition, approximately 60 kg of TDA product for every 100 tonnes of recycled PLTT and 60 tonnes of recycled OTR was taken to the laboratory for sieve analysis.

Visual examination of samples taken during TDA production showed that TDA made from PLTT produced particles that were mostly thin and plate-like in shape, and TDA made from OTR tires produced particles that were thick and mostly irregular in shape. Figure 4.1 presents pictures of the PLTT and OTR used in the project. The samples were tested to confirm the gradation satisfied Type B TDA particle size requirements and other criteria advised by the American Standard for Testing and Materials (ASTM D6270 2008). Figure 4.2 presents typical particle size distribution for both the PLTT and OTR tested during the course of TDA production. Gradation tests were conducted in accordance with ASTM C136 (2006) using large-scale sieves, with sieve openings ranging from 6-308 mm. Observation and sieve analysis showed that both the PLTT and OTR satisfied the gradation requirements of Type B TDA. At least one side wall was severed from the tread of each tire, and both the bare metal fragments and the partially-encased steel wire satisfied the ASTM D6270 (2008) requirements. Overall, the

production was free from deleterious materials, such as grease, oil, diesel fuel and so forth.



Figure 4.1: Pictures of PLTT (left) and OTR (right) used in the project.

Soil

The soil excavated from the site during the construction of the test embankment was used for the PLTT-soil mix as well as the intermediate and top soil covers. The excavated soil was classified as Clayey Sand (SC) by the Unified Soil Classification System (USCS) and has liquid and plastic limits of 25 and 16 percent, respectively. Figure 2 presents the grain size distribution for the soil established in accordance with the ASTM C136 (2006) procedure. Moreover, the maximum dry unit weight of 18 kN/m^3 and optimum moisture content of 16.5 percent were determined for the soil in the laboratory following the ASTM D698 (2007) test procedure.

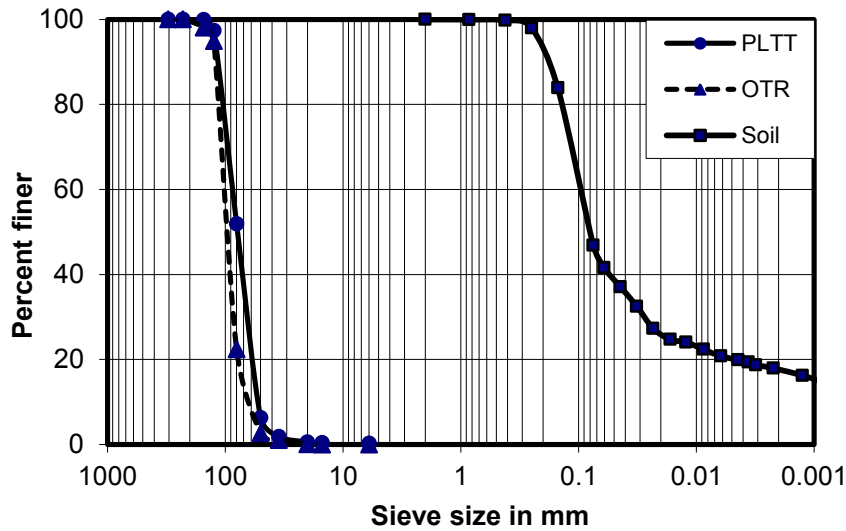


Figure 4.2: Grain size distribution of soil, PLTT and OTR used for the construction of the test embankment.

EMBANKMENT DESIGN

TDA sections

The TDA test sections were designed based on recommendations and guidelines available in Humphrey (2008) and ASTM D6270 (2008). To minimize the possibility of internal heating, the following features were considered in the design:

- The embankment was designed to contain two layers of TDA (top and bottom), each with an uncompressed thickness of 3m;
- Each 3-m-thick TDA layer was wrapped in a non-woven geotextile (Geotex 351 by Propex) that separates the TDA from the surrounding soil;
- Type B TDA ASTM D6270 (2008) was used;

- A minimum of 0.5-m-thick compacted mineral soil with a minimum of 30 percent fine was used as a separator between the two TDA layers;
- A minimum of 1-m-thick, low-permeability soil cover (including a minimum of 30 percent fines by weight) was used on the top and at the sides of the embankment above the natural ground;
- Both TDA layers were designed with three percent longitudinal slope at the base to allow water to drain out of the TDA and into the drain pipes installed at the bottom corner of each layer.

TDA and soil mixture section

The TDA (PLTT) and soil were mixed at a 50/50 ratio by volume (22/78 ratio by weight measured by taking samples of the TDA-soil mixture). The volume ratio was selected based on past experience with the TDA-soil mixture test for embankment by Yoon et al. (2006) and for ease of mixing during construction. PLTT was selected over OTR for the TDA-soil mixture due to its ample availability.

INSTRUMENTATION

The test embankment was instrumented with two types of geotechnical sensors to monitor and evaluate the construction process as well as the immediate and long-term performance of the embankment. Sensors were connected to a Campbell Scientific Corp. (Canada) CR1000 data logger that collected and recorded the data at 15-minute intervals. During the installation, the sensors were embedded in fine sand, and the wires were fed through flexible conduits to avoid any damage from the construction equipment and the TDA.

A total of 25 Vibrating Wire Liquid Settlement Systems (model SSVW105), calibrated and supplied by RST Instruments, were used to monitor the potential settlement of the embankment. Of the 25 settlement plates, seven were installed in each of the PLTT and OTR sections, six were placed in the TDA-soil mixture section, two were installed in the control section and the remaining three were installed on stable ground outside of the embankment section. These three settlement plates were used as references to correct the measurements from the others for daily changes in the atmospheric pressure. The settlement plates were installed at similar locations in the PLTT, OTR and mixture test sections as presented schematically in Figure 4.3. As seen in Figure 4.3, four settlement plates (SP 1 to SP 4) were placed on the bottom TDA layer to monitor the layer's settlement, and another three (SP 5 to SP 7) were installed on the top TDA layer. For the control section, the two settlement plates were installed at depth of 1.9 m from the finished level of the road.

Model 109AM-L thermistors, supplied by Campbell Scientific Corp. (Canada), were used to monitor the temperature changes at various depths of the embankment. A total of 18 thermistors, six in each section, excluding the control section, were utilized in the two layers.

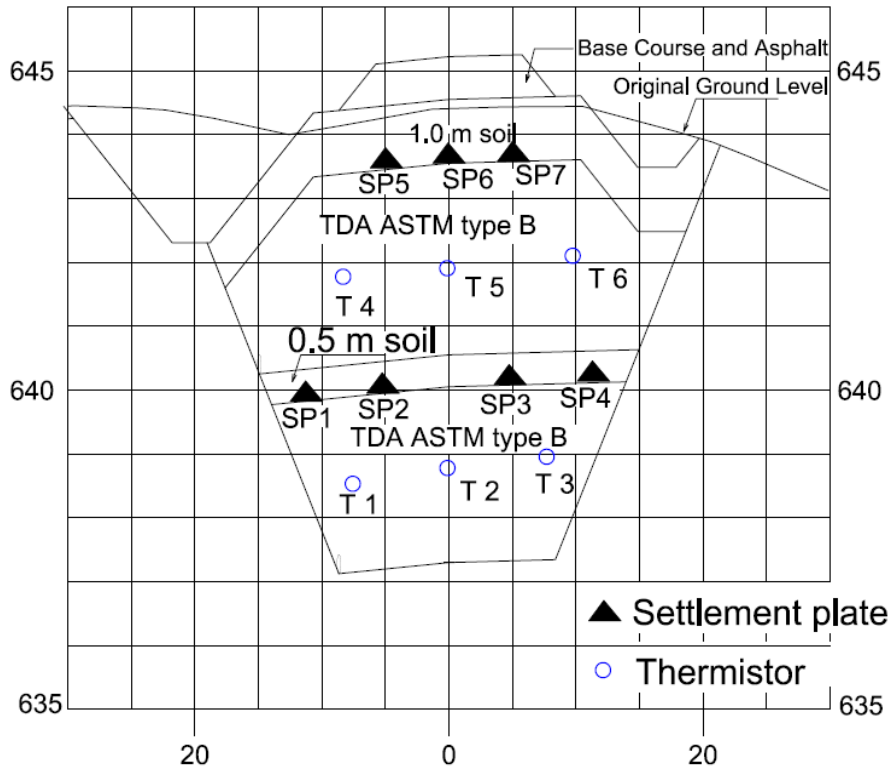


Figure 4.3: Typical cross section and instrumentation for the test embankment (all units in meters).

CONSTRUCTION

Mixing TDA and soil in the field

Mixing was performed at the site using a caterpillar excavator 345CL with a tooth-set edge bucket. The TDA and soil required for the mixture were placed near the pit in separate piles using a dump truck. The excavator then made a new pile using two buckets of TDA and two buckets of soil, which were mixed thoroughly until homogenous. Once homogeneity was obtained, the excavator prepared another TDA and soil mixture in a similar fashion by taking two buckets of TDA and two buckets of soil and adding it to the previous mix until the required volume of TDA-soil mix was achieved. At the time of mixing, the soil

moisture content was close to the optimum moisture content determined in the laboratory (16.5 percent). No segregation of the two materials was observed during mixing. Additional tests were conducted at the site to further check the homogeneity and volumetric ratio of TDA to soil during mixing and after spreading in the pit. For this test, a bucket of the TDA-soil mixture was randomly taken from the pile immediately following the mixing. Then, the TDA was separated from the soil by hand and loosely placed in another similar bucket. The loose volume of TDA and soil were compared to determine if there was a significant difference from the design volumetric ratio of TDA and soil in the mix. This test was also conducted on the TDA-soil mix already spread in the embankment. The test results indicated no significant difference in the volumetric ratio of the two materials; thus, the mixture had an acceptable level of homogeneity.

Construction process

Construction began by excavating a pit nearly 8 m deep and 60 m long, with a bottom width of 17 m and top width of 40 m. The total length of the test road is 80 m, with the last 20 m serving as the control section. During excavation, two soil profiles were revealed. The top 7 m of the test embankment contained Clayey Sand (SC) described under the “*soil*” section, while the bottom 1 m contained poorly graded sand with gravel classified as SP according to the USCS. Excavation was completed on May 15, 2012

When the excavation was complete, geotextile was spread at the bottom and on the side slopes of the excavation pit and was fixed to the ground using metal clips.

A minimum overlap of 0.6 m was maintained at every seam. Figure 4.4 shows the excavation pit covered with the geotextile. The first lifts of the TDA and TDA-soil mixture sections were then placed and spread over the geotextile.



Figure 4.4: Excavation for test embankment covered with geotextile at the bottom and on the side slopes.

Placement of TDA and TDA-soil mixture started on May 28, 2012, using conventional construction equipment. A caterpillar excavator 345CL was used for TDA and soil mixing and loading dump trucks. Three dump trucks transported the TDA from temporary storage nearby, which was approximately 800m away from the test site. The trucks also transported the soil for blending with the TDA and delivered the TDA-soil mixture to the test section. A caterpillar dozer D7R XR Series II was used to spread the TDA and the TDA-soil mixture to appropriate loose lifts. A combination of 500 mm and 300 mm loose lifts were used to place the TDA and the TDA-soil mixture. The 500 mm loose lift was used to avoid damage whenever the TDA or TDA-soil mixture was placed on top of the sensors. Additional precautions were taken to avoid damage from the construction equipment and the steel wires of the TDA by placing a layer of fine sand

underneath and on top of the sensors. The sensors installed inside the TDA layers were then further wrapped in a small piece of geotextile to avoid sand migration. A smooth drum vibratory caterpillar compactor CS-563D 109 kN was used to compact the loose lifts. For both the 500 mm and 300 mm loose lifts, six passes of the compaction equipment were completed to compact each lift in the three sections.

Observations during construction

The rate of construction was slow when placing and compacting the first two lifts as this was the first time the contractor had worked with TDA and TDA-soil mixture. However, as construction progressed, the operators became familiar with the material and continued without any major problems. No instances of tire puncture were reported during the construction. The dozer operator and the compactor operator were asked to compare the ease of construction for the three sections relative to the control section. Both operators rated PLTT as the most difficult among all sections, although it was found to be more compressible than OTR after compaction. They also stated that OTR was easier to work with compared to PLTT, and that the TDA-soil mixture was as easy as the conventional fill in the control section.

ANALYSIS OF FIELD DATA

In this section, the results and findings obtained from field data collected during construction and the monitoring phase are discussed. Based on the weight of three randomly selected truck loads and a record of load counts during construction, it was estimated that a total of 4,054 tonnes of PLTT and 2,548 tonnes of OTR were

used. Each tonne of TDA is derived from approximately 100 discarded PLTT and 20 discarded OTR tires. Thus, the project utilized an estimated 405,000 PLTT and 51,000 OTR tires, which is approximately 10 percent of the total scrap tires generated in Alberta every year (ARMA 2012). The unit weights for PLTT and OTR were computed using the geometry of the bottom TDA layer and the weight of TDA computed from load count at the end of the placement of the bottom TDA layer. The unit weights as the TDA compacted and compressed under its own weight were 7.6 and 8.1 kN/m³ for PLTT and OTR, respectively. The unit weight computed for the PLTT section is comparable to the unit weight measured in the previous project. TDA used for landslide repair project in southwest Oregon had a unit weight 7.2 kN/m³ at the end of compaction (Upton and Machan 1993).

Settlement of the test embankment

Settlement measurements were taken for the top and bottom TDA layers in the three test sections and at a depth of 1.9 m for the control section. These measurements were taken both during construction and after the placement of the asphalt layer. The settlement of the bottom TDA layers measured by SP 1 to SP 4 for the PLTT and OTR sections is presented in Figures 4.5 (a and b), respectively. Settlement of the top TDA layers measured by SP 5 to SP 7 for the PLTT and OTR sections is presented in Figures 4.5 (c and d), respectively. Settlement measurements are presented at five construction stages for the bottom layers and two construction stages for the upper layers. Stage 1 of construction corresponds to the time when the placement of the intermediate 0.5 m soil cap was finalized on June 7th; Stage 2 was completed on June 13th, when the top TDA layer reached

half its height; Stage 3 on June 20th corresponds to the placement of the top TDA layer; Stage 4 marks the placement of the top 1 m soil cover completed on July 17th; and Stage 5 is the period after the placement of the first asphalt layer on August 3rd. Post construction settlements corresponding to October 14th, December 1st and January 1st are also presented in Figure 5.

The settlements measured for the bottom TDA layers shown in Figures 4.5 (a and b) as opposed to the settlement seen for the top layers (Figures 4.5 (c and d)) were not uniform along the transverse direction for each section. The settlements measured by the two center settlement plates (SP 2 and 3) were higher than the measurements at the edges by SP 1 and 4. This behaviour is attributed to the geometry of the pit as seen in Figure 4.3, resulting in smaller amounts of the compressible TDA below SP 1 and 4 compared to SP 2 and 3.

According to Figures 4.5 (a and b) for both the PLTT and OTR sections, settlement increased as the stress level increased and the construction progressed. At all stages of construction the settlements measured in the PLTT section were higher than the measurements for the OTR section. The maximum settlement during construction for the bottom layer was observed in Stage 5 and is approximately 51 and 38 cm for the PLTT and OTR sections, respectively. It should be noted that the data for SP 3 on January 1st in Figure 4.5 (a) and SP 1 at Stage 2 on January 1st in Figure 4.5 (b) was not recorded. As presented in Figures 4.5 (c and d), the top TDA layers settled by 52 and 38 cm at Stage 5 for the PLTT and OTR sections, respectively. A possible explanation for the higher settlements of the PLTT section is that the OTR was derived from very large and thick tires.

This resulted in TDA particles with granular shapes as compared to the thin and plate-like PLTT particle shapes. The presence of more granular particle geometry in OTR may favor more efficient packing during compaction and resulted in smaller settlement compared to PLTT. This compression behavior was also observed during construction as well. OTR was stiffer than PLTT when construction equipment prepared for the next lift after the compaction.

The total settlement on October 14th, 2012, December 1st, 2012, and January 1st, 2013 for the PLTT and OTR sections are presented in Figures 4.5 (a-d). Unlike the settlement behaviours observed for the PLTT and OTR sections during construction, almost all of the settlement plates in the PLTT and OTR sections indicated additional time-dependent settlement after placement of the asphalt layer, are more for the OTR section compared to PLTT section during the monitoring period. As observed by Wartman et al. (2007), the magnitude of time-dependent compression of TDA is a function of layer height, time and TDA content. Since height and time is more or less the same for both PLTT and OTR, TDA content which is a function of compacted density, may contribute to higher time-dependent settlement in OTR compared to PLTT.

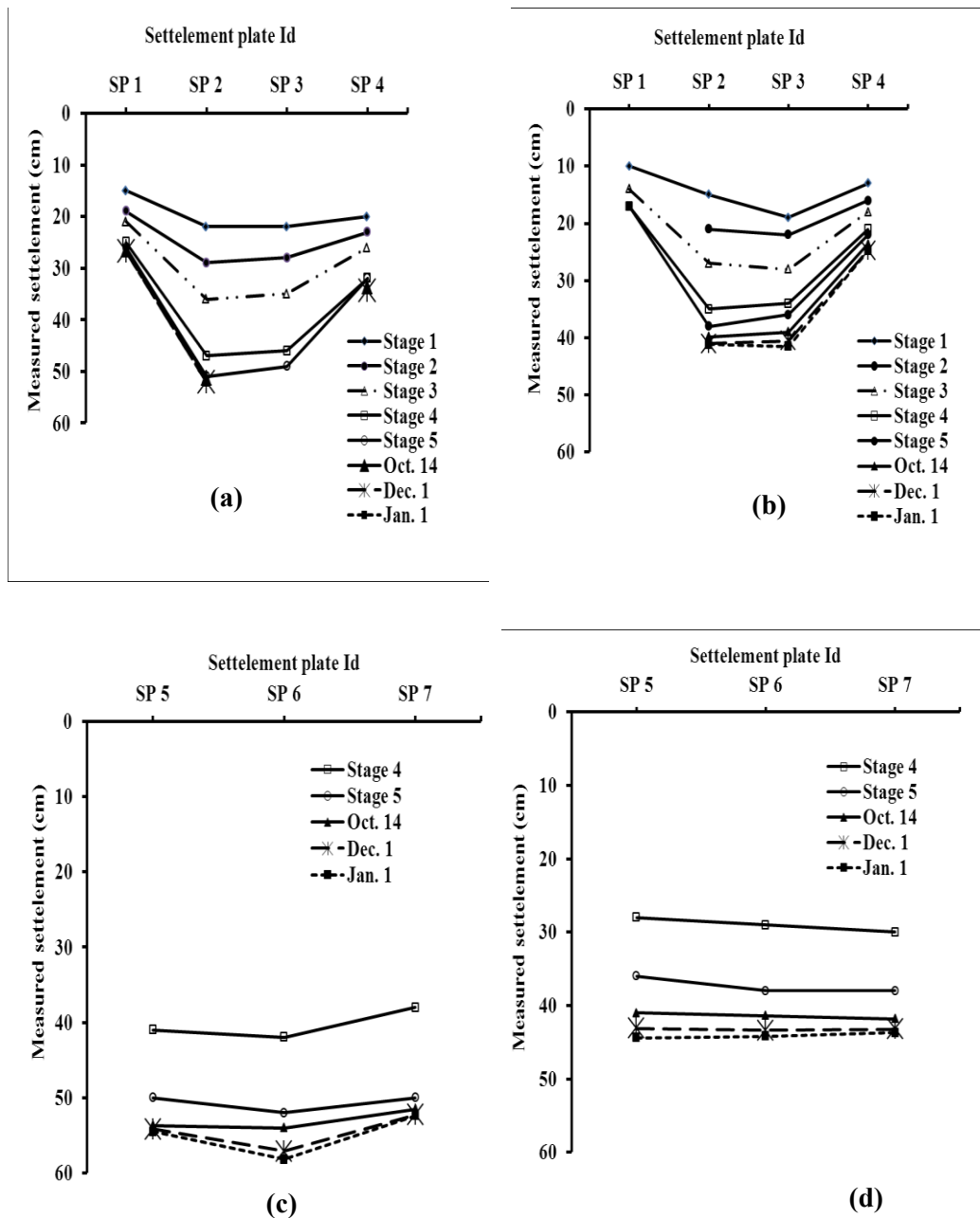


Figure 4.5: Settlement plate measurements for the: bottom layers of (a) PLTT and (b) OTR sections, and top layers of (c) PLTT and (d) OTR sections.

The short-term settlement may be of little practical significance as this settlement would occur prior to the completion of construction. Time-dependent settlement that occurs after placement of settlement sensitive structures, such as pavement,

requires consideration (Wartman *et al.* 2007). For this project, visual assessment of the road condition was conducted six months after placement of the first 160 mm Asphalt Concrete (AC) layer. During the visual assessment, a transverse crack was observed extending along the road at the east side of the embankment before the PLTT section. No other distresses were noted in the AC layer during the assessment. The transverse crack seemed to be related to the immediate placement of the AC layer in combination with the time-dependent settlement observed in PLTT and OTR sections. However, for this project to mitigate the potential effect of the embankment settlement on the long term performance of the pavement, such as the transverse crack, stage paving over two years is used. The first AC layer was placed immediately upon completion of the embankment construction, followed by the final AC layer to be placed in year two. Any distresses that occur in the first AC layer will be repaired before the placement of the final AC layer in the second stage of construction.

Settlement plates in the TDA-soil mixture section and the control section did not show significant settlement compared to the OTR and PLTT sections. The maximum settlement for the TDA-soil mixture section was measured at 4 and 3.5 cm for the top and bottom layers at Stage 5, respectively. For the TDA-soil mixture section, the soil filled the void space between the TDA particles; hence, the compression was significantly reduced. The settlement plates on the TDA-soil mixture section in stage 5 indicated that the addition of 50% soil (by volume) to PLTT reduced the compressibility of the mixture by 90% due to the addition of the 1 m soil cover. Lastly, a maximum settlement of 4 cm was measured for the

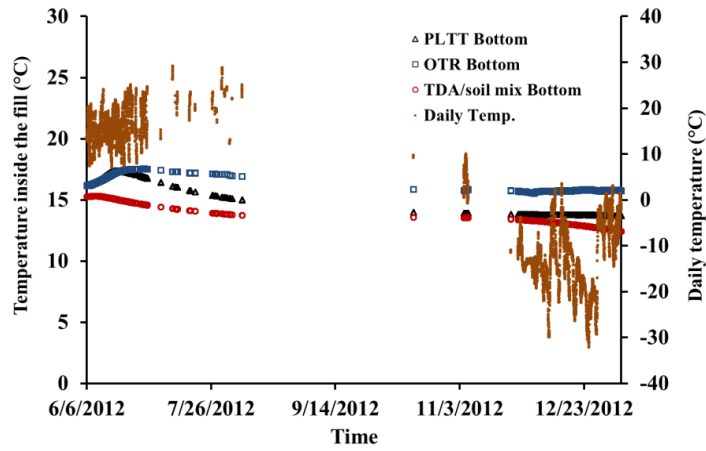
control section during construction. Most of the settlement in control and mix sections occurred during the construction, and negligible settlement occurred after the placement of the asphalt layer.

Temperature change in the test embankment

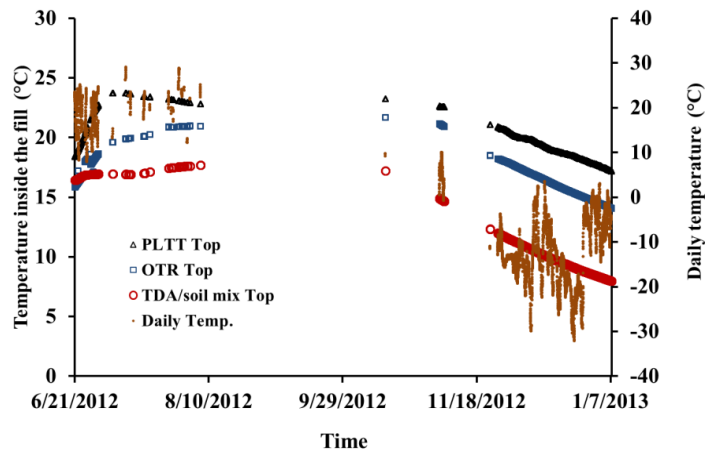
Monitoring the temperature variation in the TDA was of special interest to the project as internal heating within thick tire shred fills has been reported in literature (Humphrey 2004). The temperature measurements from June 2012 to January 2013 are presented in Figures 4.6 (a) and (b) for the bottom and upper layers in PLTT, OTR and TDA-soil mixture sections, respectively. Temperature values presented in Figure 6 for the bottom and top TDA layers are the average of T1 to T3 and T4 to T6 (in Figure 4.3), respectively. For comparison, the average daily ambient temperature during the monitoring period from the weather station located at the EWMC site is also plotted in Figures 4.6 (a) and (b). It should be noted that the data was not recorded at the site from mid-August to mid-October because power was unavailable for the data logger.

The temperature measurements for the three TDA sections indicated no internal heating during the monitoring period. For the bottom layer, temperature after placement of the asphalt layer stabilized at approximately 16 °C for PLTT and 14 °C for OTR and TDA-soil mixture sections. In all three sections, the temperature measurement for the top layer shows a decreasing trend during the monitoring period. The TDA-soil section showed the lowest temperature in both layers. The low temperature observed for the TDA-soil section during construction may have been due to wet soil used in the mixture. Each of the sensors in the three sections

showed high temperature during the summer, with the highest temperature measured in the top layer. Conversely, during the winter, all sensors showed higher temperatures in the bottom TDA layer and lower temperatures in the upper layer.



(a)



(b)

Figure 4.6: Temperature measurement for PLTT, OTR and TDA mixed with soil sections: (a) bottom layer and (b) upper layer.

FWD test results

FWD tests were conducted on top of the 1-m soil cover before the placement of the asphalt layer. Dynatest FWD was used to apply four load drops using a 300-

mm diameter load plate, resulting in target load magnitudes of 5.8, 8.1, 10.0 and 12.4 kN. The deflections were measured using seven geophones located at 1200, 900, 600, 450, 300, 200 and 0 mm from the center of the load plate. The tests were conducted at approximately 5-m intervals along the test sections. As the FWD test was applied directly on top of the subgrade layer (opposed to typical FWD tests conducted on top of the pavement surface), the maximum loads were chosen to represent the amount of stress reaching a typical subgrade layer in a full pavement structure, including an asphalt concrete, a base, and a subgrade layer. A linear elastic analysis program (KENLAYER) (Huang, 1993) was used to calculate the stress on top of the subgrade under a standard 18 kip (80kN) single wheel load. Moreover, the maximum load was adjusted during field testing so that it would not pass the deflection limit of the FWD deflection sensors due to the presence of highly compressible TDA fill below the subgrade. According to the Standard Guide for Calculating In-Situ Equivalent Elastic Moduli of Pavement Materials Using Layered Elastic (ASTM D5858–96), individual deflections must be normalized by the ratio of the reference load to the actual load when the applied loads vary by more than five percent of the reference loads. Normalization also gives the advantage of comparing the deflection among the four sections to the same scale of load (the reference load rather than the actual load applied on the load plate).

Figure 4.7 presents the reference loads versus the average normalized central deflections corresponding to the middle 10 m of each section along the centerline. According to Figure 4.7 the PLTT section, which was deemed as highly

compressible during construction, shows maximum deflections for the range of the load applied in comparison to the other three sections. The deflection for all range of loading is a minimum for the control section. Figure 4.7 also shows that under the 5.8-kN load, the central deflection for the PLTT, OTR, and TDA-soil mixture sections was nearly 5.6, 2.4, and 2 times the corresponding deflection measured for the control section, respectively. Similarly, under the 12.4-kN load, central deflection for the PLTT, OTR, and TDA-soil mixture sections was nearly 4.3, 2.3, and 2 times that of the corresponding deflection in the control section, respectively. The normalized deflection values at seven sensor locations measured under the maximum applied load (12.4 kN) is presented in Figure 4.8. The data on the deflection basin in Figure 4.8 also indicate relatively weaker subgrade resilient on PLTT and OTR section compared to TDA-soil mixture and control section.

FWD tests are performed regularly to monitor the seasonal and long-term performance of the embankment. The FWD tests conducted in stage one of construction will be used for the design or design modification in the final stage asphalt layer construction. Final AC thickness will be established through FWD tests based on the structural evaluation of the asphalt layer placed in the first stage of construction. Paving is scheduled to be finalized in stage two of construction by placing another AC layer.

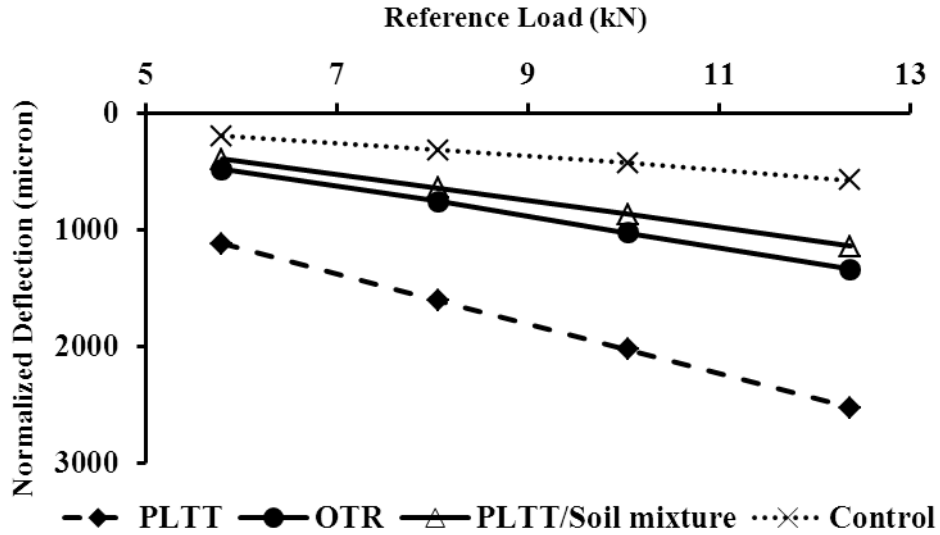


Figure 4.7: Peak deflections beneath the center of the FWD loading plate for different load drops.

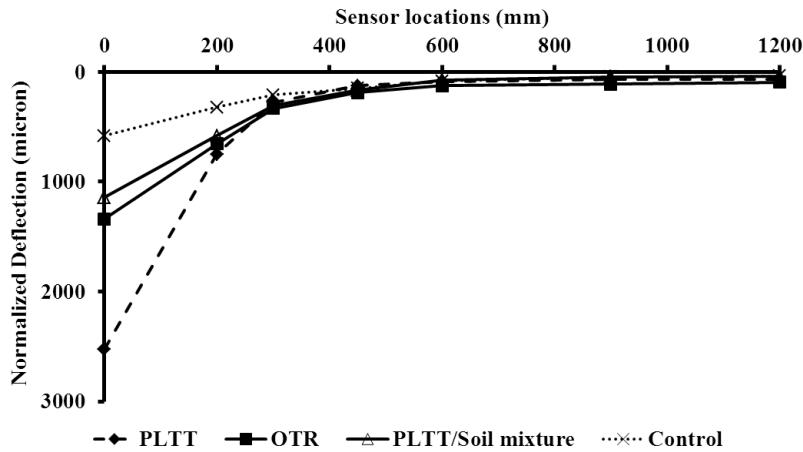


Figure 4.8: Normalized deflection basins under the maximum applied load (12.4 kN) for the four sections.

CONCLUSIONS

A test embankment containing four different sections composed of PLTT, OTR, TDA-soil mixture, and native soil was constructed for an access road to the EWMC in Edmonton, Alberta. The embankment was instrumented with various

geotechnical sensors to compare the different sections with respect to ease of construction, field mixing of TDA and soil, immediate compression, and susceptibility to internal heating and stiffness. Based on the investigation and analysis of the instrumentation data, the following observations and conclusions were drawn:

- The construction of the test embankment was completed with conventional construction equipment and without any major problems.
- Observations during construction showed that PLTT after compaction was more compressible than OTR.
- The unit weights computed based on the truck count indicated that both PLTT and OTR were lightweight, with unit weight as compacted and compressed by its weight was less than half the unit weight of normal soil fills.
- Settlement measurements indicated that PLTT and TDA-soil mixture sections show the maximum and minimum settlements at the end of the construction, respectively. Settlement measurement after completion of the asphalt layer indicated the additional time-dependent settlement was greater in the OTR section than the PLTT section.
- The TDA-soil mixture shows performance equivalent to the normal fill used in the control section; however, it requires additional activity to mix the TDA with soil.
- No evidence of internal heating was detected by the thermistors during the eight-month monitoring time for all three TDA sections.

- The FWD test results showed that the PLTT section gave maximum deflection under various load levels applied during testing.
- Stage paving can be used to mitigate any potential distresses (cracking or rutting) that will affect long term performance of the pavement.

REFERENCES

- Alberta Recycling Management Authority. 2012. Tire Recycling Program. [online] Available at: <<http://www.albertarecycling.ca/>> [Accessed on June 10, 2012].
- ASTM. 2006. Test method for sieve analysis of fine and coarse aggregates. ASTM C136–06, ASTM International, West Conshohocken, PA.
- ASTM. 2007. Test method for laboratory compaction characteristics of soil using standard effort. ASTM D 698-07, ASTM International, West Conshohocken, PA.
- ASTM. 2008. Standard practice for use of scrap tires in civil engineering applications. ASTM D 6270-08, ASTM International, West Conshohocken, PA.
- ASTM. 2008. Standard Guide for Calculating In Situ Equivalent Elastic Moduli of Pavement Materials Using Layered Elastic Theory. ASTM D5858 - 96, ASTM International, West Conshohocken, PA.
- Dickson, T.H., Dwyer D.F., and Humphrey D.N. 2001. Prototype tire-shred embankment construction. Transportation Research Record 1755, National

Research Council, Transportation Research Board, Washington, D.C.,
160-167.

Edil, T. B. 2004. A review of mechanical and chemical properties of shredded tires and soil mixtures. Recycled Materials in Geotechnics: Sessions at ASCE Civil Engineering Conference and Exposition, 1-21(ASCE, Baltimore, MD).

Huang, Y.H. 1993. Pavement Analysis and Design. Prentice-Hall Englewood Cliffs, New Jersey.

Humphrey, D.N. 2004. Effectiveness of design guidelines for use of tire derived aggregate as light weight embankment fill. Recycled Materials in Geotechniques, 61-74(ASCE, Baltimore, MD).

Humphrey, D. N. 2008. Tire derived aggregates as lightweight fill for embankments and retaining wall. International Workshop on Scrap Tire Derived Geomaterials– Opportunities and challenges, 59-81. (Yokosuka, Japan).

Humphrey, D.N., Whetten, N., Weaver, J., and Recker, K. 2000. Tire Shreds as Lightweight Fill for Construction on Weak Marine Clay. Proceeding International Symposium on Coastal Geotechnical Engineering in Practice, 611–616. (Balkema, Rotterdam, The Netherlands).

Mills, B., and McGinn, J. 2010. Design, Construction, and Performance of Highway Embankment Failure Repair with Tire derived Aggregate.

Transportation Research Record, 1345, National Research Council,
Transportation Research Board, Washington, D.C., 90-99

Strenk, P.M., Wartman, J., Grubb, D.G., Humphrey, D. N., and Natale, M. F.
2007. Variability and Scale-Dependency of Tire Derived Aggregate.
Journal of Material in Civil Engineering, ASCE, 19(3), 233-241.

Tandon, V., Velazco, D.A., Nazarian, S. and Picornell, M. 2007. Performance
monitoring of embankment containing tire chips: case study. Journal of
Performance of Construction Facilities, ASCE, 21(3), 207-214.

Upton, R. J. and Machan, G. 1993. Use of shredded tires for lightweight fill.
Transportation Research Record, 1422, National Research Council,
Transportation Research Board, Washington, D.C., 36-45.

Wartman, J., Natale, M.F., and Strenk, P.M. 2007. Immediate and time-dependent
compression of tire derived aggregate. Journal of Geotechnical and
Geoenvironmental Engineering, ASCE, 133 (3), 245-256.

Yoon, S., Prezzi, M., Sidiki, N.Z., Kim, B. 2006. Construction of test
embankment using a sand-tire shred mixtures as fill material. Journal of
Waste Management, 26, 1033-1044.

CHAPTER 5. PERFORMANCE OF HIGHWAY EMBANKMENT CONSTRUCTED FROM TIRE DERIVED AGGREGATE

This paper was submitted and under review for possible publication in the International Journal of Geomechanics (ASCE). It is modified (formatting only) and presented as submitted for possible publication part of this Ph.D. thesis as Chapter 5.

Reference: Meles, D., Yi, Y. and Bayat, A. 2014. Performance of highway embankment constructed from tire derived aggregate. International Journal of Geomechanics (ASCE). Under review for possible publication.

CHAPTER 5. PERFORMANCE OF HIGHWAY EMBANKMENT CONSTRUCTED FROM TIRE DERIVED AGGREGATE

ABSTRACT

To evaluate the performance of Tire Derived Aggregate (TDA) for use as highway embankment fill material, a test embankment was constructed in Edmonton, Alberta Canada. The test embankment was 80 m in length and contained four different test sections, each 20 m in length. The four test sections consisted of embankment material made from Passenger and Light Truck Tires (PLTT), Off-The-Road (OTR) truck tires, TDA-soil mixture, and soil without TDA. The test embankment was built using a staged construction approach, which is a common highway construction practice in Alberta. Visual assessment and Falling Weight Deflectometer (FWD) tests following the placement each pavement layer (subgrade, base course, and asphalt) were conducted, and field settlement data was collected. Settlement plates placed on top of the bottom and upper TDA layers in the PLTT and OTR sections measured the layer's maximum strains following construction; the measurements were 17 and 12 percent for the PLTT section, and 12.6 and 8.6 percent for OTR section. Moreover, the PLTT and OTR sections showed slight time-dependent deformation. However, deflection data and mean back-calculated subgrade modulus from FWD tests performed after construction indicate that the TDA fill showed satisfactory performance as highway embankment fill.

INTRODUCTION

Tire Derived Aggregate (TDA) has beneficial engineering properties; it is light-weight, and has high hydraulic conductivity and thermal insulation. Due to these properties and its widespread availability, TDA has been used as fill material for numerous highway projects (Humphrey et al. 2000; Dickson et al. 2001; Mills and McGinn 2010), and has also been mixed with soil for similar applications (Zornberg et al. 2004; Yoon et al. 2006; Tandon et al. 2007). These studies have shown that mixing TDA with soil has the advantage of reducing TDA's high compressibility. Using TDA requires knowledge of its short-term and long-term compression behavior. The short-term compression behavior may be of little significance, as deformation would occur prior to the completion of the construction. However, the long-term compression behavior is significant as it affects the road's serviceability and performance (Wartman et al. 2007).

Previous studies evaluated the time-dependent deformation behavior of TDA or TDA-soil mixture in the laboratory (Wartman et al. 2007; Humphrey 2008) and in the field (Dickson et al. 2001; Mills and McGinn 2010). These studies indicate that TDA continues to deform over a period of time well beyond the initial application of load. Wartman et al. (2007) illustrated that time-dependent deformation of TDA-soil mixture was largely a function of TDA content and time. In practice, time-dependent deformation is addressed by placing a surcharge load for a defined period of time before constructing settlement-sensitive components of the road (Humphrey et al. 2000). However, various case studies

showed that time-dependent deformation may continue for one to two years and can approach strains of 5 percent or more (Wartman et al. 2007).

Most new pavement structures in Alberta, Canada are built using the staged design and construction concept that operates by testing the roadway as it is built (Pavement Design Manual, 1997). The construction of new pavement in Alberta is usually completed in two stages. The first stage includes all construction leading up to, and including, the placement of the first asphalt layer. The second stage, which occurs a year or more after the first, includes the placement of the final asphalt layer. Staged construction is advantageous as it can use the structural evaluation of the first asphalt layer (first stage) to determine the design and modification of the second asphalt layer (second stage). Additionally, staged construction also has the advantage of reducing a roadway's lifecycle costs.

The use of Falling Weight Deflectometer (FWD) data to evaluate the structural capacity of pavement during staged construction has gradually become common practice in Alberta, Canada (Pavement Design Manual, 1997). Since 1992, pavement structural evaluation has been performed through the province based exclusively on FWD data (Pavement Design Manual, 1997). An FWD is a trailer-mounted device that measures the deflection of the pavement under a simulated vehicular load. The instantaneous deflection of the road surface is measured at a number of points at different distances moving radially outward from the center of the falling weight. Thus, the shape of the deflection bowl is obtained. Information on the structural condition of the pavement can be extracted from analysis of the FWD data. The measured deflection can be used to back-calculate the stiffness of

various pavement structural layers (Zhou et al. 1997; Rahim et al. 2003; Mehta and Roque 2003; Mohanty and Chugh 2006; Tao et al 2008). The ability to predict stiffness of various pavement structures allows engineers to evaluate its structural capacity and long-term performance. Moreover, Deflection Basin Parameters (DBPs), which are derived from FWD deflection measurements, are good indicators of selected pavement properties and conditions. Their effective use in pavement analyses, instead of relying on deflection measurements alone, has been documented in literature (Horak and Emery 2009; Horak et al. 2008; Xu et al. 2002). In this paper, apart from the backcalculated moduli computed via available commercial software, deflection basin parameters, such as Maximum Deflection (Do), Base Layer Index (BLI), Middle layer Index (MLI) and Lower Layer Index (LLI), are used to evaluate the pavement structural condition.

PURPOSE AND SCOPE

The objective of this study is to evaluate the field measured deformation and performance of an experimental test embankment that used TDA produced from Passenger and Light Truck Tire (PLTT), Off-The-Road (OTR) truck tires, TDA-soil mixture, and soil without TDA. Settlement plates installed on the top of the various TDA layers have provided measurements used to compute the field deformation. The pavement's performance is evaluated by comparing FWD data measured on the various TDA sections with that measured on a control section constructed from soil alone. The scope of this study includes analysis of settlement data measured in the field for one year, FWD test data performed on

the top of the subgrade and base course during construction, FWD test data performed on the first stage asphalt, and visual assessment of the test sections.

OVERVIEW OF THE TEST EMBANKMENT

The test embankment was part of an access road project that connects the Anthony Henday ring road to the Edmonton Waste Management Center (EWMC) in Edmonton, Alberta, Canada. This road is 80 m long, and contains four different test sections, each 20 m long. The four test sections are made of: 1) TDA from PLTT that includes passenger, light, and multipurpose passenger vehicles, with a rim diameter up to 49.5 cm (ARMA 2012); 2) TDA from OTR that includes discarded tires designed for use on vehicles or large equipment used in construction activities, with a rim diameter up to 99 cm (ARMA 2012); 3) TDA from PLTT mixed with soil at a 50/50 ratio by volume; and 4) a control section made from soil. The control section was used as a reference to determine the performance of the TDA fill sections. The soil used for the TDA-soil mixture and as subgrade in control sections is a fine-grained soil obtained from the site during excavation. It is classified as Clayey Sand (SC) by the Unified Soil Classification System (USCS) and has liquid and plastic limits of 25 and 16 percent, respectively.

The TDA used in the construction of the PLTT, OTR and TDA-soil sections is Class II fill (coarse TDA with a maximum size of 300 mm for fill from 1 to 3 m thick) according to ASTM D 6270-08 (ASTM 2008). Visual observation of samples taken during TDA production showed that PLTT contained TDA particles that are mostly thin and plate-like in shape, while OTR contained TDA

particles that are thick and mostly irregular in shape. Both PLTT and OTR satisfy the requirements of Type B TDA (ASTM 2008). Excavated soil from the site was used as intermediate and top soil cover. The embankment is instrumented with various geotechnical instruments, which are connected to a data logger that collects and records data in 15-minute intervals. However, only the settlement data collected from Vibrating Wire Liquid Settlement Systems (model SSVW105) will be discussed in this study. Further details on the material properties for TDA and soil, and field instrumentations are given in Meles et al. (2014a).

Each test section, with the exception of the control, contained TDA or TDA-soil mixture placed in two layers, each 3 m-thick with a 0.5 m thick soil cap for separation, a 1 m thick soil cover, a 45 cm base course and a 16 cm first stage asphalt layer. The design thicknesses specified for the various pavement sections did not include compression that occurred during construction. The change in thicknesses was significant for the PLTT and OTR sections. As reported by Meles et al. (2014a) the upper TDA layer in the PLTT and OTR sections settled by 42 and 28 cm after placement of the top soil cover, and 8 and 7 cm after placement of the base course material, respectively. Thus, the final thickness for the top soil cover was 1.42 and 1.28 m and base course was 53 and 52 cm at the end of construction for the PLTT and OTR sections, respectively. Figure 5.1 presents a typical cross section and the settlement plate locations of the test embankment.

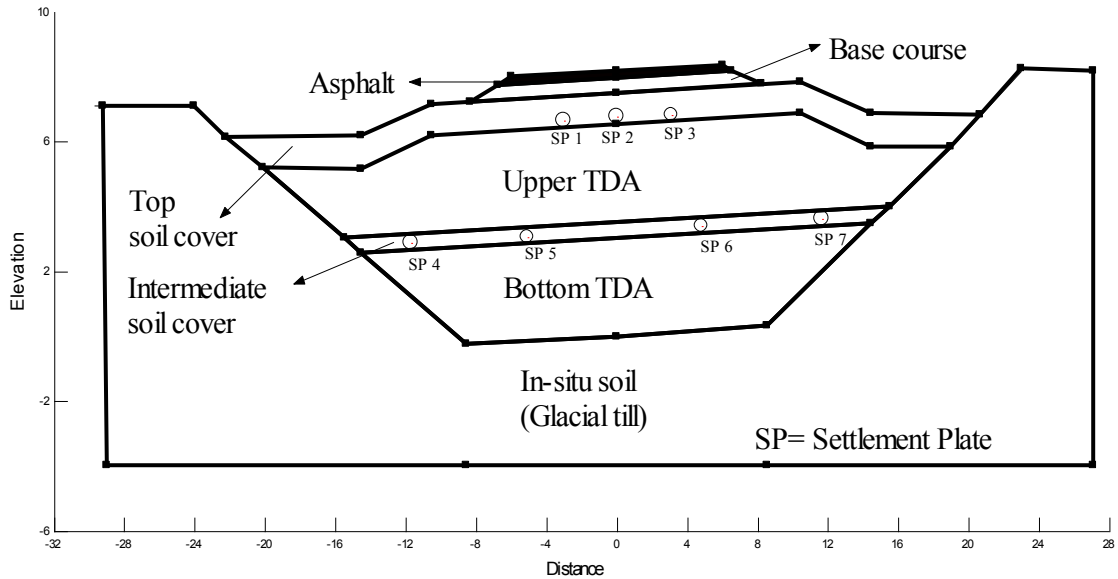


Figure 5.1: Typical cross section and instrumentation for the test embankment (all units in meters).

The TDA and TDA-soil mixture embankments were placed using conventional construction techniques. First, the geotextile was placed on the prepared base and the TDA or TDA-soil mixture was spread in 300 or 500 mm loose lifts using a caterpillar D7R XR series II dozer. A 500 mm loose lift was used whenever the TDA or TDA-soil mixture was placed on top of instrumentation to avoid damaging the sensors. Each lift was then compacted with six passes of a smooth drum vibratory caterpillar CS 563D 109 kN compactor.

IMMEDIATE SETTLEMENT DURING CONSTRUCTION

The settlement during construction was monitored by settlement plates installed on the top and bottom TDA or TDA-soil mixture layers, as shown in Figure 5.1. Only two data sets collected by the plates will be discussed in this study: those

that measured compression during construction and time-dependent settlement after construction.

TDA experiences immediate compression under an applied load, such as the weight of an overlying soil cover or pavement structure, which was measured by the settlement plates. The settlement was converted to strain by dividing the measured settlement by the initial thickness of the TDA or TDA-soil layer, which was assumed to be the design thickness of 3 m. As the foundation soil at this site is firm, little settlement was expected and the measured settlements were assumed to be from compression of the TDA. The maximum strain measured by settlement plates on top and bottom TDA layer in the PLTT and OTR sections was 12 and 17 percent, and 8.6 and 12.6 percent, respectively. Settlement plates in the TDA-soil section and the control section did not show significant settlement compared to the OTR and PLTT sections. The maximum strain measured by settlement plates on top of the bottom TDA-soil layer was 1.3 percent. The magnitude of strain computed for the PLTT section was comparable to the settlement measured in previous studies; PLTT used as approach embankment fill in the Main Turnpike in Portland, Main, U.S.A had 15.6 and 9.9 percent average strain for the lower and upper TDA layers following placement (Humphrey et al. 2000). The embankment fill in the Main Turnpike Portland contained two layers of TDA each with thickness 3 m, and topped with 1.22 m of granular soil and 1.22 m of temporary surcharge.

TIME-DEPENDENT SETTLEMENT

The time-dependent settlement measured after placement of the first stage asphalt layer between August 3, 2012 and September 1, 2013 is presented in Figure 5.2. The settlements are the average measurements collected by the three settlement plates placed on top of the upper TDA layer in the PLTT and OTR sections. The total time-dependent settlements occurred in one year period following the placement of the asphalt layer were 5.2 and 6.1 cm for the PLTT and OTR sections, respectively. A majority of this total time-dependent settlement, about 66 percent for PLTT and 68 percent for OTR section occurred in the first two months following the placement of asphalt layer. The magnitude of time-dependent settlement for the PLTT section is comparable to the settlement measured in previous studies. PLTT used for the repair of highway embankment failure in New Brunswick, Canada had approximately a 4.3 cm time-dependent settlement three months after completion of the project (Mills and McGinn 2012). The final driving surface for the highway embankment used in New Brunswick was designed to accommodate approximately 2.2 m of separation between it and the top of the TDA. Settlement plates in TDA-soil and control sections did not show any measurable time-dependent settlement. Figure 5.2 also shows that the settlements measured from January 1, 2013 to May 1, 2013 were higher than the settlement measured after May 1, 2013 for both PLTT and OTR sections. The reference settlement plate and the reservoir for the Vibrating Wire Liquid Settlement Systems (model SSVW105) were placed on stable ground on the side of the embankment 50 cm below the ground surface. The increase in settlement during the time period (January to May) may be related from frost heave of the

ground occurring around the reference settlement plate and the reservoir from the cold winter.

A review of the settlement data indicates time-dependent settlement in PLTT and OTR sections continued to occur well beyond the initial load application. However, only an additional settlement of 1.8 and 1.9 cm in PLTT and OTR sections, respectively, occurred after 2 months; settlements of this magnitude are likely to be tolerable for many geotechnical structures. Previous practice by Humphrey (2000) in addressing time-dependent settlement requires a minimum of eight weeks to elapse after TDA placement before constructing settlement-sensitive components, such as pavement. This practice may be applicable if the time-dependent settlement that occurs after 2 months is deemed tolerable for a given project. The staged construction approach used for highway construction in Alberta can also be used to address time-dependent settlement of TDA. Most time-dependent settlement occurs in the first construction stage, and any resultant distresses can be repaired before the placement of the final asphalt layer in the second stage. The data in this study also indicates that the addition of 50 percent soil by volume to the TDA highly reduces the time-dependent settlement.

Visual assessment of the road condition was conducted six months and one year after placement of the first stage asphalt layer. During the first visual assessment, a transverse crack, as shown in Figure 5.3, was observed, extending along the road where the PLTT section begins. No other distress was noted in the asphalt layer of the various test sections during this assessment. During the second visual assessment, no additional distress was noted. The transverse crack seemed to be

related to the immediate placement of the asphalt layer in combination with the time-dependent settlement observed in the PLTT sections. However, for this project to mitigate the potential effect of the embankment settlement on the long-term performance of the pavement, such as the transverse crack, staged paving was used. The first asphalt layer was placed immediately upon completion of the embankment construction, followed by the final asphalt layer. Any distresses that occur in the first asphalt layer were repaired before the placement of the final asphalt layer in the second stage of construction on September 4, 2013.

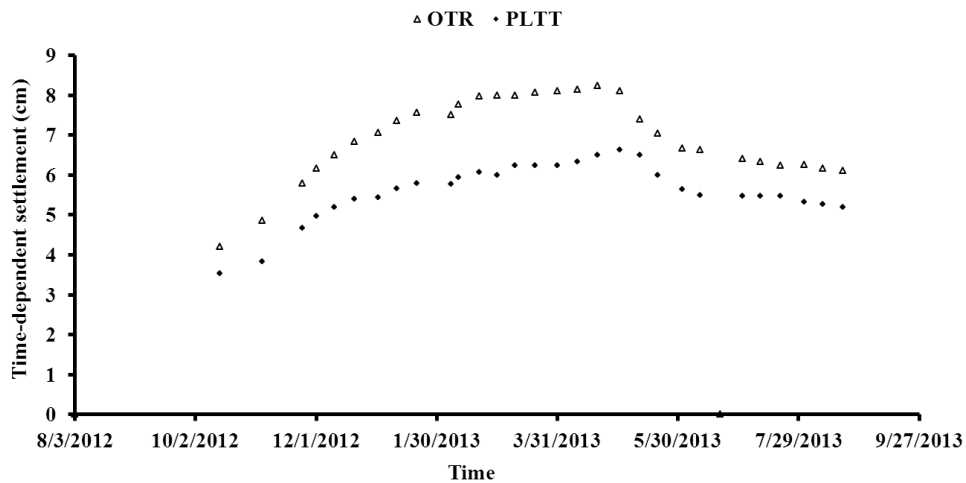


Figure 5.2: Time-dependent settlement for PLTT and OTR sections.



Figure 5.3: Photo of transvers crack observed at the start of the PLTT section.

FALLING WEIGHT DEFLECTOMETER (FWD) TESTING

A dynast FWD with a load plate diameter of 300 mm was used to perform FWD tests in this study. The FWD had nine deflection sensors placed at radial offsets from the center of the load plate. These deflection sensors were located at a distance of 0, 200, 300, 450, 600, 900, 1200, 1500, and 1800 mm away from the center of the load plate. These were fixed during the deflection testing program. FWD tests were conducted upon the completion of each pavement layer (subgrade, base course, and asphalt), and four FWD tests were performed on the first stage asphalt layer for post-construction structural performance evaluation. FWD tests on the first stage asphalt layer were conducted shortly after its placement on August 15, 2012, and the additional four tests on May 31, July 3, July 30, and finally on August 28 of 2013 before placement of the final stage asphalt layer.

The subgrade contained highly compressible TDA at shallow depth. Considering the vertical stress' ability to reach the top of the subgrade layer during traffic load, smaller FWD load drops were used. The following approximate load weights were applied: 5.8, 8.1, 10.0, and 12.4 kN. For FWD tests conducted on top of the base course and first stage asphalt layer, three consecutive load drops, approximately 21, 31 and 40 kN, and 27, 40 and 53 kN were applied, respectively. As 40 kN was the standard for pavement design and for comparison on the same base line, only the data from the 40 kN drop was used for FWD data analysis on top of the base course and asphalt layer. The tests were performed on the outer wheel path and center line of the road at 5 m intervals; this resulted in six test points per section.

PRE-SCREENING OF DEFLECTION DATA

The need to check for irregular deflection basin from raw FWD data has been discussed by Xu et al. (2002), Stubstad et al. (2000), and Rahim and George (2003). In this study, FWD tests were conducted on pavement underlined by different materials with various degrees of compressibility; the evaluation of the structural capacity of the pavement structures was based on collected FWD data. Thus, it is important to first check whether the deflection basin data is regular before performing the deflection analysis. Two criteria are used to identify the anomalous deflection basin. The first criterion used was proposed by Xu et al. (2002) as follows:

$$D_i < D_{i+1}, i = 1, 2, 3 \dots 9$$

Where D_i = the i^{th} sensor deflection, with D_1 = the deflection below the center of the load plate.

This criterion was used to check the deflection basin with negative slope (outer sensor deflection is greater than inner sensor deflection). Two sets of raw FWD deflection data, one from PLTT section and one from TDA-soil section, did not satisfy the criterion and were then excluded from the analysis.

A second criterion used in this study was proposed by Stubstad et al. (2000). In this method, R_i , the radial distance of the i^{th} sensor from the center of the load plate, is plotted against the D_1/D_i ratio in log-double log scale for $i = 2, 3, 4 \dots 9$. A second-order polynomial function is then applied to fit the relationship between R_i and D_1/D_i . A higher R^2 value indicates a normal deflection basin and a poor curve fitting usually indicates severe discontinuities in the AC layer or incorrectly recorded sensor spacing. Analysis of the deflection basin using the second criterion gave a R^2 values greater than 98 percent for all data analyzed, which implies normal deflection data.

DEFLECTION DATA

Figures 5.4 (a) and (b) present the maximum center deflection and the deflection measured by the furthest sensors from the loading plate during the construction and post-construction structural performance monitoring period for the test sections. The deflections are normalized for 12.4 and 40 kN load drops on the subgrade, and base course and asphalt layers, respectively. According to the Standard Guide for Calculating In-situ Equivalent Elastic Moduli of Pavement

Materials Using Layered Elastic (ASTM 2008), individual deflections must be normalized by the ratio of the reference load to the actual load when the applied loads vary by more than five percent of the reference load. Thus, deflection data taken at a load of approximately 40 kN on top of base course or asphalt layer were normalized to a 40 kN reference load. For subgrade, the deflections shown in Figures 5.4 (a) and (b) are for the peak load. Similarly, the deflection data taken at approximately a 12.5 kN load is normalized by a reference load of 12.4 kN. For each pavement section, the average deflection, standard deviation, and coefficient of variation (CV) at each sensor location and the deflection basin parameters for a typical FWD test are presented in Table 5.1. Moreover, the average deflection basin and DBPs for August 28, 2013 at the four sections are presented in Figures 5.5 and 5.6.

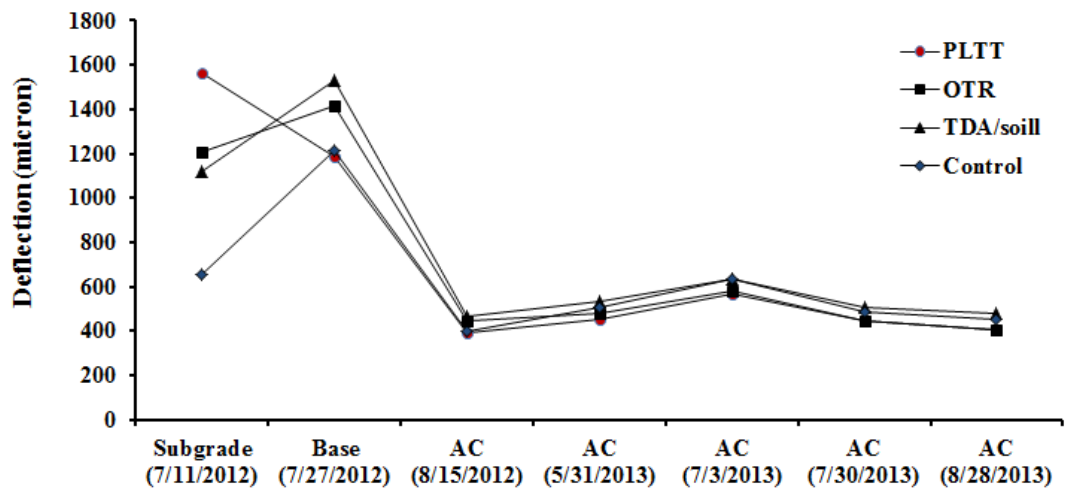
FWD peak deflection tests performed on top of the subgrade show higher values on the fill sections compared to the control section, as presented in Figure 5.4 (a). The difference in deflections decreases on the subsequent FWD tests performed on top of the base course and asphalt layers. This agrees with expected results, as the three sections contained compressible fill material (TDA) and the control section contained soil. However, the higher peak deflections observed on the subgrade were not reflected on the peak deflections measured by the FWD tests performed on the successive layers. Large-scale, one-dimensional laboratory test (Meles et al. 2014b) indicated that both OTR and PLTT show strain-hardening behavior. The strain-hardening behavior of TDA with the addition of the subsequent layers and the reduction of the applied vertical stress from FWD loads

reaching the compressible layer may explain why the higher deflections were not reflected. Comparison of peak deflections at various times on the asphalt layer indicates that the peak deflection on the asphalt layer for all sections showed maximum values for FWD test conducted on May 3, 2013. This may be related to the relatively hot temperature when FWD tests were conducted in comparison to FWD test performed on the asphalt layer. Attempt to find the effect of time-dependent settlement behavior on PLTT and OTR sections from FWD tests performed on the asphalt layer was not successful in this study.

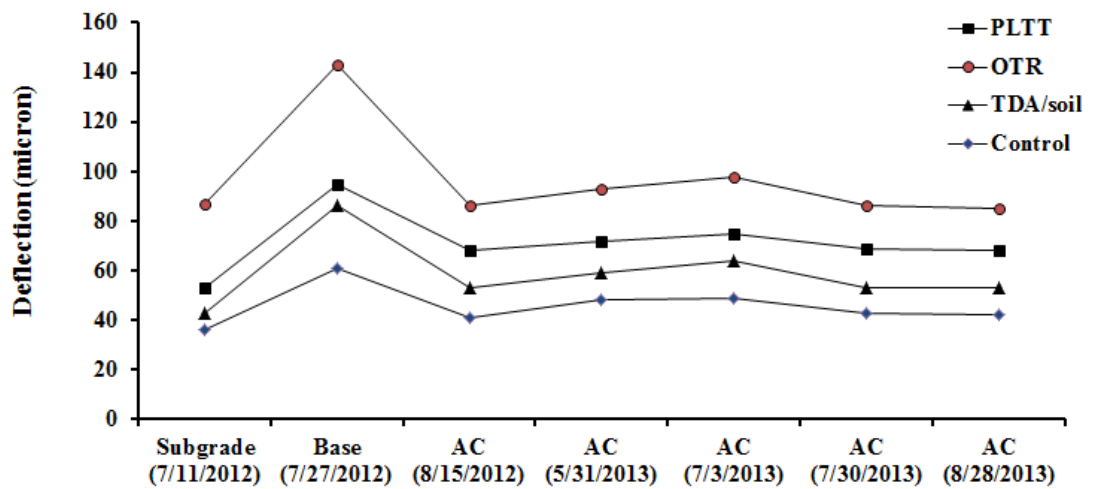
Deflections measured by the furthest sensor from the center of the load plate (1200 mm for the subgrade and 1800 mm for the base course and asphalt layer) are smaller for the control section than the fill sections in all FWD tests, as shown in Figure 5.4 (b). Though the difference was not significant, this could be due to the fill sections containing compressible material at a greater depth; the sensors furthest from the load center usually measure deflection from greater depths. This observation is supportive of the assumption that deflections measured at a great distance from the load center are primarily the response from deeper depths (Everseries © Users' Guide 2005). The average deflection basin for August 28, 2013 shown in Figure 5.5 also shows similar results. The PLTT and OTR sections show smaller deflection compared to the TDA-soil and control sections for the first six sensors located near the loading plate. However, the values of deflection reverted for the last three sensors located further from the loading plate; PLTT and OTR showed higher deflection compared to the TDA-soil and control sections. Although the deflections measured by sensors near the center of the

loading plate seems to be unrelated to the compressible fill material in the TDA sections, the deflections measured by sensors located at 1200, 1500, and 1500 mm from the center of the load plate appear to be related.

The deflection basin parameters for FWD test performed on August 28, 2013 are presented in Figure 5.6. All four sections have comparable DBP values. All three DBPs (BLI, MLI, and LLI) have lower values for the OTR and PLTT sections compared to the control section, while the TDA-soil section has DBPs values slightly higher than the control section. Horak (1998) applied DBPs parameters in the evaluation of the structural capacity of flexible pavement in South Africa. In his research, he provided correlation and tolerance limits of DBPs parameters for pavement structural condition, rehabilitation design, and analysis methodology of flexible pavement. The application of correlation and tolerance limits directly to the pavement structure with different climatic condition, such as Edmonton, may produce misleading results. However, Horak (1998)'s developed correlations relate smaller DBP values (BLI, MLI, and LLI) to better structural capacity and longer pavement life. Thus, the DBPs data indicates that pavement structures in PLTT and OTR sections have equivalent or better structural capacity and longer pavement life compared to the control section. The TDA-soil section showed slightly lower values of DBPs compared to control section, which indicates equivalent or lower structural capacity and performance life.



(a)



(b)

Figure 5.4: Deflection below: (a) center of loading plate, (b) the furthest deflection sensor.

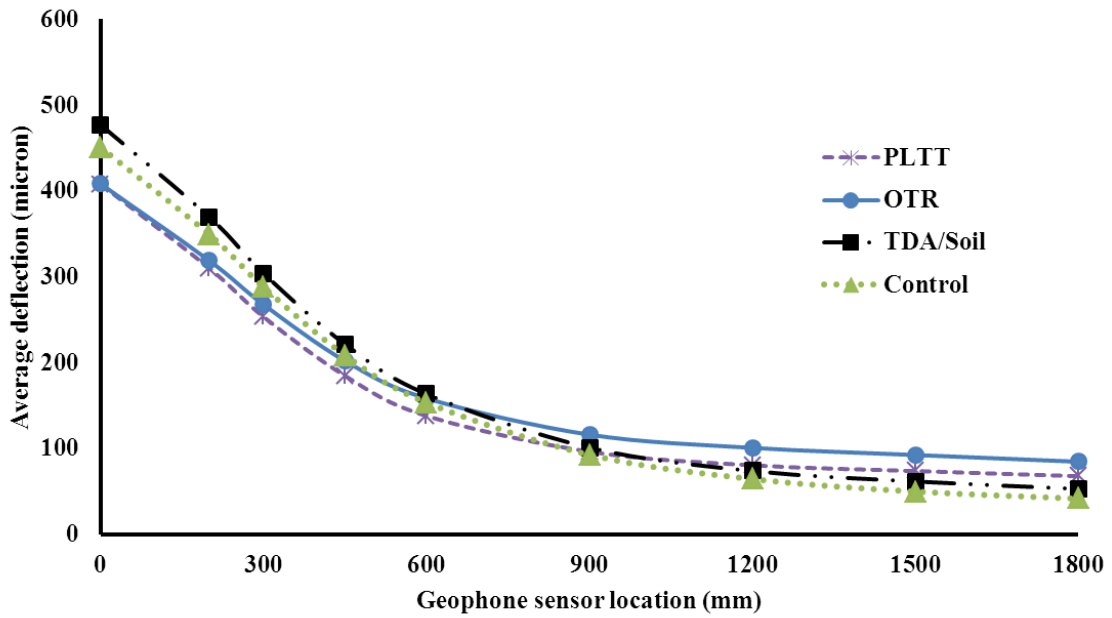


Figure 5.5: Deflection basin for FWD tests performed on August 28, 2013.

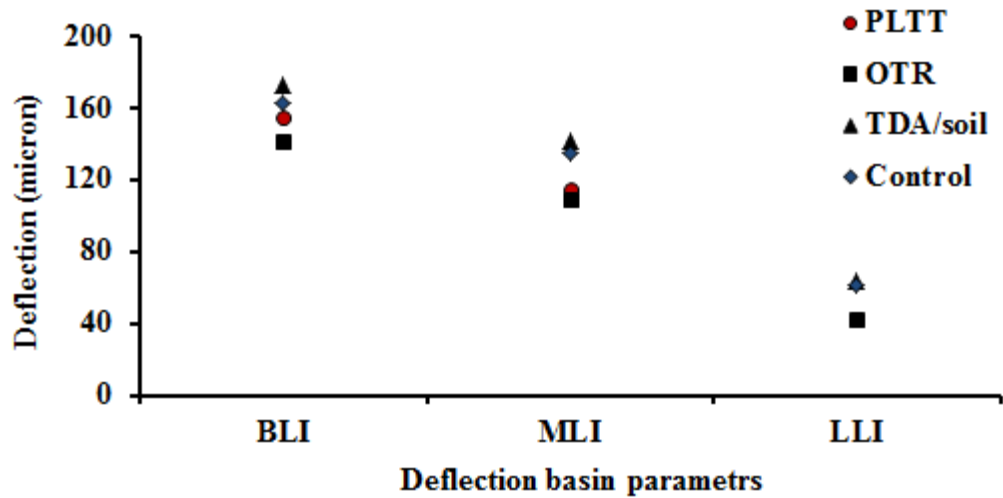


Figure 5.6: Deflection basin parameters (DBPs) for FWD test performed on August 28, 2013.

Table 5.1: Average deflection in microns and deflection basin parameters at each deflection sensor.

Section	FWD on top of	Variable	Geophone sensor location from the centre of the loading plate (mm)								Max def (micron)	BLI (micron)	MLI (micron)	LLI (micron)	
			0	200	300	450	600	900	1200	1500					1800
PLTT	Subgrade	Average	1562	502	214	116	71	58	53	NA	NA	1562	1348	143	13
		Stdev	775	268	75	27	16	13	12	NA	NA				
		CV (%)	50	53	35	23	22	23	23	NA	NA				
	Base	Average	1189	784	524	334	236	151	122	111	95	1189	665	288	85
		Stdev	123	83	85	60	39	16	9	10	11				
		CV (%)	10	11	16	18	16	11	7	9	11				
	First stage AC (Aug 15, 2012)	Average	388	307	260	199	155	102	80	73	68	388	128	105	53
		Stdev	63	58	54	46	38	20	9	6	6				
		CV (%)	16	19	21	23	24	20	11	9	8				
	First stage AC (Aug 28, 2013)	Average	408	310	253	185	138	96	81	74	68	408	155	115	42
		Stdev	15	10	12	12	12	5	5	5	4				
		CV (%)	4	3	5	6	9	6	7	6	6				
OTR	Subgrade	Average	1207	566	302	189	120	103	87	NA	NA	1207	905	183	17
		Stdev	192	88	37	14	8	6	6	NA	NA				
		CV (%)	16	16	12	8	7	6	7	NA	NA				
	Base	Average	1413	841	592	399	296	206	180	164	143	1413	821	296	91
		Stdev	222	115	103	62	44	13	15	7	8				
		CV (%)	16	14	17	16	15	6	9	4	6				
	First stage AC (Aug 15, 2012)	Average	442	355	300	231	178	120	101	93	86	442	142	123	58
		Stdev	24	22	19	17	13	6	4	3	3				
		CV (%)	5	6	6	7	7	5	4	4	3				
	First stage AC (Aug 28, 2013)	Average	408	319	268	202	159	116	101	93	85	408	141	109	42
		Stdev	8	12	14	14	11	6	4	3	3				
		CV (%)	2	4	5	7	7	5	4	4	4				
TDA/soil	Subgrade	Average	1117	517	277	159	77	51	43	NA	NA	1117	840	201	26
		Stdev	287	155	74	30	8	8	8	NA	NA				
		CV (%)	26	30	27	19	10	15	20	NA	NA				
	Base	Average	1531	994	688	449	312	184	130	104	86	1531	843	377	128
		Stdev	249	170	117	73	46	17	26	23	26				
		CV (%)	16	17	17	16	15	9	20	22	30				
	First stage AC (Aug 15, 2012)	Average	466	370	315	242	183	112	78	62	53	466	152	132	72
		Stdev	73	48	40	29	21	10	5	6	8				
		CV (%)	16	13	13	12	11	9	7	10	15				
	First stage AC (Aug 28, 2013)	Average	477	370	304	222	164	101	74	62	53	477	173	141	63
		Stdev	44	14	8	8	10	9	9	9	9				
		CV (%)	9	4	3	4	6	9	12	14	17				
Control	Subgrade	Average	651	372	218	149	80	46	36	NA	NA	651	433	138	35
		Stdev	307	170	86	54	24	14	10	NA	NA				
		CV (%)	47	46	39	36	30	31	28	NA	NA				
	Base	Average	1215	752	503	332	242	152	106	83	61	1215	712	262	89
		Stdev	143	129	93	64	59	32	16	15	11				
		CV (%)	12	17	18	19	24	21	15	18	19				
	First stage AC (Aug 15, 2012)	Average	399	307	255	189	142	88	64	50	41	399	144	113	54
		Stdev	68	51	43	33	26	15	11	9	7				
		CV (%)	17	17	17	18	18	17	17	17	18				
	First stage AC (Aug 28, 2013)	Average	451	349	288	209	154	93	64	50	42	451	163	135	61
		Stdev	34	30	28	25	20	12	9	8	6				
		CV (%)	8	9	10	12	13	13	14	15	15				

Parameters used in table are defined as follows:

$$BLI = D_0 - D_{300}, \quad MLI = D_{300} - D_{600}, \quad \text{and} \quad LLI = D_{600} - D_{900}$$

BACKCALCULATION ANALYSIS OF MODULI

The latest FWD testing data obtained on August 28, 2013 was used to calculate the subgrade modulus, which was later used to compare the performance of the four test sections. EVERCALC for Windows, a backcalculation program developed by the Washington State Department of Transportation, was used to backcalculate the modulus for the test sections. The program uses an iterative approach to find a modulus that would provide a calculated deflection basin closest to the measured deflection basin, as characterized by the root-mean-square (RMS) technique. The backcalculated moduli were analysed according to AASHTO (1993). Introduction of the compressible layer as a fourth layer in PLTT, OTR, and TDA-soil sections during backcalculation analysis resulted in unrealistic moduli and high RMS values. In some analyses, the RMS values did not converge. This problem arose due to the presence of a stiff pavement layer overlying a softer TDA layer. In this study, various options were attempted to determine more reasonable moduli and smaller RMS values; however, only two of these options will be discussed.

Option 1: the backcalculation analysis was performed from the deflection data of nine sensors with the following assumptions:

- A) The pavement structure in all sections was modeled as a three-layer system: (1) asphalt layer, (2) base course layer; and (3) subgrade layer; and

B) The thickness of the asphalt and base course for TDA-soil and control sections was based on initial design (160 mm for asphalt and 450 mm for the base course). However, the base course thicknesses of OTR and PLTT sections was modified to account for the immediate settlement of the TDA layer during construction, as reported by Meles et al. (2014a) (base course thickness of 530 and 520 mm were for PLTT and OTR sections, respectively).

Option 2: apart from the two assumptions listed in Option 1, only the first six sensors near the loading plate were considered in the backcalculation. This assumption is based on the observations made from the deflection data presented in Figure 5.4 (b) and the deflection basin presented in Figure 5.5. The deflection data in these figures seemed to indicate that the data measured by the last three sensors was related to the deflection of the deeper TDA layer rather than the subgrade material. Thus, the deflection data of the sensor located 900 mm from the load center was used to determine the subgrade modulus during the backcalculation process.

Root mean square values presented in Table 5.2 ranges from 4.75 to 11.08 percent and from 1.39 to 2.48 for options, 1 and 2 respectively. The range of RMS values for Option 2 is higher than the acceptable limit (Everseries © Users' Guide 2005). The RMS is an indicator of how closely a computed deflection basin matches a measured basin and is also an indicator of the consistency of backcalculated results for a particular analysis section. In many backcalculation procedures, the subgrade moduli are derived from the deflection data of the sensors located at the

greatest distance from the loading plate, which is also recommended by the AASHTO (1993). Thus, the higher RMS values for Option 2, especially for PLTT and OTR sections, may be related to the assumption of the three-layer systems and the use of deflection data from the furthest sensors, which seem to be the response of the TDA fill rather than the subgrade layer. The mean backcalculated subgrade modulus ranges from 70 to 110 MPa for Option 1 and from 92 to 117 MPa for Option 2. Both results are typical values of backcalculated subgrade modulus for fine grained soil (Pavement Design Manual, 1997).

Table 5.2: Backcalculated moduli from August 28, 2013 FWD data using the first six sensors nearest to the center of the loading plate.

Analysis type	Section	Backcalculated subgrade moduli (MPa)			RMS (%)
		Mean	Stdev	CV (%)	Mean
Option 1	PLTT	91	7	13	11.08
Option 2		117	8	7	2.48
Option 1	OTR	70	3	5	10.90
Option 2		92	4	5	2.13
Option 1	TDA/soil	93	10	10	7.19
Option 2		106	10	9	1.17
Option 1	Control	110	15	13	4.75
Option 2		103	12	12	1.39

PRACTICAL APPLICATIONS

The results from the settlement plates indicated a high degree of compressibility for TDA fill from the application of load on top of the TDA layer during construction. The final design thickness of various pavement layers in the PLTT and OTR sections differ from initial design thickness, as they were computed without considering the compression of the TDA layer during construction. For

example the final thickness for soil cover and base course in PLTT sections increased by 42 and 8 cm, respectively, from the initial design as a result of TDA compression following the placement of soil cover and base course. Pavement evaluation for highway embankments constructed from TDA should consider the final thickness of various pavement structures, taking into account the reduced thickness of TDA layers after construction. PLTT and OTR sections also showed time-dependent settlement, which TDA-soil and conventional fill material did not. Any highway project using TDA as a fill material should also consider this time-dependent settlement and its effect on pavement structures.

It is believed that the moduli backcalculated from FWD test alone cannot guarantee an accurate modulus value, as there is no unique solution and several combinations of modulus values could match the deflection basin accurately. A detailed evaluation of pavement may require laboratory data to verify backcalculated modulus from FWD tests. This paper outlines a combination of deflection data and backcalculated modulus to ensure a reasonable evaluation of the TDA test embankment. It is also important to observe FWD test load (40 kN), which is the standard for pavement design to evaluate embankment performance in this study.

CONCLUSION

A test embankment containing four different sections composed of PLTT, OTR, TDA-soil mixture, and soil was constructed Edmonton, Alberta, Canada using a staged construction approach. Visual assessment, settlement data, and FWD tests conducted upon completion of each pavement layer (subgrade, base course, and

asphalt) as well as four additional FWD tests performed on the asphalt layer after the first stage of construction were used to evaluate TDA's performance as a fill material. Based on this investigation, the following observations and conclusions were made:

- PLTT and OTR sections showed a high degree of immediate compression compared to TDA- soil and control sections under the weight of overlying soil placed during construction.
- The settlement plates in the PLTT and OTR sections indicated time-dependent settlement that continued to occur well beyond the initial application of load. However, most of the settlement occurred within two months after the placement of the first stage asphalt layer. Moreover, the addition of 50 percent soil by volume to TDA highly reduced the time-dependent settlement.
- Distress that may result from TDA's time-dependent settlement on the pavement structure can be minimized by allowing two months to pass before the placement of settlement sensitive structures, or by using the staged construction approach adopted in this study.
- Deflection data, DBP values, and backcalculated subgrade modulus indicated that overall performance for the PLTT, OTR and TDA-soil sections was similar to the control section, which was used as a benchmark to compare pavement performance.

The preceding conclusions support the use of PLTT, OTR, and TDA-soil mixture as a fill material for highway embankment. Moreover, TDA's application is beneficial to the environment as it promotes recycling waste material.

REFERENCES

Alberta Recycling Management Authority 2012. *Tire Recycling Program*.

[online] Available at: <<http://www.albertarecycling.ca/>> [Accessed on June 10, 2012].

AASHTO, 1993. *AASHTO Guide for Design of Pavement Structures*, Washington, D.C.

ASTM, 2008. Standard Guide for Calculating In Situ Equivalent Elastic Moduli of Pavement Materials Using Layered Elastic Theory, *ASTM D5858 - 96*, West Conshohocken, PA.

Dickson, T.H., Dwyer D.F., and Humphrey D.N., 2001. Prototype tire-shred embankment construction, *Transportation Research Record 1755*, Transportation Research Board, Washington, DC, 160-167.

Everseries © Users' Guide, 2005. *Pavement analysis computer software and case studies*, Washington State Department of Transportation.

Horak, E., Maina, J., Guiamba, D. and Hartman, A., 2008. Correlation study with the light weight deflectometer in South Africa. *Proceedings of the 27th South African transportation conference*, Pretoria, South Africa, 304-312.

- Horak, E. and Emery, S., 2009. Evaluation of airport pavements with FWD deflection bowl parameter benchmarking methodology. *2nd European airport pavement workshop*, 13-14 May 2009, Amsterdam, Netherlands
- Huang, Y. H., 1993. *Pavement analysis and design*, Prentice-Hall, Englewood Cliffs, N.J.
- Humphrey, D.N., Whetten, N., Weaver, J., and Recker, K. 2000. Tire Shreds as Lightweight Fill for Construction on Weak Marine Clay. *Proceeding International Symposium on Coastal Geotechnical Engineering in Practice*, 611–616. (Rotterdam, The Netherlands).
- Mehta, Y. and Roque, R., 2003. Evaluation of FWD data for determination of layer moduli of pavements, *Journal of Material in Civil Engineering*, 15(1), 25-31.
- Meles, D., Bayat, A, Shaffi, M., H., Nassiri, S., and Gul, M. 2014a. Investigation of Tire Derived Aggregate as a Fill Material for Highway Embankment, *International journal of geotechnical engineering*, 8(2), 182-190.
- Meles, D., Bayat, A, and Chan, D. 2014b. One-dimensional compression model for tire derived aggregate using large-scale testing apparatus, *International journal of geotechnical engineering*, 8(2), 197-204.
- Mills, B., and McGinn, J., 2010. Design, Construction, and Performance of Highway Embankment Failure Repair with Tire derived Aggregate,

Transportation Research Record 1345, Transportation Research Board, Washington, DC, 90-99.

Mohanty, S. and Chugh Y. P., 2006. Structural performance monitoring of an unstabilized fly ash-based road subbase. *Journal of Transportation Engineering*, 132:964–969.

Pavement design manual edition 1, 1997, Alberta Transportation and Utilities, Edmonton, Alberta. Edition 1 (1997).

Qiu, X. and Yang, Q. 2011. Prediction analysis of CTB asphalt pavement moduli based on FWD deflection data, *Geotechnical special publication 215*, ASCE, 16-22.

Rahim, A., and George, K. P., 2003. Falling weight deflectometer for estimating subgrade elastic moduli, *Journal of Transportation. Engineering*, 129(1), 100–107.

Stubstad, R. N., Irwin, L. H., Lukanen, E. O., and Clevenson, M. L., 2000. It's 10 o'clock—Do You Know Where Your Sensors Are?, *Transportation Research Record 1716*, Transportation Research Board, Washington, D.C., 10–19.

Tandon, V., Velazco, D.A., Nazarian, S. and Picornell, M., 2007. Performance monitoring of embankment containing tire chips: case study, *Journal of Performance of Construction Facilities.*, ASCE, 21(3), 207-214.

- Tao, M., Zhang, Z., and Wu, Z., 2008. Simple Procedure to Assess Performance and Cost Benefits of Using Recycled Materials in Pavement Construction, *Journal of Materials in Civil Engineering*, ASCE, 20(11), 718-725.
- Wartman, J., Natale, M.F., and Strenk, P.M., 2007. Immediate and time-dependent compression of tire derived aggregate, *Journal of Geotechnical and Geoenvironmental Engineering*, ASCE, 133 (3), 245-256.
- Xu, B., Ranjithan, R.S., Kim, R. Y., 2002. New condition assessment procedure for asphalt pavement layers, using falling weight deflectometer deflections, *Transportation Research Record 1806*, Transportation Research Board, Washington, DC, 57-69.
- Yoon, S., Prezzi, M., Sidiki, N.Z., Kim, B., 2006. Construction of test embankment using a sand-tire shred mixtures as fill material, *Journal of Waste Management.*, 26, 1033-1044.
- Zhou, H., Rada, G. R., and Elkins, G. E., 1997. Investigation of back-calculated moduli using deflections obtained at various locations in a pavement structure, *Transportation Research Record 1570*, Transportation Research Board, Washington, DC, 96-107.
- Zornberg, J. G., Costa, Y. D., and Volleweider, B., 2004. Performance of prototype embankment built with tire shreds and nongranular soil, *Transportation Research Record 1874*, Transportation Research Board, Washington, DC, 70-77.

CHAPTER 6 FINITE ELEMENT ANALYSIS OF HIGHWAY EMBANKMENT MADE FROM TIRE DERIVED AGGREGATE

This paper was previously submitted in the Journal of Materials in Civil Engineering (ASCE). It is modified (formatting only) and presented as submitted for possible publication part of this Ph.D. thesis as Chapter 6.

Reference: Meles, D., Dave, C., Yi, Y. and Bayat, A. 2014. Finite element analysis of highway embankment made from tire derived aggregate. Journal of Materials in Civil Engineering, ASCE, under review for possible publication.

CHAPTER 6 FINITE ELEMENT ANALYSIS OF HIGHWAY EMBANKMENT MADE FROM TIRE DERIVED AGGREGATE

ABSTRACT

Tire derived aggregate (TDA) has been used in many civil engineering applications. Despite its successful use in the past, the amount of experimental research available on TDA applications is not sufficient to provide data for the evaluation of an appropriate constitutive model. The majority of TDA constitutive models have been developed from laboratory tests performed on tire chips smaller than those used in field applications. In this study, nonlinear elastic material models, with an elastic modulus that varies as a function of vertical stress, have been developed for TDA produced from passenger and light truck tire (PLTT) and off-the-road (OTR) vehicle tires. The material model for TDA is established based on previous large-scale laboratory constrained compression tests conducted on TDA up to 300 mm in size. The model is used in a finite element (FE) analysis using geotechnical software SIGMA/W to predict the settlement of full-scale test embankment during construction. The results indicate that the settlements obtained from the FE analysis agree with the settlements measured in the field during construction of full-scale test embankment. This paper also provides design charts to compute “overbuild” required on top of TDA layer(s) to compensate immediate compression under an applied load during the placement of cover on top of TDA.

INTRODUCTION

In the Province of Alberta, Canada, over five million tires are discarded each year (ARMA 2012). As population increases, so does the volume of discard tires. This trend has promoted an interest in developing new ways to recycle end-of-life tires. An option that has been successful in the past is using the shredded form of tire derived aggregate (TDA) in civil engineering applications. In such applications, discarded tires are converted into TDA, which has many beneficial engineering properties. It is lighter in weight and has higher hydraulic conductivity and thermal insulation than conventional aggregates. Due to these properties and its widespread availability, TDA has been used as a lightweight fill material for numerous highway projects (e.g. Humphrey et al. 2000; Dickson et al. 2001; Mills and McGinn 2010).

Despite the historically successful use of TDA in civil engineering projects, limited experimental research is available to predict field deformation using constitutive model developed from laboratory tests. The use of constitutive model to predict field deformation of TDA fill has been investigated by (Gharegrat 1993; Bosscher and Edil 1997; Shalaby and Khan 2002, 2005; Youwai and Bergado 2003; Yang et al. 2002). Gharegrat (1993) determined the resilient modulus and the parameters for an hyperbolic model for tire chips in a finite element analysis of tire chips used as a fill material beneath paved roads and as backfill behind retaining walls. Bosscher and Edil (1997) used an elastic model to investigate the deformation response of large-scale model embankment made from tire chips. Lee et al. (1999) used a hyperbolic model, originally proposed by Duncan et al.

(1980), to model the deformation of a shredded tire-soil mixture in a finite element analysis of an embankment. Shalaby and Khan (2002; 2005) developed a compressibility model of shredded tire from laboratory tests and used it to predict and verify the compressibility of tire shred embankment. Youwai and Bergado (2003) proposed a hypo-plasticity model based on the critical state framework to simulate the stress-strain characteristics of the shredded rubber tire-sand mixtures. Yang et al. (2002) characterize tire chips compressibility by using the slope of the void ratio versus log stress curves from one-dimensional compression test, and provided compression index for tire chips.

In the works cited above, with the exception of Shalaby and Khan (2002; 2005), TDA was modeled based on laboratory tests using tire chips or shreds with a maximum particle size smaller than that used in field applications. TDA used for field application has a maximum size ranging from 300 to 400 mm (ASTM 2008), with large-sized particle that are typically elongated in shape and more flexible. TDA compresses under load in three mechanisms: (a) rearrangement/sliding of TDA pieces which is mostly irrecoverable; (b) bending/flattening of TDA which is responsible for a large portion of compression and is mostly recoverable upon unloading; and (c) elastic compression of TDA pieces which is also recoverable but not as influential (Ahmed and Lovell 1993). Bending/flattening also plays an important role in TDA compression; however, it is more significant at lower stress for large-sized TDA particles than small-sized TDA particles. Strenk et al. (2007) illustrated the sensitivity of TDA compression behavior (constrained modulus) with maximum TDA particle size. Meles et al. (2014a) also observed in

the laboratory that larger-sized TDA is more compressible than smaller-sized TDA. However, determining the engineering properties of TDA to be used for field applications using triaxial testing is impractical due to the size of TDA and the risk of membrane failure.

TDA compresses immediately under an applied load, such as the weight of overlying soil cover or a pavement structure, and the top elevation of TDA layer(s) should be overbuilt to compensate settlement. Humphrey (2008) developed a procedure to determine this overbuild by creating a design chart applicable to Type B TDA (300 mm maximum size). The design chart that Humphrey (2008) developed was created using a combination of laboratory compressibility tests and field compression measurements for Type B TDA, excluding the variation of TDA size and tire source of TDA production.

This paper proposes a nonlinear elastic material model for TDA produced from two tire sources. The model has been used in FE analysis to predict settlement of a test embankment. The results from the FE analysis and the settlement measured during field monitoring are then compared to verify the effectiveness of the model in calculating TDA deformation. In addition this paper provides design charts to compute the overbuild on top of TDA layer(s) to compensate immediate compression under the applied load during construction. Unlike the design charts proposed by Humphrey (2008), the design charts proposed in this study consider variation in TDA size and tire sources.

COMPRESSION MODEL FOR TDA

Materials

The TDA used in the laboratory and field tests contained both Class I fill (fine TDA with a maximum size of 200 mm and less than 1 m thick) and Class II fill (coarse TDA with a maximum size of 300 mm and 1 to 3 m thick) according to ASTM D 6270-08 (ASTM 2008) standards. Samples for laboratory testing were taken from a pile of TDA in the field, where it was used as a highway embankment fill and insulation to limit frost penetration. The TDA was produced from two different tire sources: PLTT (passenger and light truck tires) and OTR (off-the-road) vehicle tires. PLTT refers to TDA made from passenger, light, and multipurpose vehicles possessing a rim diameter of up to 49.5 cm. OTR TDA is produced from tires with a rim diameter of up to 99 cm, typical of large industrial vehicles (ARMA 2012). The PLTT and OTR used for embankment fill satisfied the requirements of Type B TDA, while the PLTT used for insulation satisfied the requirements of Type A TDA according to ASTM D 6270 (ASTM 2008) standards. Further information on the material used for the compression test is provided in Meles et al. (2014a).

Testing apparatus

The test apparatus used by Meles et al. (2014a) to determine the TDA's hyperbolic stress-strain equations was designed based on the recommendations of ASTM D6270 (ASTM 2008) standards. It consisted of a piece of PVC pipe with an inside diameter of 123 cm, a length of 150 cm, and a wall thickness of 2.7 cm. The apparatus was able to measure vertical compression and horizontal stress of

the TDA sample. The horizontal stress was measured using horizontal and vertical strain gages mounted on the outside wall of the pipe. From the vertical stress and deformation measurements, the hyperbolic stress-strain equation was determined. In addition the at-rest lateral earth pressure coefficient (K_o) was also computed from the vertical stress versus horizontal stress relationship, which later was used to determine the Poisson's ratio for the TDA. Further details on testing apparatus and method can be found in Meles et al (2014a).

Constrained compression model

The stress-strain curve for TDA is nonlinear. Meles et al. (2014a) modeled the stress-strain behavior of TDA from a large-scale one dimensional compression test using the hyperbolic equations given below (Equations 1-3) for Type B PLTT, Type B OTR, and Type A PLTT, respectively.

$$\sigma = \frac{134\varepsilon}{1-2.65\varepsilon} \quad (1)$$

$$\sigma = \frac{196\varepsilon}{1-2.77\varepsilon} \quad (2)$$

$$\sigma = \frac{163\varepsilon}{1-2.72\varepsilon} \quad (3)$$

where σ = axial stress (kPa); and ε = axial strain (%);

Derivation of nonlinear elastic stress-strain behavior for TDA

Equations 1-3 indicate that TDA becomes stiffer as the load increases. To derive the non-linear elastic stress-strain behavior for TDA, Equations 1-3 are rearranged to give Equations 4-6 for Type B PLTT, Type B OTR, and Type A PLTT, respectively:

$$\varepsilon = \frac{\sigma}{(134+2.65\sigma)} \quad (4)$$

$$\varepsilon = \frac{\sigma}{(196+2.77\sigma)} \quad (5)$$

$$\varepsilon = \frac{\sigma}{(163+2.72\sigma)} \quad (6)$$

The variation of stiffness (tangent constrained modulus) as a function of the vertical stress can be calculated from the derivative of Equations 4-6 for Type B PLTT, Type OTR, and Type A PLTT, respectively:

$$d\sigma/d\varepsilon = 134 + 5.3\sigma + 0.052\sigma^2 \quad (7)$$

$$d\sigma/d\varepsilon = 196 + 5.54\sigma + 0.039\sigma^2 \quad (8)$$

$$d\sigma/d\varepsilon = 163 + 5.44\sigma + 0.0452\sigma^2 \quad (9)$$

Figure 6.1 presents the variation of modulus as a function of the vertical stress from Equations 7-9.

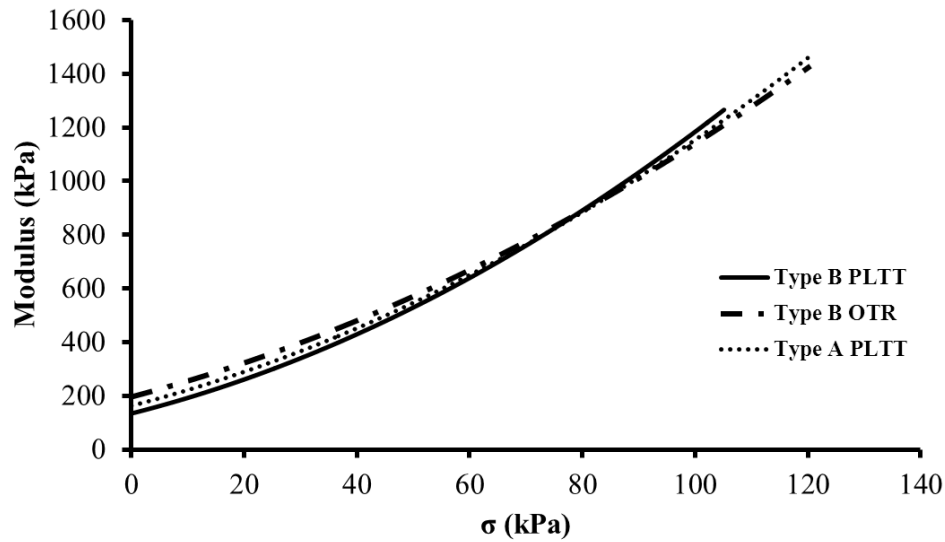


Figure 6.1: Variation of modulus as a function of vertical stress for PLTT and OTR.

FIELD EXPERIMENT

Project layout and construction of the test embankment

The test embankment in this experiment was part of the Integrated Road Research Facility (IRRF)'s research initiative aimed at evaluating the long-term performance of TDA as embankment fill and pavement insulation in Edmonton, Alberta Canada. The IRRF constructed a test road, 80 m in length with four different 20 m test sections. The four test sections are made of: 1) TDA from PLTT; 2) TDA from OTR; 3) TDA from PLTT mixed with soil at a 50/50 ratio by volume; and 4) a control section made from soil. In the PLTT, OTR, and TDA-soil mixture sections, TDA was placed in two 3 m thick layers with 0.5-m-thick soil caps for separation and 1-m thick soil cover on top. The road was finished with a 450-mm base course and 160-mm of asphalt on the surface. These

dimensions were designed without considering construction settlement during placement. Figure 6.2 shows a typical section of the test embankment.

The embankment was instrumented with various types of geotechnical instruments including the Vibrating Wire Liquid Settlement Systems (model SSVW105) which monitor the settlement of the embankment. Each section contained eight settlement plates. Four of the settlement plates were placed on top of the bottom TDA layer, three were placed on top of the upper layer, and one was placed in each section on stable ground outside of the embankment. The settlement plates on stable ground were used as references to correct measurements according to daily changes in the atmospheric pressure. All sensors were connected to a data logger that collects and records data at 15-minute intervals. The locations of the settlement plates are shown in Figure 6.2. Further details on the test embankment are given in Meles et al. (2014b).

The test embankment was constructed by excavating a pit nearly 8 m deep and 60 m long, with a bottom width of 17 m and top width of 40 m. The excavation indicated that the site mainly comprises of glacial till deposit. Detail on geology and geotechnical properties of till in the Edmonton-area are provided in May and Thomson (1978).

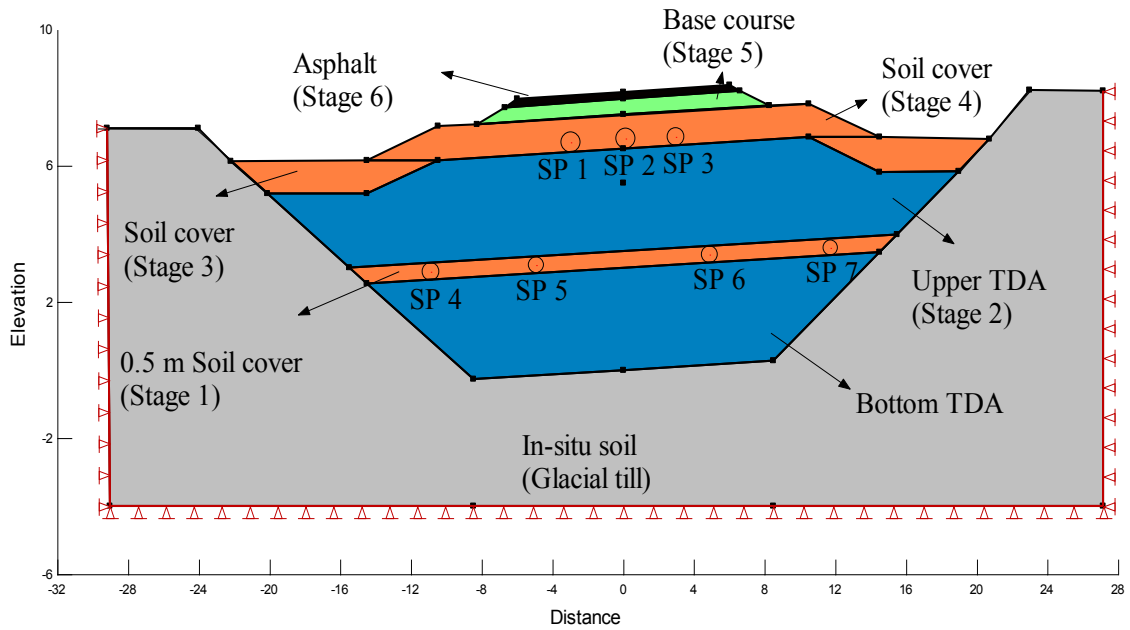


Figure 6.2: Typical section, construction stage and location of Settlement Plates (SP) for the test embankment (all units in meters).

NUMERICAL MODELING OF TEST EMBANKMENT

Finite Element Analysis using SIGMA/W

Deformations during construction of the test embankment were calculated using SIGMA/W 2007 software, GEO-SLOPE international Ltd. SIGMA/W is a powerful finite element software that uses an incremental load formulation to perform stress and deformation analyses of earth structures, such as an embankment. The use of the finite element software for deformation analysis requires an accurate constitutive model to describe the stress-strain behavior of the material. SIGMA/W includes six different soil constitutive models and an option to create a user-defined constitutive model. The built in material model that were available in the software was used in this analysis.

Material model for TDA

In SIGMA/W there are two options for modeling nonlinear elastic stress-strain behavior: hyperbolic constitutive model or linear elastic model with varying elastic modulus as a function of the vertical stress. The hyperbolic model was not used since it requires material property determined from triaxial testing, which is impractical to perform on large TDA sizes. Instead, the linear elastic model with varying modulus as a function of the vertical stress was used. The functional variations of the modulus were calculated from Equations 7-9 for PLTT and OTR. An elastic model also requires the Poisson's ratio, and unit weight for TDA. Poisson's ratio of 0.28 for Type B PLTT and 0.25 for Type B OTR previously determined by Meles et al. (2014a) using large-scale constrained compression tests, and unit weight of 7.6 kN/m^3 for Type B PLTT and 8.1 kN/m^3 for Type B OTR previously measured in the field by Meles et al. (2014b) were used in the analysis.

Selection of an appropriate modulus for TDA that simulates field condition is a challenge in numerical modelling since TDA modulus depends on many factors. Jean-Louis (2001) discussed the main factors that affect soil modulus, and classified them as state factors, loading factors, and field conditions. State factors include the density and structures of the soil, water content, past stress history, and cementation of the particles. TDA is a manufactured product with no cementation among its pieces. Therefore structure of TDA, past stress history, and cementation of TDA pieces has an insignificant effect on TDA modulus. Tatlisoz et al. (1997) showed that water also has an insignificant effect on the

compression characteristics implying that TDA modulus is also not affected by its water content. The only state parameter that affects the modulus is density. Humphrey (2008) and Meles et al. (2013) illustrated the effect of density on the compression behavior in the laboratory by varying the density of samples from loose to maximum compacted density. Moreover, TDA compression behavior is also affected by the size of TDA pieces. Strenk et al. (2007) explored the effect of TDA's size on constrained modulus. To select an appropriate model for the FE analysis for the TDA, the following issues have been considered:

1. Elastic parameters for TDA were determined from a large-scale, one-dimensional compression test. The effect of TDA size on the modulus has been considered during constrained compression test, as the TDA samples were taken directly from the field where it was used as embankment fill.

2. Load cycle has little significance since it is not considered in an elastic material model.

3. The effect of field compaction was considered while preparing samples for compression tests. Meles et al. (2014a) used a laboratory compaction method similar to the method of compaction used in the field.

4. The effect of confinement has not been considered since the results from the constrained compression test were used to develop the material model for TDA. In the present study, TDA was used as fill material by excavating in-situ soil, which has a modulus of two orders of magnitude greater than the modulus of TDA. Therefore the large-scale constrained compression test used to derive the

material model for TDA can reasonably approximate lateral stiffness from in-situ soil in the field.

Material model other than TDA

Tire Derived Aggregate is a highly compressible material with a Young's modulus 1 to 3 orders of magnitude less than typical materials used in pavement construction. Thus, deflection of TDA road embankment is primarily controlled by the modulus of the TDA. Therefore, material models other than TDA's used in the FE analysis were taken from previous studies or assigned typical values as follows:

In-situ soil: visual inspections of the in-situ soils during excavation for the test embankment and data from geotechnical investigations from nearby projects indicate that the area contains glacial till deposit. The following material properties for glacial till in Edmonton were used in the FE analysis outside the excavation boundaries: $E = 120$ MPa, $\nu=0.33$ and $\gamma = 20$ kN/m³ (Eisenstein and Morrison 1973).

TDA-soil mixture: the modulus for TDA-soil mixture was taken from previous studies conducted by Bosscher et al. (1997), and the unit weight was approximated from the compacted density of TDA and soil used in the mix ($E = 5$ MPa, and $\gamma_{comp} = 14$ kN/m³ were used during FE analysis).

Subgrade, base course, and asphalt: the material model parameters used in FE analysis for subgrade, base course, and asphalt layers was back-calculated from FWD tests conducted on the asphalt layer. Intermediate and top soil cover (E

= 35 MPa, $\Phi = 32^\circ$, and $\nu = 0.35$, γ (from field compaction) = 20 kN/m³); base course ($E = 120$ MPa, γ (assumed) = 22 kN/m³, ν (assumed) = 0.3); and asphalt ($E = 1000$ MPa, ν (assumed) = 0.3, γ (assumed) = 23 kN/m³).

Interface between TDA and in-situ soil: interaction between the TDA and the excavation boundary was modeled by introducing an interface element. The interface element was used to model relative movement between the geotextile used to wrap the TDA and the in-situ soil, and was modeled using a slip surface material model. Using slip surface material model, slippage can be modeled by specifying the frictional properties. The frictional properties for the slip surface material model were determined through direct shear tests between the geotextile and the soil. A measured friction angle of 22° from laboratory tests was used in the FE analysis.

FINITE ELEMENT ANALYSIS PROCEDURE

The numerical analysis is divided in two parts: 1) Modeling the embankment, which involves designing the mesh, defining the material properties, choosing the appropriate constitutive soil model, and defining the boundary conditions; and 2) interpreting the analysis results and comparing them with field observations.

The geometry of the model was prepared with the same dimensions as the field test embankment. Zero horizontal displacement boundary condition was used on a vertical line at a minimum distance of 5 m from the excavation boundary, and zero vertical displacement was used on a horizontal line 5 m below the base of the excavation. Considering the stiffness of the in-situ soil, which is mainly glacial till

and the light weight properties of the TDA fill material, a 5 m distance from the embankment sides for the far field boundary is deemed to be reasonable. The interface element was also used to model the interface between the in-situ soil and the geotextile that was used to wrap the TDA. The entire domain was automatically discretized into triangular elements by the software. A global size of 0.25 m was used for the mesh generation. Moreover total stress parameters were specified for the material models, and the embankment was modeled as a 2-D plane strain problem.

The FE analysis was performed in six stages following the sequence of construction. The analysis was conducted in stages to compensate for the construction settlements that occur during the placement of various layers in the FE model. The layers were activated or deactivated in each stage to simulate the construction sequence of placing the layers. The sequence of construction was performed using time stepping. First, the bottom TDA layer, considered as in-situ, was put in place to establish the initial stresses, and the construction stages progressed as follows: Stage 1 corresponds to the placement of the intermediate soil cover on top of bottom TDA layer; Stage 2 corresponds to the placement of the top TDA layer; Stage 3 corresponds to the placement of the top soil cover on the side; Stage 4 refers to the placement of the top soil cover; Stage 5 corresponds to the placement of the base course; Stage 6 corresponds to the placement of the asphalt. The various stages of modelling are shown in Figure 2.

The adjusted fill elevation with the foundation settlement option was used to compensate construction settlement during placement of each layer. SIGMA/W

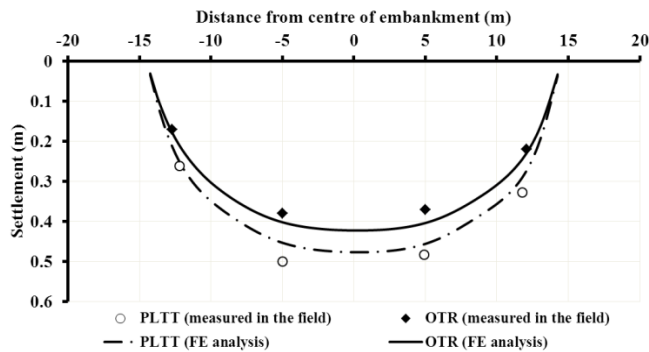
added the displacement following each layer's placement to the element nodal coordinates to compute the element weight and volume, which, in turn, were used to compute the gravitational nodal forces to simulate the placement of a layer. Addition of the displacements gives the element additional mass, which represents the additional layer placed to compensate for settlement during construction. Fundamentally, this implies that sufficient material must be placed to compensate for any settlement during construction. The intent is to build the embankment to the specified elevation during placement of each layer.

Comparisons of FE results with field observations

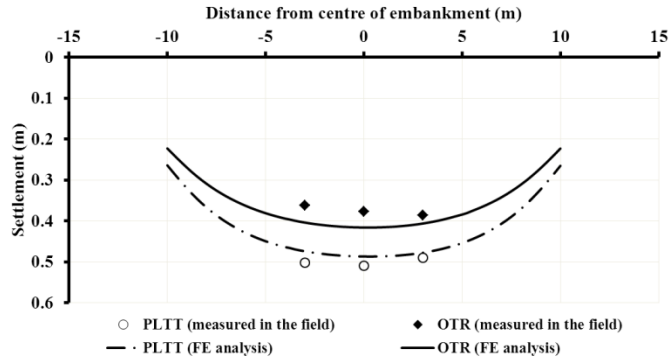
The results of the compressibility analysis from field measurements and the FE analysis conducted immediately after placement of the asphalt layer are presented in Figures 6.3 (a), (b), and (c). Figure 6.3 (a) presents settlements on the top surface of the bottom TDA layer in the PLTT and OTR sections. Figure 6.3 (b) presents settlements on the top surface of the upper TDA layer in the PLTT and OTR sections. Figure 6.3 (c) presents settlements on the top surface of the bottom TDA- soil layer in the TDA-soil section. The settlements in the control section and the top of the upper TDA-soil layer section are not presented since they were too small to be measured by the Vibrating Wire Liquid Settlement Systems used in this study. As shown in Figures 6.3 (a), (b) and (c), the FE results are in reasonably agreement with the observed settlements after the completion of the test embankment. Results from the FE analysis and field measurement in Figures 6.3 (a), (b) and (c) also indicate that PLTT is the most compressible, and that the

TDA-soil mixture has a settlement one order of magnitude less than TDA fill in the PLTT and OTR sections.

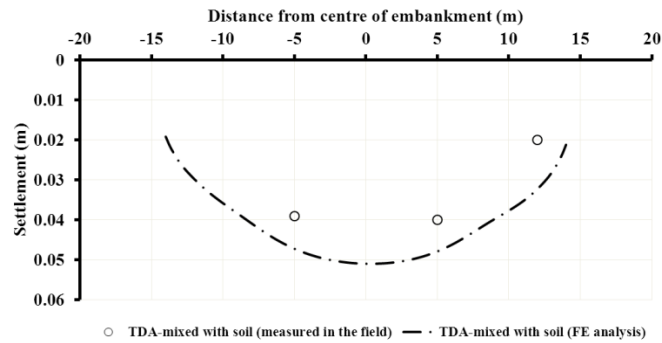
It is seen that the FE results agree reasonably well when comparing with field observations. However, the predicted settlements in the PLTT sections are underestimated up to maximum 10 percent in comparison to field measurements. The difference is partially due to the material model which was developed from large-scale constrained compression tests and possible variation between laboratory and field compaction. Similarly, the OTR section is overestimated up to maximum 7 percent in comparison to field measurements. A possible reason for this discrepancy could be the OTR, which mainly contains chunky-shaped pieces as it is produced from large thick tires, can be compacted more effectively in the field than in the large-scale laboratory compaction apparatus used by Meles et al. (2014a). The FE analysis results in the TDA-soil section overestimate the measured settlement in the field by about 20 percent. It should be noted that the material model for the TDA-soil section in the FE analysis was taken from a previous study conducted by Bosscher et al. (1997).



(a)



(b)



(c)

Figure 6.3: Settlement measured in the field and FE analysis results: (a) on top of bottom TDA layer in PLTT and OTR sections; (b) on top of upper TDA layer in PLTT and OTR sections; (c) on top of bottom TDA-soil layer in TDA- soil section.

The FE analysis in this study indicates that the settlement of the TDA embankment can be calculated with reasonably accuracy and a satisfactory design can be achieved using a material model derived from large-scale laboratory constrained compression tests. It should be emphasized that this conclusion is based on single case study of TDA. Moreover, the model may underestimate the field settlement if TDA is used as fill material under unconfined condition. However, in most geotechnical applications where TDA is used as a fill material,

it is common practice to cover the sides and top of the TDA with soil to separate it from the surrounding environment and reduce compressibility. The soil used to cover the TDA usually has stiffness much greater than that of the TDA. Under such circumstances the soil may prevent lateral deformation resulted in a constrained condition that the modulus proposed in the present study can be used in numerical analysis.

DESIGN CHARTS TO COMPUTE OVERBUILD IN TDA LAYER(S)

The proposed TDA nonlinear elastic material model has been used in the field applications for PLTT and OTR embankments with reasonably satisfactory results. Therefore the material model is used to develop design charts in preliminary design to determine overbuild required for TDA layer(s). Overbuild means the additional soil layer required on top of the TDA material in order to reach the design elevation due to deformation of the TDA layer. The design charts are simple to use and important in determining the overbuild in the TDA layers to compensate the immediate compression resulted from the applied loads during construction, such as overlying soil cover or pavement structures. The design charts are developed using FE analysis simulations that used a nonlinear material model for TDA. Each design chart is developed using ten separate models, which have similar width and boundary conditions but different TDA thicknesses. The following TDA thicknesses are used for the model: 0.3, 0.6, 0.9, 1.2, 1.5, 1.8, 2.1, 2.4, 2.7 and 3 m. A thickness increment 0.3 m is used as TDA in the field usually compacts in 0.3 m thick layers. Vertical stress is then applied in 10 kPa increments up to 100 kPa. The deformations for each 10 kPa increase

versus vertical stress are used to plot the design chart. A sample model with a 3 m thick TDA layer is presented in Figure 6.4.

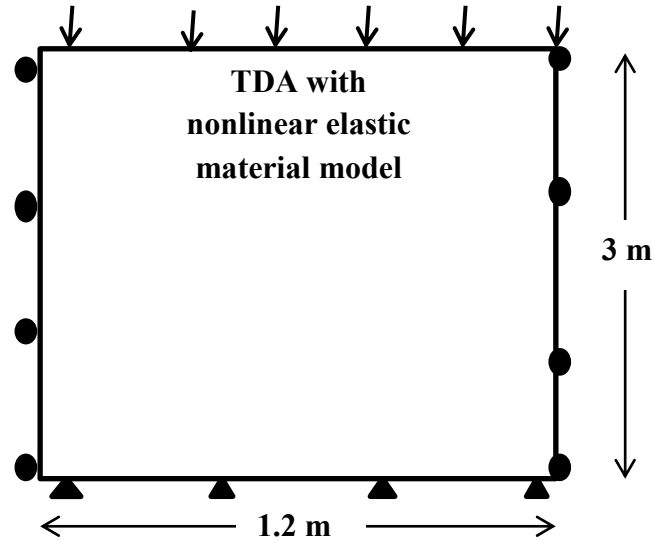


Figure 6.4: Sample model used to develop the design chart for TDA with thickness 3 m.

Figures 6.5 (a), (b), and (c) present design charts for Type B PLTT, Type B OTR, and Type A PLTT, respectively. The design charts are applicable when TDA fill is placed and compacted in 300 mm thick layers. The procedure for the use of the design chart is similar to the procedure proposed by Humphrey (2008). It requires the type of TDA used as fill material (Type A PLTT, Type B PLTT, or Type B OTR), thickness of the TDA layer, and vertical stress to be applied to the top of the layer. The calculation procedure for the overbuild is outlined below:

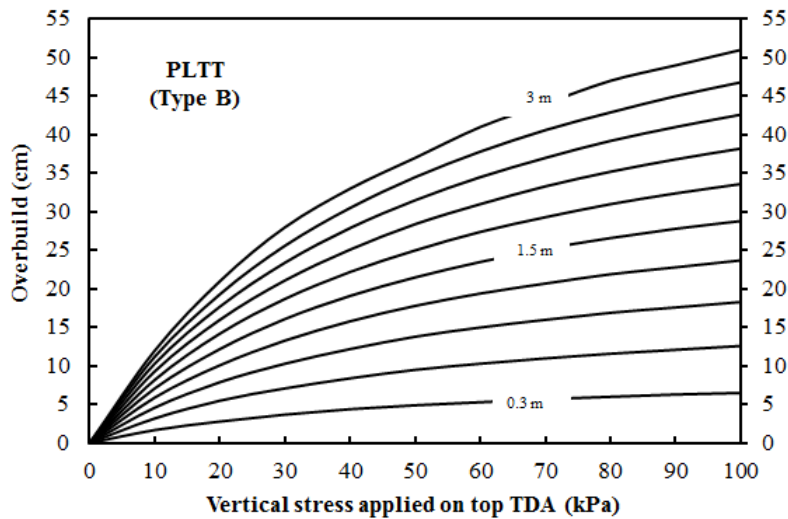
- Calculate the vertical stress acting on top of the TDA layer;
- Select the appropriate chart from Figure 6.5 for the type and size of TDA used as fill material;

- Enter the chart with vertical stress computed above, and the overbuild can be determined using the line which has equivalent thickness with the TDA layer;
- Round down the overbuild to the nearest 0.1 m.

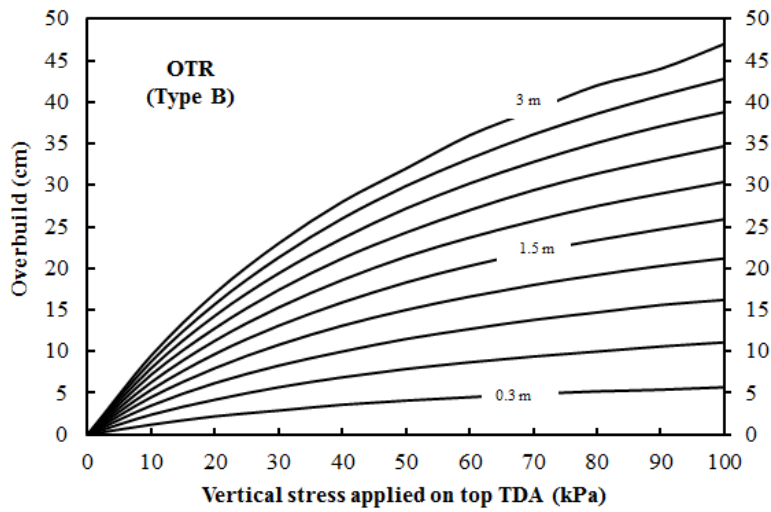
Consider the following example, an overbuild for a single Type B PLTT layer with a thickness of 3 m, soil cover of 1 m ($\gamma = 20 \text{ kN/m}^3$), base course of 0.45 m ($\gamma = 22 \text{ kN/m}^3$) and an asphalt layer of 0.16 m ($\gamma = 23 \text{ kN/m}^3$) on top of the TDA is computed as follows: calculate the vertical stress applied on top of the TDA layer ($20*1 + 0.45*22 + 0.16*23 = 34 \text{ kPa}$); find 34 kPa in Figure 6.5 (a) and cross-reference both the line for Type B PLTT and the layer thickness of 3 m. Subsequently, determine the overbuild and round down the thickness to the nearest 0.1 m. In this case, the overbuild for a vertical stress of 34 kPa according to Figure 6.5 (a) will be 0.31 m. However, rounded down to the nearest 0.1 m, the overbuild will be 0.3 m. A similar procedure can be used for TDA fill constructed with Type B OTR or Type A PLTT by using the appropriate curve for each from Figure 6.5 (b) and (c). Although Type A PLTT is generally used for fill thickness less than 1 m, it is reported by Humphrey et al. (2000) that type A TDA has been used for fill thickness greater than 1 m. Thus, the design chart for Type A TDA has also been developed for fill thickness of up to 3 m.

This procedure was used to predict settlement at the end of fill placement during construction of Portland Jetport interchange in Portland, Maine (Humphrey et al. 2000). Overbuild was not considered during construction Portland Jetport interchange. However data collected during construction indicated that the strain

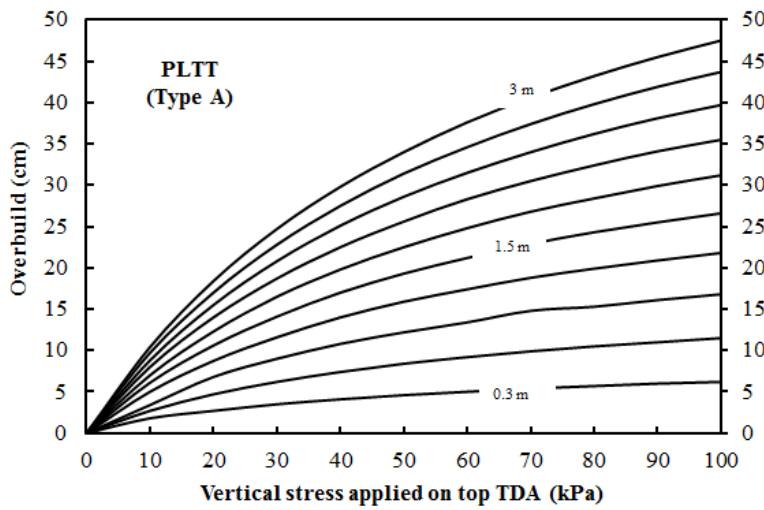
at the end of fill placement was 9.9 percent for the overlying-fill thickness of 2.9 m. If an average unit weight of 19 kN/m^3 is assumed for overlying-fill material, the vertical stress on the top of upper TDA layer will be 55 kPa ($19 \text{ kN/m}^3 * 2.9 \text{ m}$). Using the procedure outlined in the previous paragraph, the overbuild round down to the nearest 0.1 m will be 0.3 m (9.1 percent in terms of strain). Had the upper TDA was overbuild by additional 0.3 m from design thickness during construction, most of vertical settlement that occurred at the end of fill placement would have been accommodated by TDA layer. This demonstrates the applicability of the design charts presented in Figure 6.5 (a), (b) and (c).



(a)



(b)



(c)

Figure 6.5: Overbuild design chart: (a) Type B PLTT; (b) Type B OTR; and (c) Type A PLTT.

CONCLUSION

Nonlinear elastic material models have been developed for TDA produced from PLTT and OTR based on previous large-scale, one-dimensional compression tests for TDA up to 300 mm in size. The material models have been verified with FE

analysis results used to predict the settlement of a full-scale test embankment in Edmonton. Based on the results from the FE analysis and data measured in the field during construction of the full-scale field experiment, the following conclusions can be made:

- Compressibility is the governing parameter in the design of structural fill using TDA. The compressibility of TDA can be determined from large-scale, one-dimensional laboratory compression tests performed on compacted samples.
- The incremental tangent constrained modulus for TDA derived from the large-scale, one-dimensional compression test increases as vertical stress increases. The functional relation can be represented by a second degree polynomial function.
- The computed settlements of an embankment using the FE analysis agree reasonably well with field measurements. Thus, the material model proposed for PLTT and OTR in this study can be used to calculate deformation in geotechnical TDA applications, such as highway embankment fill material and backfill behind retaining walls.

The design charts proposed in this study can be used for preliminary design to determine the overbuild for TDA layer(s) to compensate for immediate compression under applied loads, such as the weight of an overlying soil cover or pavement structure.

REFERENCES

- Alberta Recycling Management Authority, 2012. Tire Recycling Program.
[online] Available at: <<http://www.albertarecycling.ca/>> [Accessed on June 10, 2012].
- Ahmed, I., and Lovell, C. W. 1993. Rubber soils as lightweight geomaterial. Transportation Research Record, 1422, National Research Council, Transportation Research Board, Washington, D.C., 61–70.
- ASTM, 2008. Standard practice for use of scrap tires in civil engineering applications. ASTM D 6270-08, West Conshohocken, PA.
- Bosscher, P. J., Edil, T. B., and Kuraoka, S. 1997. Design of highway embankments using tire chips. Journal of geotechnical and geoenvironmental engineering, 123(4), 295–304.
- Dickson, T.H., Dwyer D.F., and Humphrey D.N. 2001. Prototype tire-shred embankment construction. Transportation Research Record., No. 1755, 160-167, National Research Council, Transportation Research Board, Washington, D.C.
- Duncan, J. M., Byrne, P., Wong, K. S., and Mabry, P. 1980. Strength, stress-strain and bulk modulus parameters for finite element analyses of stress and movements in soil masses, Geotech. Engrg. Res. Rep. No. UCB/GT/80-01, University of California, Berkeley, Calif.

- Eisenstein, Z., and Morrison, A. 1973. Prediction of foundation deformation in Edmonton using an in situ pressure probe. *Canadian geotechnical journal*, 10, 193-210.
- Gharegrat, H. 1993. Finite element analyses of pavements underlain by a tire chip layer and of retaining walls with tire chip backfill. MSCE thesis, University of Maine, Orono, Me.
- Jean-Louis, B. 2001. Introduction to soil moduli. *Geotechnical news*, June 2001, BiTech Publisher Ltd, Richmond, B.C., Canada.
- May, R. M., and Thomson, S. 1978. The geology and geotechnical properties of till and related deposits in the Edmonton, Alberta, area. *Canadian geotechnical journal*, 15, 362-370.
- Meles, D., Bayat, A., and Chan, D. 2014a. One-dimensional compression model for tire derived aggregate using large-scale testing apparatus. *International journal of geotechnical engineering*, 8(2), 197-204.
- Meles, D., Bayat, A., Shaffi, M., H., Nassiri, S., and Gul, M. 2014b. Investigation of Tire Derived Aggregate as a Fill Material for Highway Embankment. *International journal of geotechnical engineering*, 8(2), 182-190.
- Meles, D., Bayat, A., and Soleymani, H. 2013. Compression behavior of large-sized Tire Derived Aggregate for embankment application. *Journal of Material in Civil Engineering*, ASCE, 25(9), 1285-1290.

- Mills, B., and McGinn, J. 2010. Design, Construction, and Performance of Highway Embankment Failure Repair with Tire derived Aggregate. Transportation Research Record., No 1345, 90-99. National Research Council, Transportation Research Board, Washington, D.C.
- Humphrey, D.N., Whetten, N., Weaver, J., and Recker, K. 2000. Tire Shreds as Lightweight Fill for Construction on Weak Marine Clay. Proc., Int. Symp. on Coastal Geotechnical Engineering in Practice, 611–616. (Balkema, Rotterdam, The Netherlands).
- Humphrey, D. N. 2008. Tire derived aggregates as lightweight fill for embankments and retaining wall. International workshop on Scrap Tire Derived Geomaterials– Opportunities and challenges, 59-81. (Yokosuka, Japan).
- Lee, J. H., Salgado, R., Bernal, A. and Lovell, C. W. 1999. Shredded Tires and Rubber-Sand as Lightweight Backfill. Journal of geotechnical and geoenvironmental engineering , 125(2), 132-141.
- Shalaby, A. and Khan, R.A. 2002. Temperature monitoring and compressibility measurement of a tire shred embankment: Winnipeg, Manitoba, Canada, Transportation Research Record., No 1808, 67-75. National Research Council, Transportation Research Board, Washington, D.C.
- Shalaby, A. and Khan, R.A. 2005. Design of unsurfaced roads constructed with large-size shredded rubber tires: a case study. Resource, Conservation and Recycling Journal, Elsevier B.V., 44, 318-332.

- Strenk, P.M., Wartman, J., Grubb, D.G., Humphrey, D. N., and Natale, M. F. 2007. Variability and Scale-Dependency of Tire Derived Aggregate. *Journal of Material in Civil Engineering*, ASCE, 19(3), 233-241.
- Tatliso, N., Benson, C. H., and Edil, T. B. 1997. Effect of fines on mechanical properties of soil-tire chip mixtures. Testing soil mixed with waste or recycled materials, *STP 1275*, M. Wasemiller, and K.Hodding, eds., ASTM, West Conshohocken, PA., 93–108.
- Yang, S., Lohnes, R. A., and Kjartanson, B. H. (2002). Mechanical properties of shredded tires. *Geotechnical testing journal*, 25(1), 44-52.
- Youwai, S., and Bergado, D. T. (2003). Strength and deformation characteristics of shredded rubber tire-sand mixtures. *Canadian geotechnical journal*, 40(1), 254-264.

CHAPTER 7. SUMMARY, CONCLUSIONS AND RECOMMENDATIONS

GENERAL SUMMARY

One of the major problem to use TDA as a fill material is lack of large-scale laboratory experiments that used to predict the deformation behavior of TDA in the field. Moreover, previous studies focus mainly on PLTT, there is no laboratory or field experiment reported in literature for TDA made from OTR. Thus, the focus of this study was to develop material model for TDA based on large-scale laboratory compression experiment, and verify the material model using the compression data measured during construction of full-scale field experiment. Characterizing TDA from OTR using laboratory and field experiment was performed for the first time in this study.

The research used field experiment that used state-of-the-art field instrumentation and data acquisition system. The field experiment besides being used for verification of the developed material model; it also provided important information to compare PLTT, OTR, TDA-mixed with soil with respect to ease of construction, and long and short performance of TDA or TDA-mixed with soil. Most importantly the information provided in this research will help build confidence and facilitate use of TDA as a fill material in Alberta, Canada and benefit the environment by recycling waste tire.

A number of contributions have been produced from this research to use TDA or TDA-mixed with soil as fill material:

- Compression behavior of TDA has been investigated using various large-scale laboratory experiments. The effect of sample initial unit weight, TDA particle size and source of tire for TDA production has been investigated.
- The compression behavior of TDA from OTR has been investigated for the first time.
- A method of compaction for preparing large-scale TDA samples has been proposed.
- Nonlinear material models for TDA based on large-scale laboratory compression experiment have been proposed for various TDA size and tire sources for TDA production.
- Construction difficulties and short- and long-term performances of TDA and TDA-mixed with soil as a fill material for highway embankment have been identified.

COMPRESSION BEHAVIOR OF TDA

Compression behavior of TDA has been investigated using two laboratory experimental set-ups: 570-mm diameter polyethylene pipe thick enough not to allow any lateral deformation of the TDA sample; and 1230-mm diameter Polyvinyl chloride (PVC) pipe that allow small lateral deformation to compute lateral earth pressure coefficient at-rest (K_o) from measurement of vertical and horizontal stress that later used to compute Poisson's ratio.

The first laboratory experiment provided important information to characterize stress-strain behaviour of PLTT and OTR under one-dimensional condition.

Results for the compression test of PLTT in this study agree well with Warith and Raio (2006). Moreover, results obtained to see effect of sample unit weight on compression behaviour for PLTT compares well with Humphrey (2008). Once the experimental set-up was validated by comparing test result for PLTT with the data reported in the literature, one-dimensional compression models as a function of sample unit weight are provided for OTR. This experiment also used to compare compression behaviour of OTR and PLTT for samples with the same initial void ratio. The result showed PLTT and OTR have more or less the same compression curve when compared at the same initial void ratio. Moreover, the experiment is used as a base to design the second experiment (1230-mm diameter PVC pipe) and also used to recommend OTR for similar applications as PLTT.

The second experiment (1230-mm diameter PVC pipe) provided stress-strain behaviour of TDA expressed using hyperbolic equation. The experiment considered TDA particle size and tire source as experimental variables. Samples for laboratory testing were taken from a pile of TDA in the field, where it was used as highway embankment fill and insulation to limit frost penetration. In this experiment, a compaction method similar to field compaction procedure was used. The PVC pipe used for the test also allows small lateral deformation that was used to compute TDA Poisson's ratio. It should be noted that TDA laboratory compaction method used in this study: besides being similar to the field compaction procedure, it was compared with previous method of TDA laboratory compaction by Humphrey and Sandford (1993) for its effectiveness in compacting TDA. The stress-strain relation in terms of hyperbolic equations for Type A

PLTT, Type B PLTT and Type B OTR and other design parameters such as K_o and μ were provided from this study.

MATERIAL MODEL FOR TDA

The study proposed and verified nonlinear elastic material model for TDA. TDA from PLTT as well as OTR showed strain hardening with increase in vertical stress. For compacted samples tested in the second experiment (1230-mm diameter PVC), the strain was recoverable. Thus, nonlinear elastic material models for TDA (incremental tangent modulus) were developed from the derivative hyperbolic stress-strain equation developed using 1230-mm diameter laboratory experiment.

The incremental tangent modulus as a function of vertical stress was given by second degree polynomial function for Type A PLTT, Type B PLTT and Type B OTR. The material model for Type B PLTT and Type B OTR was further used in Finite Element (FE) analysis to predict the settlement measured during construction of instrumented test embankment that used Type B PLTT and Type B OTR as fill material. The comparison of FE analyses result with the measured data in the field shows FE analyses agree well. Thus, the comparison indicated that deflection of highway embankment with TDA as fill material can be predicted and a satisfactory design can be achieved using material model proposed in this study.

DATA COLLECTED FROM INSTRUMENTED FULL SCALE FIELD EXPERIMENT

The study also provided data collected during and after the construction of an instrumented test section that used PLTT, OTR, TDA-mixed with soil and soil without TDA as a fill material. The data collected from field experiment were used to compare the characteristics of PLTT, OTR, TDA-soil mixture and conventional soil, including the ease of construction, field mixing of TDA and soil, immediate and time-dependent settlement, potential for internal heating and deflection under Falling Weight Deflectometr (FWD) test. Moreover, data collected on field settlement and temperature monitoring for PLTT section has been compared with previous case studies (e.g., Humphrey *et al.* 2000; Dickson *et al.* 2001; Shalaby and Khan 2002, 2005; Mills and McGinn 2010). The results in this study agree well with the data reported from previous case histories.

CONCLUSIONS

The following conclusion can be drawn from this research:

- Laboratory experiment using 560-mm diameter one-dimensional test apparatus indicated that:
 - The compression curve obtained for OTR has the same shape with PLTT, and in both PLTT and OTR the compression curve depends on the initial unit weight of the sample
 - The laboratory loading-unloading compression test indicated that only the first load cycle result in significant plastic deformation for both TDA sources.

- Comparison of compression behaviour indicates that both PLTT and OTR show more or less similar stress-strain behaviour when compared at the same initial void ratio.
- Laboratory experiment from 310-mm diameter test apparatus to investigate the applicability of the proposed method of compaction indicated that:
 - Using the method of compaction proposed in this study, it is possible to achieve a compacted unit weight similar to the dynamic compacted unit weight.
 - TDA strips initially placed at random are aligned perpendicularly to the direction of the application of loads after compaction, similar to observations made after field compaction.
 - The method of compaction developed in this study can be used to prepare large-size compacted TDA samples.
- Laboratory experiment from 1230-mm diameter test apparatus conducted on TDA sample collected from field where TDA used as insulation layer and embankment fill applications indicated that:
 - The stress-strain relation for compacted Type A PLTT, Type B PLTT and Type B OTR can be described by hyperbolic equations.
 - Type B PLTT gives the smallest unit weight under both loose and compacted states compared to Type A PLTT and Type B OTR.

- For TDA produced from PLTT, the study indicates that TDA containing large pieces compresses more than TDA containing smaller pieces.
- The laboratory results also suggest that there may be some advantages to use Type B PLTT compared to Type A PLTT as retaining wall backfill since it has a lower K_o value.
- Compression models described in terms of incremental tangent modulus as a function of vertical stress are developed for Type A PLTT, Type B PLTT and Type B OTR. The functional relation can be represented by second degree polynomial function.
- The construction of the test embankment was completed with conventional construction equipment and without any major problems.
- Observations during construction of the test embankment showed that PLTT after compaction was more compressible than OTR.
- The unit weights computed based on the truck count during construction of the test embankment indicated that both PLTT and OTR were lightweight, with unit weight as compacted and compressed by its weight was less than half the unit weight of normal soil fills.
- Settlement measurements in the field indicated that PLTT and TDA-soil mixture sections show the maximum and minimum settlements at the end of the construction, respectively.

- The TDA-soil mixture shows performance equivalent to the normal fill used in the control section; however, it requires additional activity to mix the TDA with soil.
- No evidence of internal heating was detected by the thermistors during the eight-month monitoring time for all three TDA sections.
- PLTT and OTR sections showed high degree of immediate compression compared to TDA-mixed with soil and control sections during construction under the weight of overlying soil.
- The settlement results in PLTT and OTR sections indicated time-dependent settlement that continued to occur well beyond the initial application of the load. However, most of the settlement occurred within 2 months after the placement of the first stage asphalt layer. Moreover the addition of 50 % of soil by volume to TDA highly reduces the time-dependent settlement.
- Distress that may result from TDA time-dependent settlement on the pavement structure can be minimized using the usual practice of allowing 2 months period to pass before placement of settlement sensitive structures or by using the stage constructor approach adopted in this study.
- Deflection data, DBPs value, and back-calculated subgrade modulus indicated overall performance for the PLTT, OTR and TDA-mixed with soil sections is similar to the control section which was used as a bench mark to compare pavement performance.
- Validation of material model developed for Type B PLTT and Type OTR using FE analysis indicated the material models developed in this study can be

used to make deformation analysis where TDA used as fill material in geotechnical applications such as highway embankment fill material.

- The study proposed design charts for Type A PLTT, Type B PLTT and Type B OTR that can be used to determine overbuild that top elevation of TDA layer(s) should be overbuilt to compensate immediate compression under an applied load, such as the weight of an overlying soil cover or pavement structures.

In conclusion, the research provides TDA properties important to engineering applications, including compression behavior, elastic modulus, the coefficient of lateral earth pressure at rest, and Poisson's ratio. The field experiment also support the use of PLTT, OTR, and TDA mixed with soil as a fill material for highway embankment. The performance is quite satisfactory. Moreover, this application is beneficial to the environment by recycling a waste material.

RECOMMENDATIONS FOR FUTURE WORK

The following recommendations are suggested for future studies:

- TDA production mostly results in protruding steel wire that extends from the cutting surface of TDA particles. The effect of protruding wire from the cutting surface of TDA particles on the compression behavior requires further study.
- The data collected from the field experiment in this study indicated that OTR was relatively easy from construction perspective. Thus, it requires further

laboratory and field study to investigate the application of OTR-mixed with soil for the same application.

- TDA has been used successfully used in USA to reduce vibration and sound absorption for dynamic loading such as under light rail way truck line. The planned and on-going expansion of the light rail transit system in Edmonton, Canada may be a good opportunity to further expand and study application of PLTT and OTR to reduce sound and vibration for dynamic loading.
- Both PLTT and OTR have shown creep settlement in the field. The creep settlement requires further study in the laboratory
- Data to evaluate the performance of the field test embankment was only taken for one year. However, further observation longer than one year required to evaluate long-term performance under traffic load.
- Full understanding on engineering properties of OTR require study on shear strength and hydraulic conductivity in the laboratory.

REFERENCES

- AB-Malek, K., and Stevansson, A. 1986. The effects of 42 years immersion in sea water on natural rubber. *Journal of Materials Science*, 21, 147-154.
- Ahmed, I. 1993. Laboratory study on properties of rubber soils. Rep.No. FHWA/IN/JHRP-93/4, Dept. of Civil Engineering, Purdue Univ., West Lafayette, Ind.
- Ahmed, I., and Lovell, C. W. 1993. Rubber soils as lightweight geomaterial. *Transportation Research Record*, 1422, National Research Council, Transportation Research Board, Washington, D.C., 61–70.

- Alberta Recycling Management Authority. 2013. Tire recycling program. Edmonton, AB. [online] Available: <<http://www.albertarecycling.ca/>>. [Accessed on June 1, 2013].
- ASTM. 2008. Standard practice for use of scrap tires in civil engineering applications. ASTM D 6270-08, ASTM International, West Conshohocken, PA.
- ASTM. 2009. Standard test methods for laboratory compaction characteristics of soil using modified effort. ASTM D 1557-09, ASTM international, West Conshohocken, PA.
- ASTM. 2007. Standard test methods for laboratory compaction characteristics of soil using standard effort. ASTM D 698-07, ASTM International, West Conshohocken, PA.
- Benda, C.C. 1995. Engineering properties of scrap tires used in geotechnical applications. Report 95-1, Materials and Research Division, Vermont agency of transportation, Montpelier, VT.
- Beaty, J.R. 1981. Physical properties of rubber compounds. Chapter 10 of mechanics of pneumatic tires, Clark, S.K. ed., United States Department of Transportation, Highway Traffic Safety Administration, Washington, D.C.
- Bosscher, P. J., Edil, T. B. and Eldin, N. N. 1992. Construction and performance of a shredded waste tire test embankment. Transportation Research Record 1345, National Research Council, Transportation Research Board, Washington, D.C., 44–52.

- Bosscher, P. J., Edil, T. B., and Kuraoka, S. 1997. Design of highway embankments using tire chips. *Journal of Geotechnical and Geoenvironmental Engineering*, 123(4), 295–304.
- Chu, C-J. 1998. A geotechnical investigation of the potential use of shredded scrap tires in soil stabilization. Ph.D. Dissertation, Kent State University, Kent, Ohio.
- Dickson, T.H., Dwyer D.F., and Humphrey D.N. 2001. Prototype tire-shred embankment construction. *Transportation Research Record 1755*, National Research Council, Transportation Research Board, Washington, D.C., 160-167.
- Drescher, A., and Newcomb, D.E. 1994. Development of design guidelines for use of shredded tires as a lightweight fill in road subgrade and retaining walls. Report No. MN/RC-94/04, Department of Civil and Mineral Engineering, University of Minnesota, Minneapolis, MN, 1994.
- Drescher, A., Newcomb, D, and Heimdahl, T. 1999. Deformability of shredded tires. Minnesota Department of Transportation, MN/RC -1999-13.
- Edeskar, T. 2004. Technical and environmental properties of tire shreds focusing on ground engineering applications. SE-971 87 Lulea, Department of Civil and Mining Engineering, Lulea University, Lulea, Sweden.
- Edil, T. B., and Bosscher, P. J. 1992. Development of engineering criteria for shredded or whole tires in highway applications. Report No. WI 14-92, Department of Civil and Environmental Engineering, University of Wisconsin, Madison, Wisconsin.

- Edil, T. B., and Bosscher, P. J. 1994. Engineering properties of tire chips and soil mixtures. *Geotechnical Testing Journal*, Vol. 17, No. 4, pp. 453-464.
- Eyles, J., Sider, D., Baxter, J., Taylor, S. M., and Willms, D. 1990. The impacts and effects of the Hagersville tire fire: Preliminary analysis and findings. In *Environment Ontario (Ed.), The challenge of a new decade (Vol. 2, pp. 818-829)*. Toronto: Environment Ontario.
- Geosyntec consultants 2008. *Guidance manual-for engineering use of Scrap Tires*. Prepared for Maryland Department of the Environmental Scrap Tire Program, Geosyntec project No: ME0012, Maryland, USA.
- Gharegrat, H. 1993. Finite element analyses of pavements underlain by a tire chip layer and of retaining walls with tire chip backfill. MSCE thesis, University of Maine, Orono, ME.
- Heimdahl, T. C., and Drescher, A. 1999. Elastic anisotropy of tire shreds. *Journal of Geotechnical and Geoenvironmental Engineering*, 125(5), 383-389.
- Humphrey, D.N. 1999. Water quality results for Whitter farm road tire shred field trial. Department of Civil and Environmental Engineering, University of Maine, Orono, ME.
- Humphrey, D. N. 2008. Tire derived aggregates as lightweight fill for embankments and retaining wall. *International Workshop on Scrap Tire Derived Geomaterials– Opportunities and Challenges*, Yokosuka, Japan, 59-81.
- Humphrey, D.N., and Katz, L.E. 2000. Five-year field study of the effect of tire shreds placed above the water table on groundwater quality.

- Transportation Research Record 1714, National Research Council, Transportation Research Board, Washington, DC, 18-24.
- Humphrey, D. N., and Manion, W. P. 1992. Properties of tire chips for lightweight fill. Proceeding: Grouting, Soil Improvement, and Geosynthetics, ASCE, New York, 1344–1355.
- Humphrey, D. N. and Sandford, T.C. 1993. Tire chips as lightweight subgrade fill and retaining wall backfill. Symposium on Recovery and Effective Reuse of Discarded Material and By-Products for Construction of Highway Facilities, Federal Highway Administration, Washington, DC.
- Humphrey, D. N., Sandford, T. C., Cribbs, M. M., and Manion, W. P. 1993. Shear strength and compressibility of tire chips for use as retaining wall backfill. Transportation Research Record 1422, National Research Council, Transportation Research Board, Washington, D.C., 29–35.
- Humphrey, D.N., and Swett, M. 2006. Literature review of the water quality effects of tire derived aggregate and rubber modified asphalt pavement. Department of Civil and Environmental Engineering, University of Maine, Orono, ME, for U.S. Environmental Protection Agency Resource Conservation Challenge, November 29, 2006.
- Humphrey, D. N., Whetten, N., Weaver, J., and Recker, K. 2000. Tire shreds as lightweight fill for construction on weak marine clay. Proceeding International Symposium on Coastal Geotechnical Engineering in Practice, Balkema, Rotterdam, The Netherlands, 611–616.

- Manion, W. P., and Humphrey, D. N. 1992. Use of tire chips as light weight and conventional embankment fill, Phase I-laboratory. Technical paper 91-1, Technical Services Division, Maine department of transportation, Maine.
- Lamb, T.W. and Whitman, R.V. 1969. Soil Mechanics. John Wiley & Sons, New York.
- Lee, J. H., Salgado, R., Bernal, A. and Lovell, C. W. 1999. Shredded tires and rubber-sand as lightweight backfill. Journal of Geotechnical and Geoenvironmental Engineering, 125(2), 132-141.
- Leclercq, B., Schaeffner, M., Delmas, P., Blivet, J. C., and Matichard, Y. 1990. Durability of geotextiles: Pragmatic approach used in France. Geotextiles, Geomembranes and Related Products, Ed. Hoedt, D., Balkema, Rotterdam, 679-684.
- Masad, E., Taha, R., Ho, C., and Papagiannakis, T. 1996. Engineering properties of tire/soil mixtures as lightweight fill material. Geotechnical Testing Journal, 193, 297-304.
- Mills, B and McGinn, J. 2010. Design, construction, and performance of highway embankment failure repair with Tire-derived Aggregate. Transportation Research Record 2170, National Research Council, Transportation Research Board, Washington, D.C., 90-99.
- Moo-Young, Sellasie, K., Zeroka, D., and Sabnis, G. 2003. Physical and chemical properties of recycled tire shreds for use in construction, Journal of Environmental Engineering, 129(10), 921-929.

- Newcomb, D. E. and Drescher, A. 1994. Engineering properties of shredded tires in lightweight fill applications. Transportation Research Record 1437, National Research Council, Transportation Research Board, Washington, D.C., 1-7.
- Nickels, W.L. 1995. The effect of tire shreds as subgrade fill on paved roads. M.S. Thesis, Department of Civil Engineering, University of Maine, Orono, Maine, 215.
- Pehlken, A., and Essadiqi, E. 2005. Scrap tire recycling in Canada. CANMET material technology laboratory, MTL 2005-08 (CF).
- Reddy, K. R. and Saichek, R. E. 1998. Assessment of damage to geomembrane liners by shredded scrap tires. Geotechnical Testing Journal, 21 (4), 307-316.
- Shalaby, A. and Khan, R.A. 2002. Temperature monitoring and compressibility measurement of a tire shred embankment: Winnipeg, Manitoba, Canada. Transportation Research Record 1808, National Research Council, Transportation Research Board, Washington, D.C., 67-75.
- Shalaby, A., and Khan, R.A. 2005. Design of unsurfaced roads constructed with large-size shredded rubber tires: a case study. Resource Conservation and Recycling Journal, Elsevier B.V., Vol. 44, 318-332.
- Strenk, P.M., Wartman, J., Grubb, D.G., Humphrey, D. N. and Natale, M. F., 2007. Variability and scale-dependency of tire derived aggregate. Journal of Material in Civil Engineering, ASCE, 19(3), 233-241.

- Tandon, V., Velazco, D.A., Nazarian, S. and Picornell, M. 2007. Performance monitoring of embankment containing tire chips: case study. *Journal of Performance of Construction Facilities*, ASCE, 21(3), 207-214.
- Tweedie, J.J., Humphrey, D.N., and Sandford, T.C. 1998. Full scale field trials of tire shreds as lightweight retaining wall backfill, at-rest condition. *Transportation Research Record* 1619, National Research Council, Transportation Research Board, Washington, D.C., 64-71.
- Upton, R.J., and Machan, G. 1993. Use of shredded tires for lightweight fill. *Transportation Research Record* 1422, National Research Council, Transportation Research Board, Washington, D.C., 36-45.
- Warith, M.A., Sundhakar, M.R. 2006. Predicting the compressibility behavior of tire shred samples for landfill applications. *Journal of Waste Management*, 26 (3), 268-277.
- Wu, W., Benda, C., and Cauley, R. 1997. Triaxial determination of shear strength of tire chips. *Journal of Geotechnical and Geoenvironmental Engineering*, ASCE, 123 (5), 479-482.
- Warith, M.A., Sundhakar, M.R. 2006. Predicting the compressibility behavior of tire shred samples for landfill applications. *Journal of Waste Management*, 26 (3), 268.
- Wartman, J., Natale, M.F., and Strenk, P.M. 2007. Immediate and time-dependent compression of tire derived aggregate. *Journal of Geotechnical and Geoenvironmental Engineering*, ASCE, 133 (3), 245-256.

- Winnipeg Sun 2001. The fire started accidentally continues to smolder just west of Winnipeg. Winnipeg free press.
- Yang, S., Lohnes, R. A., and Kjartanson, B. H. 2002. Mechanical properties of shredded tires. *Geotechnical Testing Journal*, 25(1), 44-52.
- Youwai, S., and Bergado, D. T., 2003. Strength and deformation characteristics of shredded rubber tire-sand mixtures. *Canadian Geotechnical Journal*, 40(1), 254-264.
- Yoon, S., Prezzi, M., Sidiki, N.Z., and Kim, B. 2006. Construction of test embankment using a sand-tire shred mixtures as fill material. *Journal of Waste Management*, 26(9), 1033-1044.
- Zornberg, J. G., Costa, Y. D., and Vollenweider, B. 2004. Performance of prototype embankment built with tire shreds and nongranular soil. *Transportation Research Board 1874*, National Research Council, Transportation Research Board, Washington, D.C., 70-77.